Development of lattice density functionals and applications to structure formation in condensed matter systems

Dissertation

zur Erlangung des akademischen Grades

Doctor rerum naturalium

an der Universität Osnabrück

Fachbereich Physik

vorgelegt von

Benaoumeur Bakhti
aus
Algerien

Betreuer: Prof. Dr. Philipp Maaß

Osnabrück, 2013

Abstract

Lattice Density Functional Theory (LDFT) is a powerful tool in the calculation of the density functionals in condensed matter systems. In this work we used a LDFT approach based on the Markov chain to set up an exact density functionals for some lattice models. At first, we considered the lattice hard rod mixtures. In this case, a set of multi-component random variables were introduced to refer to each species of rods. This set reflects the property of the zero dimensional cavity to hold at most one particle. With this connection, our results were reduced to those previously derived within Lattice Fundamental Measure Theory (LFMT). Following the Markov chain approach, we then considered hard rods with arbitrary nearest neighbour interactions extending over two rods lengths. Explicit results for the thermodynamics of the homogeneous hard rods with contact interactions were derived from the corresponding free energy functional. The results show the dramatic effects of thermal interactions over the simple athermal hard core exclusion. Combining strategies from the previous work, we could set up an exact density functional for hard rod mixtures with contact interactions. An interesting aspect of the Markov chain approach is that its density functionals have the same form as the fundamental measure functionals. This feature makes it possible the extension of the exact density functional in one dimension to approximate density functional in higher dimensions using the dimensional crossover. In the presence of interactions, we identified two types of zero-dimensional cavities as expected. The first one is 1-particle cavity, which is a cavity that cannot hold more than one particle (in our language, at most one occupation number can be one in the range of the cavity). The second type is a 2-particle cavity, which is a cavity that cannot hold more than two particles (at most, two occupation numbers can be one in the range of the cavity). In order to account for time dependent phenomena, we have also considered the lattice Time-Dependent Density Functional Theory (LTDFT), applying it to hard rods with contact interactions. By taking some appropriate limits, the corresponding results reproduce those of the standard totally asymmetric exclusion process (TASEP) with interactions and those of the driven hard rods with pure hard core exclusion.

Zusammenfassung

Die Gitter-Dichtefunktionaltheorie (LDFT) ist eine wichtige Methode zur Berechnung von Dichtefunktionalen in der Festkörperphysik. In dieser Arbeit wird die LDFT-Methode auf Basis der Markovkette verwendet, um genauere Dichtefunktionale für einige Gittermodelle zu berechnen. Zu Beginn untersuchen wir Mischungen harter Stäbe. Hierfür wurden eine Reihe von Zufallsvariablen eingeführt, die jeder Stabspezies zugeordnet werden können. Das garantiert die Gültigkeit der "nulldimensionalen Cavity" zumindest für das Ein-Teilchen-Modell. Unsere Ergebnisse konnten mit den zuvor abgeleiteten Resultaten aus der "Fundamental Measure Theory" in Einklang gebracht werden. Anschliessend haben wir harte Stäbe mit beliebigen nächste-Nachbar-Wechselwirkungen betrachtet. Explizite Ergebnisse für die Thermodynamik homogener harter Stäbe mit Kontaktwechselwirkungen wurden aus den entsprechenden Dichtefunktionalen abgeleitet. Die Ergebnisse zeigen die drastischen Auswirkungen der thermischen Wechselwirkungen, die zusätzlich zu den Hard-Core-Wechselwirkungen eingeführt wurden. Durch Überlegungen früherer Arbeiten waren wir in der Lage die genauen Dichtefunktionale für Mischungen harter Stäbe mit Kontaktwechselwirkungen herzuleiten. Es ist davon auzugehen, dass die Dichtefunktionale, die durch die Markovketten-Methode hergeleitet wurden, die gleiche Form aufweisen, wie die "Fundamental Measure Functionals". Diese Tatsache erlaubt uns, die gewonnenen Dichtefunktionale aus einer Dimension in Dichtefunktionale höherer Dimensionenen unter Verwendung dimensionaler Crossover zu erweitern. Unter Berücksichtigung von Wechselwirkungen werden zwei Arten von nulldimensionalen Cavities erwartet. Zum einen ist es die Ein-Teilchen-Cavity, die höchstens ein Teilchen beinhaltet, das heisst höchstens einmal besetzt ist. Zum anderen ist es die Zwei-Teilchen-Cavity, die im Gegensatz zur Ein-Teilchen-Cavity bis zu zwei Teilchen beinhalten kann. Des Weiteren werden dynamische Phänomene unter Anwendung der zeitabhängigen Gitter-DFT harter Stäbe mit Kontaktwechselwirkungen untersucht. Unter bestimmten Bedingungen, die für einen Vergleich nötig waren, konnten die früheren Ergebnisse des Standard-TASEPs und Resultate getriebener harter Stäbe mit Hard-Core-Wechselwirkungen reproduziert werden.

To my parents

Contents

Chapter 1

Introduction

The classical density functional theory (DFT) has been proposed as an alternative way to investigate the equilibrium thermodynamic properties of classical many-body systems [1–4]. Its basic idea is that the free energy functional of a physical system is a unique functional of the density. At equilibrium, this free energy functional is minimum and equals to the grand canonical free energy functional. The corresponding thermodynamics quantities can be inferred from the free energy functional via functional differentiation and integration. This consists a great advance in the treatment of the many body problems in statistical physics over the traditional way of calculating the partition function, because various exact and approximate methods have been introduced to calculate the free energy functional. The theory has been successfully applied to a wide range of physical systems including liquid-gas transition [1, 5], wetting phenomena [6], fluids in porous media [7, 8], surface and interface behaviour [9–11] as well as confinements effects on bulk phase transition [12, 13]. It has even been extended to nonspherical hard bodies [14–19] and time dependent phenomena [20–44].

Based on the same theoretical basis of classical DFT, a lattice version of this theory was constructed to account for the appropriate discrete description for many systems in condensed matter and statistical mechanics. This includes ordering phenomena in metallic alloys, submonolayer adsorbate systems [45], glasses and fluids in porous media [46], roughening [47] and DNA denaturazion [48].

In order to also account for the dynamics of structure formation and phase transitions in lattice condensed matter systems, the LDFT has been extended to time dependent phenomena [45, 49–54]. The LTDFT has been constructed based on the local equilibrium approximation, in which the non-equilibrium distribution function is expressed by the Boltzmann distribution with a time-dependent external potential that needs to be calculated self-consistently. The LTDFT has been successfully applied to the kinetics of ordering transitions and time evolution of density profiles in Ising and Potts models [52] as well as in the asymmetric exclusion process of stochastic interacting lattice gas [53,54]. The results were in a good agreements with kinetic Monte Carlo simulations.

A great deal of attention has been focused on the exactly solvable models in one dimension. It is known that the latter played a crucial rule in the development of classical DFT. The importance of these models has recently grown due to the discovery of the dimensional crossover [5, 55–62], which means that an exact free energy functional in one dimension can be used to build an approximate free energy functionals in higher dimensions. Various schemes have been introduced to set up an exact free energy functionals, including the Robledo-Varia approach [63], the Markov chain approach [64, 65] and lattice fundamental measure theory (LFMT) [60–62, 66–69].

Despite the tremendous progress in using LDFT for systems with hard core exclusion, very few results have been achieved for systems with thermal interactions [70]. The latter have been proved to be realistic for many physical phenomena including crystallization of polymers [71], micelles [72], protein solutions [73], DNA coated colloids [74, 75], as well as ionic fluids [76].

It is along this line, that we are interested in this work in deriving some exact density functionals in one dimension. A paradigm model of our study is the one dimensional hard rods system with thermal interactions. Both one-component and multi-components hard rod systems are considered. The interactions are of arbitrary shape and range and can be repulsive or attractive [77–79].

In Chap. 2 and 3, we present a short introduction to the basic of classical DFT and its lattice version.

In Chap. 4, we use the Markov chain approach to re-derive the exact density functional for a hard rod mixtures on a one-dimensional lattice, which forms the basis of LFMT. The transition probability in the Markov chain depends on a set of occupation numbers, which reflects the property of a zero-dimensional cavity to hold at most one particle. For a given mean occupation numbers, an exact expression of the equilibrium distribution of microstats is obtained, that means an expression for the unique external potential that generates the density profile in equilibrium. By considering the rod ends to fall onto the lattice sites, the mixture is always additive [77].

In Chap. 5, we derive an exact free energy functional for a hard rods with arbitrary nearest neighbour interactions on a one-dimensional lattice. The derivation is based on the Markov property of the system, which allows us to express the exact joint probability distributions. Application was made to rods interacting via sticky core (contact) interactions. The free energy functional and the pair densities of the Ising model were recovered by taking an appropriate limits and the results coincide with those derived earlier using the LFMT. However, our derivation extends previous work, as we have also investigated the case of in-homogeneous coupling. An explicit expression for the entropy, free energy and chemical potential were derived for homogeneous hard rods with contact interactions [78, 79].

In Chap. 6, we extend our results to hard rod mixtures with contact interactions. In the derivation, we combined strategies from the two previous chapters. The density functional is shown to have the fundamental measure form. The free energy functional contains two different contributions. One due to the hard core

exclusion, is encoded in the 1-particle cavity. The second due to the 2-particle cavity and it contains the effects of the interactions. For rods of size one, results previously derived for the Potts model were recovered. Once we have the free energy functional, equilibrium thermodynamics could be worked out using the DFT formalism. Some of the thermodynamic functions are presented at the end of the chapter.

In Chap. 7, we extend the DFT to the pair level. We start by generalizing the Marmin theory to the pair DFT. The formulation makes use of the invariance of the Hamiltonian under the two particles partition of the system. Based on the same previous theoretical bases, we prove that the same theory holds for lattice systems. The results combined with the generalized Markov property permit us to construct an exact pair free energy functional for one dimensional hard rods. The latter has the same form as a fundamental measure functionals and hence can be extended to higher dimensions using the cavity theory.

In Chap. 8, We investigate the steady state dynamics of hard rods with contact interactions within the LTDFT. The dynamics of this system attracted much attention recently because of its numerous applications in condensed matter systems and biophysics as for example, ribosomes moving along mRNA and large molecules or vesicles that are transported by motor proteins along microtubules. An important model in this field is the asymmetric exclusion process (ASEP) which constitutes one of the few models in non-equilibrium statistical mechanics that can be solved exactly. This model describes the diffusion of particles along one-dimensional channels. Our system of interacting driven hard rods is a generalization of the TASEP. Rods of size l are moving in one direction on a one dimensional lattice with some rates and they are interacting through a contact interactions. Current-density relation and phase diagram of system with periodic and open boundary conditions are calculated. Results for a rods with pure hard core interactions and those for lattice gas with nearest neighbour interactions are recovered by taking an appropriate limits.

In Chap. 9 we conclude with a summary and some outlooks for future work.

Chapter 2

Density functional theory

2.1 Introduction

Classical Density Functional Theory (DFT) has become one of the most important tools in statistical mechanics [1–4]. Its basic idea is that for a classical system at some temperature and chemical potential, the free energy functional is a unique functional of the density for a given inter-atomic interactions and external potential. It was first introduced as a technique for treating the quantum mechanical many body problems [80–83] and its development is based on two theories of Hohenberg and Kohn [84]. The first theory states that the energy of the system is a unique functional of the density

$$E = E[\rho(r)] \tag{2.1}$$

The second theory states that the minimization of the energy functional $E[\rho]$ with respect to the density ρ yields the ground state energy E_0 and the ground state density ρ_0. As a result, the ground state problem is reduced to a variation principle

$$\frac{\delta E[\rho(r)]}{\delta \rho(r)} = 0 \tag{2.2}$$

Despite being crucial for the development of the DFT, the Hohenberg-Kohn theory does not give any recipes to calculate the energy functional. This was later provided by the Kohn-Sham theory [85]. Kohn and Sham set up an exact theory that maps the Hamiltonian of the interacting many body electrons system to a Hamiltonian of non-interacting electrons system that can be treated exactly plus some exchange and correlation terms that need to be incorporated as a perturbation. Initially, they developed the Local Density Approximation (LDA) to approximate the exchange and correlation terms. The aim of all subsequent works in DFT is to develop an exact or approximate methods to calculate the exchange and correlation terms for a wide range of applications in condensed matter systems.

These theories (Hohenberg-Kohn and Kohn-Sham), which had a great impact on the electronic structure theory of matter, are only valid for systems where the

quantum effects are dominated over the thermal fluctuations. Mermin made a crucial improvement of the DFT by extending the Hohenberg-Kohn theory to no zero temperature systems. He wrote down a variational principle for the grand canonical free energy functional [86]. The new theory leads to the formulation of DFT for classical many body theory in statistical physics. The Mermin recipe consists of first proving that the free energy functional of a system at finite temperature is a unique functional of the density and second that the free energy functional at equilibrium is minimum and equals to the grand canonical free energy functional. The minimization principle provides a unique relation between the equilibrium density and the external potential. Following Mermin [86], let us consider an inhomogeneous electrons system at finite temperature T and chemical potential μ in the grand canonical ensemble. The states of the system are described by the matrix density $\hat{\rho}$ defined by

$$\hat{\rho} = \psi^*(\mathbf{r})\psi(\mathbf{r}) \tag{2.3}$$

with $\psi(\mathbf{r})$ is the wave function associated with the Hamiltonian $\mathcal{H}$ of the system. $\hat{\rho}$ fulfills the normalization condition $\mathsf{Tr}\hat{\rho} = 1$, where the trace denotes a sum over diagonal elements. The maximum entropy principle yields the following expression for the density matrix at equilibrium

$$\hat{\rho}_0 = \frac{e^{-\beta(\mathcal{H}-\mu N)}}{\mathsf{Tr}e^{-\beta(\mathcal{H}-\mu N)}} \tag{2.4}$$

N is the operator number of particles. The equilibrium grand potential is defined by

$$\begin{aligned}\Omega[\hat{\rho}_0] =& \mathsf{Tr}\hat{\rho}_0(\frac{1}{\beta}\ln\hat{\rho}_0 + \mathcal{H} - \mu N) \\ =& -k_B T \ln Z\end{aligned} \tag{2.5}$$

where

$$Z = \mathsf{Tr}\, e^{-\beta(\mathcal{H}-\mu N)} \tag{2.6}$$

is the grand canonical partition function. To prove that $\Omega[\hat{\rho}]$ is minimum at $\hat{\rho}_0$ let us calculate the difference

$$\begin{aligned}\Omega[\hat{\rho}] - \Omega[\hat{\rho}_0] &= \mathsf{Tr}\left[\hat{\rho}(\frac{1}{\beta}\ln\hat{\rho} + \mathcal{H} - \mu N) - \frac{1}{\beta}\ln Z\right] \\ &= \frac{1}{\beta}\mathsf{Tr}[\hat{\rho}(\ln\hat{\rho} - \ln\hat{\rho}_0)] \\ &\geq 0\end{aligned} \tag{2.7}$$

The inequality fellows from an equivalent relation to the Gibbs-Bogoliubov inequality proved by Mermin for finite temperature quantum systems [86].

To prove the second assumption of Mermin, let suppose that there are two external potentials $V(\mathbf{r})$ and $V'(\mathbf{r})$ differing by more than a constant and leading to

the same equilibrium density $\rho(\mathbf{r})$. We refer respectively by $\mathcal{H}^{'}$, $\hat{\rho}_0^{'}$ and $\Omega^{'}$ to the Hamiltonian, the probability distributions and the grand potential associated with the external potential $V^{'}(\mathbf{r})$. Making use of the minimization principle (2.2) for the free energy functional, we have

$$\begin{aligned}\Omega^{'} &= \mathsf{Tr}\left[\hat{\rho}_0^{'}(\frac{1}{\beta}\ln\hat{\rho}_0^{'} + \mathcal{H}^{'} - \mu N)\right] \\ &< \mathsf{Tr}\left[\hat{\rho}_0(\frac{1}{\beta}\ln\hat{\rho}_0 + \mathcal{H}^{'} - \mu N)\right] \\ &= \Omega + \int d\mathbf{r}(V^{'}(\mathbf{r}) - V(\mathbf{r}))\end{aligned} \tag{2.8}$$

By the same way and interchanging the primed and un-primed quantities we find

$$\Omega < \Omega^{'} + \int d\mathbf{r}(V(\mathbf{r}) - V^{'}(\mathbf{r})) \tag{2.9}$$

Adding the two Eqs (2.8) and (2.9), we arrive to the contradiction

$$\Omega + \Omega^{'} < \Omega + \Omega^{'} \tag{2.10}$$

and hence the density uniquely determines the external potential and vice versa.

The same formalism above holds for classical systems at finite temperature [87, 88]. The density matrix becomes the joint probability distributions

$$\chi(\mathbf{r}_1, \ldots, \mathbf{r}_N, \mathbf{p}_1, \ldots, \mathbf{p}_N) = \frac{e^{-\beta(\mathcal{H}-\mu N)}}{Z} \tag{2.11}$$

and the partition function is given by

$$Z = \mathsf{Tr}_{cl}\left[e^{-\beta(\mathcal{H}-\mu N)}\right] \tag{2.12}$$

where the trace denotes

$$\mathsf{Tr}_{cl} = \sum_N^{\infty} \frac{1}{N!h^{3N}} \int d\mathbf{r}_1 \ldots d\mathbf{r}_N d\mathbf{p}_1 \ldots d\mathbf{p}_N \tag{2.13}$$

One important aspect of the Gibbs free energy functional is that it can be separated on two parts

$$\Omega[\rho] = F[\rho] + \int d\mathbf{r}\rho(\mathbf{r})(V(\mathbf{r}) - \mu) \tag{2.14}$$

$F[\rho]$ is the intrinsic Helmholtz free energy functional. It is independent of the external potential and contains two contributions

$$F[\rho] = F_{id}[\rho] + F_{ex}[\rho] \tag{2.15}$$

$F_{id}[\rho]$ is the ideal gas part and it has a universal form

$$F_{id}[\rho] = \int d\mathbf{r}\rho(\mathbf{r})[\ln\rho(\mathbf{r}) - 1] \tag{2.16}$$

$F_{ex}[\rho]$ is the excess free energy functional and It contains the inter-particles interactions. Once the free energy functional has been calculated, we can get in principle all the equilibrium thermodynamic properties of the system. In particular the equilibrium density profiles which can be inferred from the condition that Ω is minimum at equilibrium

$$\frac{\delta F[\rho]}{\delta \rho(\mathbf{r})} = \mu - V(\mathbf{r}) \tag{2.17}$$

Eq (2.17) is the Euler-Lagrange equation of the system. It gives a unique relation between equilibrium density profiles and the external potential.

The total Helmholtz free energy functional is the legend transform of the Gibbs free energy functional and it is given by [2]

$$A = F[\rho] + \int d\mathbf{r}\rho(\mathbf{r})V(\mathbf{r}) \tag{2.18}$$

The direct correlation functions (DCF) can be generated from the excess free energy functional

$$c^{(1)}(\mathbf{r}) = -\frac{\delta F_{ex}[\rho]}{\delta \rho(\mathbf{r})} \tag{2.19}$$

for the one point DCF and

$$c^{(2)}(\mathbf{r}_1, \mathbf{r}_2) = -\frac{\delta^2 F_{ex}[\rho]}{\delta \rho(\mathbf{r}_1)\delta \rho(\mathbf{r}_2)} \tag{2.20}$$

for the two pint DCF and

$$c^{(n)}(\mathbf{r}_1, \ldots, \mathbf{r}_n) = \frac{\delta c^{(n-1)}(\mathbf{r}_1, \ldots, \mathbf{r}_{n-1})}{\delta \rho(\mathbf{r}_n)} \tag{2.21}$$

for the n-point DCF.

The first derivative of Ω with respect to the external potential is the one-body density

$$\rho(\mathbf{r}) = -\frac{\delta \Omega[\rho(\mathbf{r})]}{\delta u(\mathbf{r})} \tag{2.22}$$

where $u(\mathbf{r}) = \mu - V(\mathbf{r})$. The second derivative is the density-density correlation function

$$\begin{aligned} -G(\mathbf{r}_1, \mathbf{r}_2) &= \frac{1}{\beta}\frac{\delta^2 \Omega[\rho(\mathbf{r})]}{\delta u(\mathbf{r}_2)\delta u(\mathbf{r}_1)} \\ &= -\frac{\delta \rho(\mathbf{r}_1)}{\delta u(\mathbf{r}_2)} \\ &= \rho(\mathbf{r}_1)\rho(\mathbf{r}_2)h(\mathbf{r}_1, \mathbf{r}_2) + \rho(\mathbf{r}_1)\delta(\mathbf{r}_1 - \mathbf{r}_2) \end{aligned} \tag{2.23}$$

the structure function (or the total correlation function) $h(\mathbf{r}_1, \mathbf{r}_2)$ is given by

$$h(\mathbf{r}_1, \mathbf{r}_2) = g(\mathbf{r}_1, \mathbf{r}_2) - 1 \tag{2.24}$$

where $g(\mathbf{r}_1, \mathbf{r}_2)$ is the radial (pair) distribution function.
From (2.15), (2.20) and (2.23) we find

$$-\beta\frac{\delta u(\mathbf{r}_1)}{\delta\rho(\mathbf{r}_2)} = -G^{-1}(\mathbf{r}_1, \mathbf{r}_2) = -\frac{\delta(\mathbf{r}_1 - \mathbf{r}_2)}{\rho(\mathbf{r}_1)} + c^{(2)}(\mathbf{r}_1, \mathbf{r}_2) \tag{2.25}$$

Inserting $G(\mathbf{r}_1, \mathbf{r}_2)$ and $G^{-1}(\mathbf{r}_1, \mathbf{r}_2)$ in the expression

$$\int d\mathbf{r}_3 G^{-1}(\mathbf{r}_1, \mathbf{r}_3)G(\mathbf{r}_3, \mathbf{r}_2) = \delta(\mathbf{r}_1 - \mathbf{r}_2) \tag{2.26}$$

we get

$$h(\mathbf{r}_1, \mathbf{r}_2) = c^{(2)}(\mathbf{r}_1, \mathbf{r}_2) + \int d\mathbf{r}_3 h(\mathbf{r}_1, \mathbf{r}_3)\rho(\mathbf{r}_3)c^{(2)}(\mathbf{r}_3, \mathbf{r}_2) \tag{2.27}$$

Eq (2.27) is the Ornstein-Zernike (OZ) equation for an in-homogeneous systems. It relates the DCF to the total correlation function [89]. Different methods have been proposed to solve the OZ equation, include the Percus-Yevick [90], the Hypernetted chains [91, 92], Born-Green [93] and Mean spherical approximations [94]. All these approximations are based on introducing a closer relation between the two unknowns of the OZ equation, namely the total correlation function h and the two-point direct correlation function $c^{(2)}$. The Percus-Yevick approximation supplements the OZ equation with the relation

$$c^{(2)}(\mathbf{r}) = g(\mathbf{r})[1 - e^{-\beta v(\mathbf{r})}] \tag{2.28}$$

where $v(\mathbf{r})$ is the inter-particle interactions. To get a more simpler form for the OZ equation, Percus and Yevick introduced the function $y(\mathbf{r}) = g(\mathbf{r})e^{-\beta v(\mathbf{r})}$. Accordingly, the DCF can be written as

$$c^{(2)}(\mathbf{r}) = f(\mathbf{r})g(\mathbf{r}) \tag{2.29}$$

$f(\mathbf{r})$ is the Mayer function. Inserting Eq (2.29) in (2.27) yields the Percus-Yevick equation

$$y(\mathbf{r}_{12}) = 1 + \rho \int d\mathbf{r}_3 f(\mathbf{r}_{13})y(\mathbf{r}_{13})h(\mathbf{r}_{23}) \tag{2.30}$$

where $\rho = N/L^3$ is the density of the homogeneous system.

The hypernetted chain approximation supplements the OZ equation with

$$c^{(2)}(\mathbf{r}) = h(\mathbf{r}) - \ln(g(\mathbf{r})) - \beta v(\mathbf{r}) \tag{2.31}$$

These procedures have been applied to many systems, such as the hard spheres and sticky hard spheres. The resulting DCF's have been used as a building block to build the free energy functionals using Eq (2.20). Integration of Eq (2.20) between two densities through a path of integration parameterized as [4]

$$\rho_\lambda(\mathbf{r}) = (1 - \lambda)\rho_0(\mathbf{r}) + \lambda\rho_1(\mathbf{r}) \tag{2.32}$$

yields the expression

$$\frac{1}{V}\beta F_{ex}[\rho_1] = \beta f_{ex}(\bar{\rho}_0) + \frac{\partial \beta f_{ex}(\bar{\rho}_0)}{\partial \bar{\rho}_0}(\bar{\rho}_1 - \bar{\rho}_0) - \frac{1}{V}\int_0^1 d\lambda \int_0^\lambda d\lambda' \int d\mathbf{r}_1 d\mathbf{r}_2 c^{(2)}(\mathbf{r}_1, \mathbf{r}_2, [(1-\lambda')\rho_0 + \lambda'\rho_1]) \times (\rho_1(\mathbf{r}_1) - \bar{\rho}_0)(\rho_1(\mathbf{r}_2) - \bar{\rho}_0) \tag{2.33}$$

where the reference state is taken to be a uniform liquid with excess free energy functional $f_{ex}(\rho)$ and density $\rho_0(\mathbf{r}) = \bar{\rho}_0$. To make (2.33) tractable, the direct correlation function has been expanded as Taylor series and only the leading terms in the development has been taken into account [4]

$$c^{(2)}(\mathbf{r}_1, \mathbf{r}_2, [\rho_\lambda]) = c^{(2)}(\mathbf{r}_{12}, \bar{\rho}(\lambda)) + \sum_{n=3}^{\infty} \frac{1}{(n-2)!} \int d\mathbf{r}_3 \dots d\mathbf{r}_N c^{(n)}(\mathbf{r}_3, \dots, \mathbf{r}_N, \bar{\rho}(\lambda)) \times (\rho_\lambda(\mathbf{r}_3) - \bar{\rho}(\lambda)) \dots (\rho_\lambda(\mathbf{r}_N) - \bar{\rho}(\lambda)) \tag{2.34}$$

$c^{(n)}$ is the n-point direct correlation function. Eqs. (2.33) and (2.34) which are exact have been extensively used to derive a free energy functionals for an inhomogeneous systems such as solids, based on the knowledge of the properties of the homogeneous ones. The most simplest DFT based on (2.33) and (2.34) is the Ramakrishnan-Yussouff approximation. It has been developed for the case where the target system is a uniform fluids with density $\bar{\rho}_0 = \bar{\rho}_1$. In this case, the series is truncated at a second order [95]. The theory has been successfully applied to the study of freezing.

2.2 Approximate DFT

2.2.1 Effective Liquid Approximation

In order to build a DFT for freezing, Baus and Colot [96] developed a perturbative theory based on eqs (2.33) and (2.34) with $\bar{\rho}_0 = \bar{\rho}_1$. They approximated the direct correlation function by that of a liquid at density $\bar{\rho}(\lambda) = \bar{\rho}_{ELA}$ for which the first peak of the structure factor of the liquid occurs at the smallest reciprocal lattice vector. Replacing the density in eq (2.33) yields [4]

$$\frac{1}{V}\beta F_{ex}[\rho_1] = \beta f_{ex}(\bar{\rho}_1) - \frac{1}{2V}\int d\mathbf{r}_1 d\mathbf{r}_2 c^{(2)}(\mathbf{r}_{12}, \bar{\rho}_{ELA})(\rho_1(\mathbf{r}_1) - \bar{\rho}_1)(\rho_1(\mathbf{r}_2) - \bar{\rho}_1) + \dots \tag{2.35}$$

A modified version of the ELA has been introduced later by Baus [97] under the name Self-Consistent effective liquid approximation (SCELA). It consists of taking

$\bar{\rho}_0 = 0$ and choose $\bar{\rho}(\lambda) = \lambda\bar{\rho}_{SCELA}$ which leads to [4]

$$\frac{1}{V}\beta F_{ex}[\rho_1] = -\frac{1}{V}\int_0^1 d\lambda \int d\mathbf{r}_1 d\mathbf{r}_2 (1-\lambda) c^{(2)}(\mathbf{r}_{12}, \lambda\bar{\rho}_{SCELA})\rho_1(\mathbf{r}_1)\rho_1(\mathbf{r}_2) + ... \tag{2.36}$$

$\bar{\rho}_{SCELA}$ is chosen so that the free energy per atom of liquid is equal to those of solid.

The last version of the ELA named the Generalized ELA has been introduced by Lutsko and Baus [2, 98, 99] . The idea of the theory is based on a mapping of the the nonuniform system to a uniform one leading to a self-consistence equations. The first mapping which is termed the thermodynamics mapping consists of equating the excess free energy functional of a nonuniform fluid with those of an effective fluid at density $\hat{\rho}_1$. This can be done as follows [2, 4]: Taking the initial density to be zero in the exact expression of the excess free energy

$$\beta F_{ex}[\rho] = \beta F_{ex}[\rho_i] - \int d\mathbf{r}(\rho(\mathbf{r}) - \rho_i(\mathbf{r}))c^{(1)}([\rho_i], \mathbf{r}) \tag{2.37}$$
$$- \int_0^1 d\lambda \int d\mathbf{r}_1(\rho(\mathbf{r}_1) - \rho_i(\mathbf{r}_1)) \int_0^\lambda d\lambda' \int d\mathbf{r}_2(\rho(\mathbf{r}_2) - \rho_i(\mathbf{r}_2))c^{(2)}(\rho_{\lambda'}, \mathbf{r}_1, \mathbf{r}_2)$$

leads to

$$\beta F_{ex}[\rho] = -\int_0^1 d\lambda \int d\mathbf{r}_1\rho(\mathbf{r}_1) \int_0^\lambda d\lambda' \int d\mathbf{r}_2\rho(\mathbf{r}_2)c^{(2)}(\lambda'\rho, \mathbf{r}_1, \mathbf{r}_2) \tag{2.38}$$

and for a uniform system it becomes

$$\beta F_{ex}[\rho] = -N\rho \int d\mathbf{r} \int_0^1 d\lambda \int_0^\lambda d\lambda' c^{(2)}(\lambda'\rho, \mathbf{r}) \tag{2.39}$$

Equating the two excess free energies gives

$$\hat{\rho}_1[\rho] = \frac{1}{N}\int d\mathbf{r}_1\rho(\mathbf{r}_1) \int d\mathbf{r}_2\rho(\mathbf{r}_2)\omega(\mathbf{r}_1, \mathbf{r}_2, \rho) \tag{2.40}$$

and the weighted density is given by

$$\omega(\mathbf{r}_1, \mathbf{r}_2, [\rho]) = \frac{\int_0^1 d\lambda \int_0^\lambda d\lambda' c^{(2)}(\lambda'\rho, \mathbf{r}_1, \mathbf{r}_2)}{\int d\mathbf{r}_1 \int_0^1 d\lambda \int_0^\lambda d\lambda' c^{(2)}(\lambda'\hat{\rho}_1, \mathbf{r})} \tag{2.41}$$

The second mapping which is called the structural mapping consists of equating the density averaged direct correlation function of the nonuniform fluid with those of an effective liquid at a density $\hat{\rho}_2$

$$\int d\mathbf{r}_1 \int d\mathbf{r}_2\rho(\mathbf{r}_1)\rho(\mathbf{r}_2)c^{(2)}([\rho], \mathbf{r}_1, \mathbf{r}_2) = \int d\mathbf{r}_1 \int d\mathbf{r}_2\rho(\mathbf{r}_1)\rho(\mathbf{r}_2)c^{(2)}(\hat{\rho}_2[\rho], |\mathbf{r}_1 - \mathbf{r}_2|)$$

demanding the two mapping to hold simultaneously at density $\hat{\rho}_1[\rho] = \hat{\rho}_2[\rho] = \hat{\rho}[\rho]$ leads to the expression for $\hat{\rho}[\rho]$ with the same form as in Eq (2.40) and the weight function is given by

$$\omega^{GELA}(|\mathbf{r}_1 - \mathbf{r}_2|, [\rho]) = -\hat{\rho}\frac{\int_0^1 d\lambda \int_0^\lambda d\lambda' c^{(2)}([\lambda'\rho], |\mathbf{r}_1 - \mathbf{r}_2|)}{\beta\psi_{ex}(\hat{\rho})} \tag{2.42}$$

where $\psi_{ex}(\hat{\rho})$ is the GELA excess free energy functional per atom

$$\beta\psi_{ex}(\hat{\rho}) = -\frac{1}{N}\int_0^1 d\lambda \int d\mathbf{r}_1\rho(\mathbf{r}_1)\int_0^\lambda d\lambda' \int d\mathbf{r}_2\rho(\mathbf{r}_2)c^{(2)}(\hat{\rho}[\lambda'\rho], |\mathbf{r}_1-\mathbf{r}_2|) \tag{2.43}$$

By taking an appropriate limits the previous effective liquid approximations can be recovered from the GELA. The GELA has been used to describe the freezing of hard spheres and the results were in good agreement with simulation and even better than previous density functional approximations but it fails in describing of freezing into the bcc or fcc lattice for an inverse power low potentials.

2.2.2 Weighted Density Approximation

The weighted density approximation has been proposed by Nordholm et al [100] as a theory for the in-homogeneous hard spheres fluid. It consists of approximating the excess free energy functional as

$$F_{ex}[\rho(\mathbf{r})] = \int d\mathbf{r}\rho(\mathbf{r})\psi_{ex}[\bar{\rho}(\mathbf{r})] \tag{2.44}$$

$\psi_{ex}(\rho) = \Phi(\rho)/\rho$ is the excess free energy per particle of the homogeneous system and the weighted density $\bar{\rho}$ is given by [3]

$$\bar{\rho}(\mathbf{r}_1) = \int d\mathbf{r}_2\rho(\mathbf{r}_1 + \mathbf{r}_2)w(\mathbf{r}_2, \bar{\rho}(\mathbf{r}_1)) \tag{2.45}$$

where $w(\mathbf{r}', \bar{\rho}(\mathbf{r}))$ is a normalized wight function. The choice of the wight functions is a key element in the WDA because it determines the non-local dependence of $F_{ex}[\rho(\mathbf{r})]$. Different choices have been proposed leading to different versions of the WDA.

Local density approximation

The choice:

$$w(\mathbf{r}) = \delta(\mathbf{r}) \tag{2.46}$$

corresponds to the local density approximation earlier introduced to set up an approximate free energy functionals. It is the simplest scheme used to build approximate free energy functionals for nonuniform systems from the knowledge of the

properties of the uniform ones. The LDA approximate the excess free energy functional as

$$F_{ex}[\rho] = \int_V d\mathbf{r}\psi_{ex}(\rho(\mathbf{r})) \tag{2.47}$$

It is well known that the LDA gives an acceptable results only if the density varies very smoothly over the molecular size distances. It fails for sharp interface like the liquid-vapor interface, because the gradient of the density will generate a forces applied on volumes with different densities. This effect has not been incorporated in the LDA [4]. An improved version of the LDA is when the density functional depends not only on the density but on also on square gradient of the density

$$F_{ex}[\rho] = \int_V d\mathbf{r}\left[\psi_{ex}(\rho(\mathbf{r})) + \psi(\rho)(\nabla\rho(\mathbf{r}))^2\right] \tag{2.48}$$

the second coefficient can be determined by imposing additional requirement on the excess free energy functional $F_{ex}[\rho]$. It is given by [2]

$$\psi(\rho) = \frac{1}{12\beta}\int d\mathbf{r}\,\mathbf{r}^2 c^{(2)}(\mathbf{r}, \rho(\mathbf{r})) \tag{2.49}$$

This approximation named the square gradient approximation (SGA) has been introduced earlier than the WDA [101]. It was discussed even by Boltzmann himself in study of the liquid-vapor interface [102]. The SGA is useful for a wide range of inter-facial problems and it has been extended to the case of mixtures. Another close version of the SGA has been introduced by Ebner *et al* and it consists of the following functional

$$F[\rho] = \int d\mathbf{r}\psi(\rho(\mathbf{r})) + \frac{1}{4\beta}\int d\mathbf{r}_1 \int d\mathbf{r}_2 c^{(2)}(\mathbf{r}_{12}, \rho^m)[\rho(\mathbf{r}_1) - \rho(\mathbf{r}_2)]^2 \tag{2.50}$$

where $\rho^m = (\rho(\mathbf{r}_1) + \rho(\mathbf{r}_2))/2$. The previous functional reduces to the gradient approximation one for slowly varying density and it is consistent with the linear response theory. The SGA is failed when the local density achieves a high values and the WDA has been introduced as a refined DFT [4].

Mean field approximation

The choice:

$$w(\mathbf{r}) = \frac{v(\mathbf{r})}{v_0} \tag{2.51}$$

where $v(\mathbf{r})$ is the iner-molecular interactions and $v_0 = \int d\mathbf{r}v(\mathbf{r})$ corresponds to the mean field approximation (MFA). The free energy functional has the form

$$F[\rho] = \frac{1}{2}\int d\mathbf{r}_1 d\mathbf{r}_2 \rho(\mathbf{r}_1)\rho(\mathbf{r}_2)v(\mathbf{r}_1 - \mathbf{r}_2) \tag{2.52}$$

The MFA has been used for soft interactions where the particles can be assumed to be uncorrelated and it gives an accurate results for systems with ultra-soft interactions, like the case of polymer chains in bad solvents [3].

WDA of Nordholm et al

The first density dependent wight function has been proposed by Nordholm et al [100]. The weight functions were tailored to reproduce the direct correlation function of the homogeneous fluid. The results largely improve the previous DFT such as the LDA and the SGA for the homogeneous systems, but on the other side this complicated the derivation or the numerical minimization of Ω because the weight function becomes now an equation for $\bar{\rho}(\mathbf{r})$ which needs to be solved at every point $\mathbf{r}$. The following forms have been used for $\bar{\rho}(\mathbf{r})$

$$\bar{\rho}(\mathbf{r}) = \int d\mathbf{r}' w_0(|\mathbf{r} - \mathbf{r}'|)\rho(\mathbf{r}') \tag{2.53}$$

where

$$w_0(r) = \frac{3}{4\pi\sigma^3}\theta(\sigma - r) \tag{2.54}$$

the excess density functional $\psi_{ex}[\bar{\rho}(\mathbf{r})]$ is chosen to be

$$\psi_{ex}[\bar{\rho}] = -\ln(1 - \frac{2}{3}\pi\sigma^3\rho) \tag{2.55}$$

The theory has been used to study the hard spheres near wall and the results for density present an oscillatory profile not in good agreement with simulations and it fails also in the study of phase transitions.

WDA of Tarazona

The choice of Tarazona for the weight functions consists of [103]

$$w(r) = w_0(r) + \rho w_1(r) + \rho^2 w_2(r) \tag{2.56}$$

where $w_0(r)$ and $w_1(r)$ are calculated by comparison with the virial expansion of $c_{hs}^{(2)}$. $w_2(r)$ which is purely empirical has been obtained from a fit to the Percus-Yevick results. $w_0(r)$ has been calculated exactly and it has the same form as the Nordholm *et al* wight function

$$w_0(r) = \frac{3}{4\pi\sigma^3}\theta(\sigma - r) \tag{2.57}$$

$w_1(r)$ is a solution of the equation

$$\begin{aligned} &\frac{10\pi}{3}\sigma^3 w_0(r) + 8w_1(r) + \frac{5\pi}{3}\sigma^3 \int d\mathbf{r}' w_0(r')w_0(|\mathbf{r} + \mathbf{r}'|) \\ &+ 8\int d\mathbf{r}' w_0(r')w_1(|\mathbf{r} + \mathbf{r}'|) = \left[8 - 6\frac{r}{\sigma} + \frac{1}{2}\left(\frac{r}{\sigma}\right)^3\right]\theta(\sigma - r) \end{aligned} \tag{2.58}$$

which can be obtained by the inverse Fourier transform

$$w_1(k) = \frac{\sigma^3}{12\pi r}\int_0^\infty dk\, k \sin(kr)\frac{\hat{f}(k) - 20\hat{w}_0(k) - 10\hat{w}_0(k)^2}{8[1 + \hat{w}_0(k)]} \tag{2.59}$$

where $\hat{w}_0(k)$ and $\hat{f}(k)$ are the Fourier transforms of $w_0(r)$ and $f(r)$ respectively. $w_2(r)$ has the form

$$w_2(r) = \frac{5\pi\sigma^3}{24}\left[1 - 2\frac{r}{\sigma} + \frac{5}{6}\left(\frac{r}{\sigma}\right)^5\right]\theta(\sigma - r) \tag{2.60}$$

The requirement that the weighted density $\bar{\rho}(\mathbf{r})$ reduces to ρ in the case of homogeneous fluids implies

$$\int d\mathbf{r}\, w_0(\mathbf{r}) = 1 \tag{2.61}$$

and

$$\int d\mathbf{r}\, w_\nu(\mathbf{r}) = 0 \text{ for } \nu = 1, 2 \tag{2.62}$$

$\bar{\rho}(\mathbf{r})$ in this case is given by

$$\bar{\rho}(\mathbf{r}) = \frac{2\bar{\rho}_0(\mathbf{r})}{1 - \bar{\rho}_1(\mathbf{r}) + [(1 - \bar{\rho}_1(\mathbf{r}))^2 - 4\bar{\rho}_0(\mathbf{r})\bar{\rho}_2(\mathbf{r})]^{1/2}} \tag{2.63}$$

This approximation makes use of the Carnahan-Starling equation of state to fix

$$\psi_{CS}(\rho) = \frac{4\eta - 3\eta^3}{(1-\eta)^2} \tag{2.64}$$

where the packing fraction is given by $\eta = \pi\sigma^3\rho/6$. The theory has been applied to study hard spheres near hard wall and the results for density profiles and surface tension are in good agreement with simulations. It yields also a realistic oscillatory density profiles for fluids near hard wall and realistic equation of state for two dimensional fluid. It has been extended straightforwardly to the case of mixtures [3].

WDA of Curtin and Ashcroft

Curtin and Ashcroft's theory [104] consists of avoiding the expansion of the weighted density used by Tarazona. Curtin and Ashcroft fixed the weight function by requiring that the resulting direct correlation function for the in-homogeneous system leads to those derived from the Percus-Yevick equation for all fluid densities. The weight function is determined from

$$\begin{aligned} k_B T\tilde{c}^{(2)}(k,\bar{\rho}) = &- 2\frac{\partial\psi_{ex}(\bar{\rho})}{\partial\bar{\rho}}\tilde{w}(k,\bar{\rho}) - \bar{\rho}\frac{\partial^2\psi_{ex}(\bar{\rho})}{\partial\bar{\rho}^2}\tilde{w}^2(k,\bar{\rho}) \\ &- 2\frac{\partial\psi_{ex}(\bar{\rho})}{\partial\rho}\tilde{w}(k,\bar{\rho})\frac{\partial\tilde{w}(k,\bar{\rho})}{\partial\bar{\rho}} \end{aligned} \tag{2.65}$$

where $\tilde{w}(k,\bar{\rho})$ is the Fourier transform of $w(\mathbf{r},\bar{\rho})$, and $\psi_{ex}(\bar{\rho})$ is the free energy density functional. The direct correlation function and the density functional of the uniform fluid constitute an input for the theory. This approximation has been extended to the case of mixtures by Denton and Ashcroft [105].

2.2.3 Fundamental Measure Theory

Original FMT

The idea behind the previous DFT's is to construct an approximate free energy functionals of in-homogeneous systems based on information from the corresponding uniform systems. A new theory for the in-homogeneous systems has been proposed by Rosenfeld with the aim to find the properties of the uniform systems as an output rather than an input [55]. Inspired by the exact results for one dimensional hard rods of Percus [106] and the Scaled Particle Theory (SPT) [107, 108], Rosenfeld observed that two fundamental quantities enter in the construction of the exact free energy functional of hard rods which is given by

$$F_{ex}[\rho] = -\int dx n(x) \ln(1-\eta(x)) \tag{2.66}$$

The two fundamental quantities are

$$n(x) = \frac{1}{2}(\rho(x+R) + \rho(x-R)) \tag{2.67}$$

$$\eta(x) = \int_{-R}^{R} dy \rho(x+y) \tag{2.68}$$

where R is the radius of the rod. These two quantities (called the weighted densities) can be re-written as a convolution between the density and some weight functions as

$$n(x) = \int dy \rho(y) \omega_n(x-y), \tag{2.69}$$

and

$$\eta(x) = \int dy \rho(y) \omega_\eta(x-y) \tag{2.70}$$

The weight functions (fundamental measures)

$$\begin{aligned} \omega_n(x) =& \delta(|x|-R) \\ \omega_\eta(x) =& \theta(|x|-R) \end{aligned} \tag{2.71}$$

are constructed based on the geometry of the rod. The first one restricts the integration to the two surfaces of the rod, while the second restricts integration to the volume of the rod. A further important observation is that the convolution of the two fundamental measures gives the Mayer function of the system. This suggests a connection to the SPT. Rosenfeld generalized the exact results of hard rods in one dimension to 3D hard spheres using the following recipes [61]
"(i) decomposing the Mayer function into a sum of convolution of the one-particle measures;
(ii) using these measures to define a set of weighted densities;

(iii) determining the functional form by restoring to SPT."
In 3D and in addition to the two weight functions $\omega_n(\mathbf{r})$ and $\omega_\eta(\mathbf{r})$, the first step led to a new vector weight function given by

$$\mathbf{w}(\mathbf{r}) = \frac{\mathbf{r}}{R}\frac{\delta(|\mathbf{r}| - R)}{s_D} \tag{2.72}$$

and the corresponding vector weighted density

$$\mathbf{v}(\mathbf{r}) = \int d\mathbf{r}'\rho(\mathbf{r} + \mathbf{r}')\mathbf{w}(\mathbf{r}') \tag{2.73}$$

here R is the radius of the hard sphere. s_D being the total molecular surface in D dimensions ($s_1 = 2, s_2 = 2\pi R, s_3 = 4\pi R^2$) [3]. The three weighted densities (result from the convolution of the weight functions and the density) are the building blocks for the free energy functional of hard spheres in three dimensions $\Phi_{FMT}([\rho], \mathbf{r}) = \phi(\eta(\mathbf{r}), n(\mathbf{r}), \mathbf{v}(\mathbf{r}))$. By requiring the consistency of the resulting free energy functional with the SPT, Rosenfeld proposed the following form for the free energy density functional

$$\Phi_{FMT}([\rho], \mathbf{r}) = \sum_{i=1}^{3} \phi_i^{(3D)}(\eta(\mathbf{r}), n(\mathbf{r}), \mathbf{v}(\mathbf{r})) \tag{2.74}$$

where $\phi_i^{(3D)}(\eta(\mathbf{r}), n(\mathbf{r}), \mathbf{v}(\mathbf{r}))$ are given by

$$\phi_1^{(3D)}(\eta, n) = -n(\mathbf{r})\ln(1 - \eta(\mathbf{r})), \tag{2.75}$$

$$\phi_2^{(3D)}(\eta, n, \mathbf{v}) = 4\pi R^3 \frac{n^2 - \mathbf{v}\mathbf{v}}{1 - \eta}, \tag{2.76}$$

and

$$\phi_3^{(3D)}(\eta, n, \mathbf{v}) = 8\pi^2 R^6 n \frac{n^2/3 - \mathbf{v}\mathbf{v}}{(1 - \eta)^2}. \tag{2.77}$$

The resulting free energy functional has been proved to be better than those of the WDA in studying hard spheres against hard wall. However, it fails to describe the structure of the crystal because the convolution of delta function used for the density in this case with the weight delta function leads to a strong divergence of the free energy functional [3]. This failure leads later to a new versions of the FMT and to the cavity theory developed by Tarazona [58, 59].

Dimensional reduction and cavity theory

The original version of the FMT has been proposed to reproduce the PY correlation function and equation of state, but it fails in the crossover of the free energy functional to lower dimension, where only the two first terms in the free energy density functional (2.74) reproduce the exact results of hard rods. The dimensional

crossover [5, 56–59] has been introduced as a solution for this failure. The dimensional crossover means that the approximate free energy functionals for higher dimensional (3D) systems contain predictions for free energy functionals for lower dimensional systems (2D and 1D) and vise versa. It played a crucial role in subsequent developments and applications of the FMT. The dimensional reduction from 3D to 2D can be recovered by replacing the z-dependence in the 3D distribution by delta function along this direction ($\rho(x,y,z) = \rho(x,y)\delta(z)$). By the same way the dimensional reduction to 1D can be recovered by taking $\rho(x,y,z) = \rho(x)\delta(y)\delta(z)$. Observing that the third term in the total free energy density functional (2.74) must vanish in this limit, and to produce the exact free energy functional of the 0D cavity (a cavity so narrow that it cannot hold more than one particle), Tarazona enlarged the two fundamental measure by a new tonsorial term which has the following weighted density components [58, 59]

$$\mathcal{T}_{\alpha,\beta}(\mathbf{r}) = \int d\mathbf{r}'\rho(\mathbf{r}+\mathbf{r}')\frac{r'_\alpha r'_\beta}{R^2}\frac{\delta(R-|\mathbf{r}'|)}{4\pi R^2} \tag{2.78}$$

α and β refer to the Cartesian coordinates x, y, z. The unique combination of n, η, $\mathbf{v}$ and $\mathcal{T}$ such that the resulting total free energy density functional recovers the bulk PY direct correlation function and the exact free energy functional in the limit of 0D cavity is given by $\phi_1^{(3D)}$ and $\phi_2^{(3D)}$ with the same form as the original FMT and the third term $\phi_3^{(3D)}$ is given by

$$\phi_3^{(3D)} = 12\pi^2 R^6 \frac{\mathbf{v}.\mathcal{T}.\mathbf{v} - n\mathbf{v}\mathbf{v} - \mathrm{Tr}[\mathcal{T}^3] + n\mathrm{Tr}[\mathcal{T}^2]}{(1-\eta)^2} \tag{2.79}$$

the resulting free energy has very appealing features [59]¨
(i) It reproduces the exact density functional for hard rods with arbitrary 1D distributions of hard spheres.
(ii) It is free from the divergences for any 0D distribution and it reproduces the free energy of the cavity which is given by

$$F[\rho] = \eta + (1-\eta)\ln(1-\eta) \tag{2.80}$$

(iii) It reproduces the PY direct correlation function and compressibility equation of state in the bulk fluid.¨
The original fundamental measure functional can be recovered from the last one by taking an isotropic form for the tensor, $\mathcal{T}_{\alpha,\beta}(\mathbf{r}) \approx \delta_{\alpha,\beta} n(\mathbf{r})$. This explains the good results obtained via the original fundamental measure functional for the planar wall-fluid interface, and its complete failure in describing the hard spheres crystal where the tensor measure is strongly anisotropic.

2.3 Exact DFT in one dimension

Exactly solvable models in one dimension are important tools in the development of DFT. This is due to the fact that they hint the internal structure of the theory and

also that they have been used as a basis to develop approximate methods in higher dimensions. As it is mentioned in sec. 2.2.3, the FMT has its roots partly in the exact free energy functional of Percus. In addition, the semi-empirical weighted density approximation has been motivated by this functional as well [4]. The first exact derivation of free energy functional in one dimension has been presented by Percus for hard rods in arbitrary external potential using the inverse problem approach [106]. The free energy density functional of simple hard rods is known to have the form

$$\Phi_{ex}[\rho] = -n(x)\ln(1-\eta(x)) \tag{2.81}$$

where the weighted densities $n(x)$ and $\eta(x)$ are given respectively by Eqs. (2.67) and (2.68). They have been written as a convolution between the density ρ and some weight functions ω_n and ω_η. This free energy functional has been re-derived by Robledo and Varea [63] using a more simpler approach. They started by writing down an exact free energy functional for lattice hard rods rods of size m and it is given by

$$\beta F[\rho] = \sum_s \{\rho_s(\ln\rho_s + \beta u_s) + (1-t_m)\ln(1-t_m) - (1-t_{m-1})\ln(1-t_{m-1})\} \tag{2.82}$$

where ρ_s and u_s are respectively the density and the external potential at site s and t_m is given by

$$t_m = \sum_{l=0}^{m} \rho_{s-l} \tag{2.83}$$

To obtain the free energy functional for continuum system, they employed the following transformations

$$\frac{1}{N!} \to \prod_s \left(\frac{e}{N}\right)^{\rho_s}, \qquad \text{for large } m \tag{2.84}$$

and

$$\left[1 - \frac{\rho_s}{1-t_m}\right]^{(1-t_m)/\rho_s} \to e, \qquad \text{for large } m \tag{2.85}$$

Inserting in the expression of the lattice free energy functional yields those for continuum space hard rods and it coincides exactly with the Percus's functional.

The inverse problem approach of Percus has been generalized to the case of hard rods mixture by Vanderlick *et al* [109]. Let us summarize their approach. The grand canonical partition function can be written as

$$Z_T = 1 + \langle 1|\omega(I - e\omega)^{-1}|1\rangle \tag{2.86}$$

where ω is a matrix representation of

$$\omega_{\alpha\beta}(x,y) = \omega_\alpha(x)\delta_{\alpha\beta}\delta(x-y) \tag{2.87}$$

where $\omega_\alpha(x) = e^{\beta(\mu_\alpha - u_\alpha(x))}$, α denote the species of particles, μ_α is the chemical potential of particles of type α and u_α is the external potential. e is a matrix representation of

$$e_{\alpha\beta}(x, y) = \theta(x - y - d_{\alpha\beta}) \tag{2.88}$$

in the (α, x) space. $d_{\alpha\beta} = (d_\alpha + d_\beta)/2$, d_α is the diameter of rod of type α. In Eq (2.86), I is the vector $I_\alpha(x) = 1$ and the notation $\langle\rangle$ denotes a sum of the number of particles and integration over coordinates. The density which is defined by

$$\rho_\alpha(x) = \frac{1}{\omega_\alpha(x)} \frac{\delta Z_T}{\delta \omega_\alpha(x)} \tag{2.89}$$

can be written as

$$\rho_\alpha(x) = \frac{\omega_\alpha(x)\hat{Z}_\alpha(x)Z_\alpha(x)}{Z_T} \tag{2.90}$$

where the truncated partition functions satisfy

$$Z_\alpha = 1 + e_\alpha \wedge, \qquad \wedge = \sum_\beta \delta_\beta \omega_\beta Z_\beta \tag{2.91}$$

$$\hat{Z}_\alpha = 1 + \hat{\wedge} e_\alpha, \qquad \hat{\wedge} = \sum_\beta \hat{Z}_\beta \omega_\beta \delta_\beta \tag{2.92}$$

In deriving (2.91) and (2.92), $e_{\alpha\beta}$ has been written as a convolution of two functions as $e_{\alpha\beta}(x, y) = e_\alpha \delta_\beta$ where

$$\begin{aligned} e_\alpha(x, y) &= \theta(x - y - R_\alpha) \\ \delta_\beta(x, y) &= \delta(x - y - R_\beta) \end{aligned} \tag{2.93}$$

R_α is the radius of rods of type α. Some algebra leads to the following equations

$$\begin{aligned} \frac{dZ(x)}{dx} &= \frac{\rho_-(x)}{\hat{Z}(x)} Z_T \\ \frac{d\hat{Z}(x)}{dx} &= \frac{\rho_+(x)}{Z(x)} Z_T \end{aligned} \tag{2.94}$$

where

$$\begin{aligned} \rho_-(x) &= \sum_\beta \rho_\beta(x - R_\beta) \\ \rho_+(x) &= \sum_\beta \rho_\beta(x + R_\beta) \end{aligned} \tag{2.95}$$

and

$$\begin{aligned} Z_\alpha(x) &= Z(x - R_\alpha) \\ \hat{Z}_\alpha(x) &= \hat{Z}(x + R_\alpha) \end{aligned} \tag{2.96}$$

Solving the system of equations (2.96) yields the following expressions for the truncated partition functions

$$\begin{aligned} Z(x) &= \exp\left[\int_{-\infty}^{x} \frac{\rho_-(y)}{1+\int_{-\infty}^{y} dz[\rho_-(z)-\rho_+(z)]} dy\right] \\ \hat{Z}(x) &= Z_T \exp\left[\int_{-\infty}^{x} \frac{-\rho_+(x)}{1+\int_{-\infty}^{y} dz[\rho_-(z)-\rho_+(z)]} dy\right] \end{aligned} \tag{2.97}$$

Inserting (2.97) in the expression (2.89) yields

$$\begin{aligned} \beta(\mu_\alpha - u_\alpha(x)) = \ln\rho_\alpha(x) &- \int_{-\infty}^{x-R_\alpha} \frac{\rho_-(y)}{1+\int_{-\infty}^{y} dz[\rho_-(z)-\rho_+(z)]} dy \\ &+ \int_{-\infty}^{x+R_\alpha} \frac{\rho_+(x)}{1+\int_{-\infty}^{y} dz[\rho_-(z)-\rho_+(z)]} dy \end{aligned} \tag{2.98}$$

and the free energy functional can be integrated from the following expression

$$\mu_\alpha - u_\alpha(x) = \frac{\delta F[\rho]}{\delta\rho_\alpha(x)} \tag{2.99}$$

and it leads to

$$\begin{aligned} \beta F[\rho] = \sum_\alpha \int dx[\rho_\alpha(x)\ln\rho_\alpha(x) - \rho_\alpha(x)] + \int \sum_\alpha \frac{1}{2}\left[\rho_\alpha(y+R_\alpha) + \rho_\alpha(y-R_\alpha)\right] \\ \times \ln\left[1 - \sum_\beta \int_{y-R_\beta}^{y+R_\beta} \rho_\beta(z)dz\right] dy \end{aligned} \tag{2.100}$$

The inverse problem approach has been used also to derive an exact free energy functional for sticky hard rods system [110]. It leads to an exact partition function

$$\begin{aligned} Z_T = \exp \int_{-\infty}^{\infty} \frac{1}{2\gamma} \Bigg\{ \Bigg[1 + 2\gamma \frac{n(x+R)+n(x-R)}{1-\int_{x-R}^{x+R} n(y)dy} \\ + \gamma^2 \left(\frac{n(x+R)-n(x-R)}{1-\int_{x-R}^{x+R} n(y)dy} \right)^2 \Bigg]^{1/2} - 1 \Bigg\} dx \end{aligned} \tag{2.101}$$

The free energy functional can be inferred from the previous partition function and the expression for external potential $u(z)$ as a function of the density. The latter is

given by

$$\beta(\mu - u(z)) = \ln[K(z+d)\tilde{K}(z-d)/n(z)] + \frac{1}{2}\ln\left(1 - \int_{z-d}^{z} n(y)dy\right)\left(1 - \int_{z}^{z+d} n(y)dy\right)$$
$$+ \frac{1}{2\gamma}\int_{z-d}^{z}\frac{1}{2\gamma}\left\{\left[1 + 2\gamma\frac{n(x+d)+n(x)}{1-\int_{x}^{x+d} n(y)dy}\right.\right.$$
$$\left.\left. + \gamma^2\left(\frac{n(x+d)-n(x)}{1-\int_{x}^{x+d} n(y)dy}\right)^2\right]^{1/2} - 1\right\}dx \tag{2.102}$$

where $\tilde{K}(x)$ and $K(x)$ are defined by

$$\tilde{K}(x) = \frac{1}{2\gamma}\left\{\left[\left(1 - \gamma\frac{n(x+d)-n(x)}{1-\int_{x}^{x+d} n(y)dy}\right)^2 + \frac{4n(x+d)\gamma}{1-\int_{x}^{x+d} n(y)dy}\right]^{1/2}\right.$$
$$\left. - \left(1 - \gamma\frac{n(x+d)-n(x)}{1-\int_{x}^{x+d} n(y)dy}\right)\right\} \tag{2.103}$$

$$K(x) = \tilde{K}(x-d) - \frac{n(x)-n(x-d)}{1-\int_{x-d}^{x} n(y)dy} \tag{2.104}$$

$n(x)$ is the density at position x, γ is related to the stickiness of the rod and d is its diameter.

Brannock and Percus [111] have extended the Vanderlick *et al*'s strategy to the case of hard rod mixtures with arbitrary nearest neighbour interactions. In the latter case, the Boltzmann factor e contains an additive term related to the finite range interactions. In this new approach, and based on the Wertheim theory [112, 113], the terms of the grand canonical partition function are reorganized in such a way that the additive term in the inter-particles potential is absorbed in the activity and the new Boltzmann factor is given by a modified step function. This transformation maps the hard rod mixtures with arbitrary nearest neighbour interactions to a pure hard rod mixtures. This mapping can be reached by collecting the particles into a blocks of any numbers of particles and rewrite the grand canonical partition function in terms of blocks of particles rather than a single particles. Within this method an exact expression for the free energy functional of a mixtures of hard rod with sticky and square well potential has been derived with closure relations for the weighted densities. The same approach has been extended by Percus [114] and Tutschka and Cuesta [115] to hard rods with next nearest neighbour interactions where applications are made to the sticky core interactions.

Chapter 3

Lattice density functional theory

3.1 Overview of LDFT

Despite the success of continuum classical DFT in applications to a wide varieties of systems, there are still many systems where the description in terms of discrete molecular configuration is more appropriate. These include the ordering phenomena in metallic alloys, submonolayer adsorbate systems, glasses [46], and fluids in porous media [116].

Based on this necessity, the DFT has been formulated for lattice systems [45, 60–65, 67, 68, 117–121]. For a system at temperature T, chemical potential μ, and external potential u_i, the free energy functional is known to have the form [45]

$$\Omega[\rho] = F[\rho] + \sum_i (u_i - \mu)\rho_i \tag{3.1}$$

where ρ_i is the density at site i. The first term on the rhs of (3.1), which is known to be universal (independent of the external potential), can be written as

$$F[\rho] = F_{id}[\rho] + F_{ex}[\rho] \tag{3.2}$$

$F_{id}[\rho]$ is the ideal gas part and $F_{ex}[\rho]$ is the excess part. The later one includes the inter-particles interactions. The equilibrium density profiles can be obtained from the minimization principle which reads

$$\frac{\delta F[\rho]}{\delta \rho_i} = \mu - u_i \tag{3.3}$$

The n-points direct correlation function is the n-th derivative of the excess free energy functional with respect to the density

$$c^{(n)}_{i_1 \ldots i_n} = \frac{\delta^n F_{ex}[\rho]}{\delta\rho_{i_1} \ldots \delta\rho_{i_n}} \tag{3.4}$$

A closer relation between the direct correlation function and the pair correlation function $h_{i,j}$ is given by the discrete Ornstein-Zernicke equation [52]

$$h_{i,j} = c_{i,j} + \sum_k c_{i,k}\rho_k h_{k,j} \tag{3.5}$$

where $c_{i,j}$ is related to the two-point direct correlation function by

$$c_{i,j} = c^{(2)}_{i,j} - \frac{\delta_{i,j}}{1-\rho_i} \tag{3.6}$$

The radial distribution function is given by

$$g_{i,j} = h_{i,j} - 1 \tag{3.7}$$

In analogy to the continuum DFT, the aim of LDFT is to find exact or approximate methods to calculate the excess free energy functionals. In one dimension, various exact methods have been constructed to set up a free energy functionals. These methods include the Robledo-Varea approach, the Markov chain, and the lattice fundamental measure theory (LFMT).

3.2 Robledo and Varea approach

The first derivation of the exact free energy functional of hard rods on a lattice has been reported by Robledo and Varea [63]. Their approach is based on the observation that for a uniform ideal lattice gas of N particles on a one dimensional lattice of L sites, the probability for any configuration to happen is given by

$$\chi[\rho] = \frac{1}{N!}\rho^N(1-\rho)^{L-N} = \frac{1}{N!}\left[\rho^\rho(1-\rho)^{1-\rho}\right]^L \tag{3.8}$$

which for a nonuniform lattice gas becomes

$$\chi[\rho] = \frac{1}{N!}\prod_{s=0}^{L-1}\rho_s^{\rho_s}(1-\rho_s)^{1-\rho_s} \tag{3.9}$$

For particles with size l and due to the $l-th$ neighbour exclusion, Eq. (3.9) becomes

$$\chi[\rho] = \frac{1}{N!}\prod_{0}^{L-1}\rho_s^{\rho_s}\frac{(1-t_l)^{1-t_l}}{(1-t_{l-1})^{1-t_{l-1}}} \tag{3.10}$$

where

$$t_l = \sum_{l=0}^{l}\rho_{s-l} \tag{3.11}$$

The free energy functional inferred from Eq. (3.10) is

$$\beta F[\rho] = \sum_s\Big[\rho_s(\ln\rho_s + \beta u_s) + (1-t_l)\ln(1-t_l) - (1-t_{l-1})\ln(1-t_{l-1})\Big] \tag{3.12}$$

where u_s is the external potential at site s and $\beta = 1/k_BT$ is the inverse temperature.

3.3 Markov chain approach

Buschle *et al* [64, 65] have been derived an exact free energy functional for lattice hard rods system using the Markov chain approach. To summarize their derivation, let us consider a system of N hard rods of length l in the presence of an external potential. The rods are located on a one-dimensional lattice with L sites. The lattice is defined in such a way that the ends of the rods coincide with lattice sites. A set of occupation numbers n_j, $j = 1, \ldots, L$, are introduced to specify the microstates of the system. If the left end of a rod is at site j then $n_j = 1$, while $n_j = 0$ otherwise. The mutual exclusion of hard rods implies the constraint $n_k n_j = 0$ for $j = k, \ldots, k + l - 1$. In a grand canonical description the chemical potentials μ specify the mean numbers of rods. A fixed boundary conditions are considered here where site 0 and $L + 1$ are supposed to be occupied by a rod. Here we assume that $\beta = 1/k_B T = 1$ where T is the temperature and k_B is the Boltzmann constant. The joint probabilities $\chi(n_1, \ldots, n_L)$ of the microstates can be decomposed as

$$\chi(n_1, \ldots, n_L) = \prod_{j=1}^{L} \psi(n_k | n_{k-1}, \ldots, n_1) \tag{3.13}$$

where $\psi(.|\ldots)$ denotes the corresponding conditional probabilities. By using the Boltzmann expression for the joint probabilities of microstates in the grand canonical ensemble, Buschle *et al* proved that the conditional probabilities satisfy the following Markov property

$$\psi(n_k | n_{k-1}, \ldots, n_1) = \psi(n_k | n_{k-1}, \ldots, n_{k-l+1}) \tag{3.14}$$

The previous equation results from the hard core exclusion and the rhs denotes the probability to observe occupation number n_k at site k given that $\{n_j | k - l + 1 \leq j \leq k - 1\}$ are given. The conditional probabilities $\psi(n_k | n_{k-1}, \ldots, n_{k-l+1})$ can be calculated based only on constraint of mutual exclusion between rods. We have

$$\psi(n_k | n_{k-1}, \ldots, n_{k-l+1}) = \frac{\phi(n_k, \ldots, n_{k-l+1})}{\phi(n_{k-1}, \ldots, n_{k-l+1})} \tag{3.15}$$

where $\phi(.)$ denotes joint probabilities which can be calculated as following: By definition, the mean occupation at site i, $\rho_i = \langle n_i \rangle$ is given by

$$\begin{aligned} \rho_i &= \sum_{\mathbf{n}} n_i \phi(n_k, \ldots, n_{k-l+1}) \\ &= \phi(0_k, \ldots, 0_{i+1}, 1_i, 0_{i-1}, \ldots, 0_{k-l+1}) \end{aligned} \tag{3.16}$$

and we further have from the normalization condition

$$\phi(0_k, \ldots, 0_{k-l+1}) + \sum_{i=k-l+1}^{k} \rho_i = 1 \tag{3.17}$$

From Eqs (3.16) and (3.17) we get

$$\psi(n_k|0_{k-1},\ldots,0_{k-l+1}) = \begin{cases} \dfrac{\rho_k}{1-\sum\limits_{j=k-l+1}^{k-1}\rho_j} & \text{for } n_k = 1 \\ \dfrac{1-\sum\limits_{j=k-l+1}^{k}\rho_j}{1-\sum\limits_{j=k-l+1}^{k-1}\rho_j} & \text{for } n_k = 0 \end{cases} \tag{3.18}$$

The total conditional probabilities are given by

$$\psi(n_k|n_{k-1},\ldots,n_{k-l+1}) = \rho_k^{n_k}\frac{\left[1-\sum\limits_{j=k-l+1}^{k}\rho_j\right]^{(1-\sum\limits_{j=k-l+1}^{k}n_j)}}{\left[1-\sum\limits_{j=k-l+1}^{k-1}\rho_j\right]^{(1-\sum\limits_{j=k-l+1}^{k-1}n_j)}} \tag{3.19}$$

Inserting the total conditional probabilities (3.19) in Eq (3.13) we get an exact expression for the joint probability distributions.

Based on the Gibbs-Bogoliubov inequality the density functional for N hard rods in an external potential $U(\mathbf{n}) = \sum_k u_k n_k$ is defined as

$$\begin{aligned}\Omega[\rho] &= \sum_{\mathbf{n}}\chi_\rho(\mathbf{n})\left[k_\mathrm{B}T\log\chi_\rho(\mathbf{n}) + U(\mathbf{n}) - \mu N\right] \\ &= F[\rho] + \sum_{k=1}^{L}(u_k-\mu)\rho_k \end{aligned} \tag{3.20}$$

where $F[\rho] = k_\mathrm{B}T\sum_{\mathbf{n}}\chi_\rho(\mathbf{n})\log\chi_\rho$ is the free energy functional.
Inserting the expression of the joint probability distributions in Eq (3.20), we get an exact expression for the free energy functional,

$$\begin{aligned}\Omega[\rho] = \sum_{k=1}^{L}\Bigg\{&\rho_k\ln\rho_k + (1-\sum_{j=k-l+1}^{k}\rho_j)\ln(1-\sum_{j=k-l+1}^{k}\rho_j) \\ &-(1-\sum_{j=k-l+1}^{k-1}\rho_j)\ln(1-\sum_{j=k-l+1}^{k-1}\rho_j) + \beta(u_k-\mu)\rho_k\Bigg\}\end{aligned} \tag{3.21}$$

The previous expression coincides exactly with the earlier result of Robledo and Varea [63].

3.4 Lattice fundamental measure theory

3.4.1 Free energy functional of hard rod mixtures

Despite its successful applications to continuum systems [5,55–59], the FMT stays for longer time away from application to lattice systems. The challenge is that the

simple recipe for constructing the free energy functionals for continuum systems is not directly transferable to the discrete case. The reason for that on one hand is that there is no equivalent to the SPT for lattice systems and on the other hand the decomposition of the discrete Mayer function is not unique which precludes a definition of the weight functions [60, 61].

In 2002, Lafuente and Cuesta have succeeded to extend the fundamental measure theory to lattice systems by constructing an exact free energy functional for hard rod mixtures in one dimension [60, 61]. The derivation is based on the approach suggested by Vanderlick *et al* [109], explained in Chap. (2). The resulting free energy functional has the same form as the fundamental measure functionals, and this makes it possible to extend the free energy functional to higher dimensions. Within this construction, it was possible to set up a lattice version for the cavity theory and hence makes the dimensional reduction possible as well. This theory permits to construct free energy functionals for hard cubes and hard squares form free energy functional of hard hypercubes in d dimensions.

To briefly review the basic idea behind the LFMT, let us consider a hard rod mixtures on a one dimensional lattice. The inter-particles potential between rod of type α at site i, and rod of type β at site j is given by

$$v_{\alpha\beta}(i,j) = \begin{cases} \infty & \text{when } |i-j| < \sigma_{\alpha\beta} \\ 0 & \text{when } |i-j| \geq \sigma_{\alpha\beta} \end{cases} \tag{3.22}$$

where $\sigma_{\alpha\beta} = (l_\alpha + l_\beta)/2$, l_α is the length of rod of type α. The grand canonical partition function can be written as

$$Z_T = 1 + \sum_{N=1}^{\infty} \mathrm{Tr}\left[\omega_{\alpha_1(s_1)} \prod_{i=1}^{N-1} e_{\alpha_i\alpha_{i+1}}(s_i, s_{i+1})\omega_{\alpha_{i+1}}(s_{i+1})\right] \tag{3.23}$$

where the trace denotes a summation over all positions and all species of the rods. The Mayer function $e_{\alpha\beta}(i,j) = \theta(i-j-\sigma_{\alpha\beta})$, and $\omega_{\alpha\beta}(i,j) = \omega_\alpha(i)\delta_{\alpha\beta}\delta_{ij}$ are represented here as a matrices in the (α, s) space. The density of rods of species α can be written as

$$\begin{aligned} \rho_\alpha(i) &= \frac{\omega_\alpha(i)}{Z_T}\frac{\delta Z_T}{\delta\omega_\alpha(i)} \\ &= \frac{\hat{Z}_\alpha(i)\omega_\alpha(i)Z_\alpha(i)}{Z} \end{aligned} \tag{3.24}$$

where the left and right truncated partition functions are defined by

$$\begin{aligned} Z_\alpha(i) &= 1 + \sum_{(\beta,j)} (e\omega)_{\alpha\beta}(i,j)Z_\beta(j) \\ \hat{Z}_\alpha(i) &= 1 + \sum_{(\beta,j)} \hat{Z}_\beta(j)(\omega e)_{\beta\alpha}(j,i) \end{aligned} \tag{3.25}$$

As noted by Lafuente and Cuesta, the system of equations (3.25) can be solved exactly only if the Boltzmann factor has rank one. Depending on this observation,

two cases arise for lattice systems. The additive case, where all the rods have an even or an odd diameters. In this case the Boltzmann factor has rank one and the system can be solved exactly. The second is the non-additive case where some of the rods have an even diameters and others have odd diameters. In the latter case the Boltzmann factor is not of rank one, nevertheless, Lafuente and Cuesta could calculate the free energy functional in the non-additive case by mapping the additive mixtures to non-additive mixtures [60]. First consider the additive mixtures, where the rods diameters can be written as: $l_\alpha = 2a_\alpha + \epsilon$ with $a_\alpha \in N$ and $\epsilon = 0, 1$.

Let us write the Mayer function as a convolution of two functions $e_{\alpha\beta}(i, j) = e_\alpha * \delta_\beta(i - j)$, where

$$\begin{aligned} e_\alpha(i) &= \theta(i - a_\alpha - \epsilon) \\ \delta_\alpha(s) &= \delta(s - a_\alpha) \end{aligned} \tag{3.26}$$

Because $e_\alpha(i + a_\alpha) = \theta(i - \epsilon)$ (independent of α), we define

$$\begin{aligned} Z(i) &= Z_\alpha(i + a_\alpha) \\ \hat{Z}(i) &= \hat{Z}_\alpha(i - a_\alpha) \end{aligned} \tag{3.27}$$

$$\rho^{\pm}(i) = \sum_\alpha \rho_\alpha(i \pm a_\alpha) \tag{3.28}$$

Inserting Eqs (3.27) and (3.28) in Z_α at $i + a_\alpha$ and $\hat{Z}_\alpha$ at $i - a_\alpha$ we find

$$\begin{aligned} Z(i) &= 1 + Z_T \sum_{r=-\infty}^{i-\epsilon} \frac{\rho^-(r)}{\hat{Z}(r)} \\ \hat{Z}(i) &= 1 + Z_T \sum_{r=i+\epsilon}^{\infty} \frac{\rho^+(r)}{Z(r)} \end{aligned} \tag{3.29}$$

Applying the discrete differential operator on the two Eqs (3.29), we get

$$\begin{aligned} \Delta Z(i) &= Z_T \frac{\rho^-(i + 1 - \epsilon)}{\hat{Z}(i + 1 - \epsilon)} \\ \Delta \hat{Z}(i) &= Z_T \frac{\rho^+(i + \epsilon)}{Z(i + \epsilon)} \end{aligned} \tag{3.30}$$

using the discrete Leibniz rule for the discrete differential operator $\Delta(fg)(i) = f(i+1)\Delta g(i) + g(i + 1)\Delta f(i)$, the two Eqs (3.30) reduce to

$$\Delta(Z\hat{Z})(i) = Z_T \left\{\rho^-(i + 1 - \epsilon) - \rho^+(i + \epsilon)\right\} \tag{3.31}$$

With the following boundary conditions

$$\begin{aligned} Z_\alpha(\mp\infty) &= Z_T \\ \hat{Z}_\alpha(\pm\infty) &= 1 \end{aligned} \tag{3.32}$$

the solution of (3.32) can be written as

$$Z(i)\hat{Z}(i) = Z_T \left\{ 1 - \sum_{\alpha} \sum_{r=i-a_\alpha+1-\epsilon}^{i+a_\alpha-1+\epsilon} \rho_\alpha(r) \right\} \tag{3.33}$$

Eq (3.33) permits to decouple the system of equations (3.30), and the final results are

$$\begin{aligned} \frac{Z(i)}{Z_T} &= (1 - n^{(0)}(i-\epsilon)) \prod_{r=i-\epsilon}^{\infty} \frac{1-n^{(1)}(r)}{1-n^{(0)}(r)} \\ \hat{Z}(i) &= \prod_{r=i}^{\infty} \frac{1-n^{(1)}(r)}{1-n^{(0)}(r)} \end{aligned} \tag{3.34}$$

where Lafuente and Cuesta introduced the weighted densities $n^{(k)}(i) = \sum_{\alpha} w_\alpha^{(k)} * \rho_\alpha(i)$ and the weight functions $w_\alpha^{(k)}$ are given by

$$w_\alpha^{(k)} = \begin{cases} 1 & \text{if } -a_\alpha - k - \epsilon < i < a_\alpha \\ 0 & \text{else} \end{cases} \tag{3.35}$$

form Eq (3.32) and (3.34) , the total partition function is given by

$$Z_T = \prod_{r=-\infty}^{\infty} \frac{1-n^{(1)}(r)}{1-n^{(0)}(r)} \tag{3.36}$$

Z_T and $\omega_\alpha(i)$ determine the free energy functional. It is given by

$$\beta F[\rho_\alpha] = \beta F_{id}[\rho_\alpha] + \sum_i \Big[\Phi_0(n^{(1)}(i)) - \Phi_0(n^{(0)}(i)) \Big] \tag{3.37}$$

F_{id} is the ideal gas part and the second term represents the excess part which is due to the inter-particles interactions. Φ_0 has the form

$$\Phi_0(n^{(k)}(i)) = n^{(k)}(i) + (1 - n^{(k)}(i)) \ln(1 - n^{(k)}(i)) \tag{3.38}$$

Comparing with its continuum counterpart, $\Phi_0(\eta)$ represents the excess free energy functional for a zero-dimensional cavity and η represents the mean occupancy of the cavity.

The free energy functional of the non additive hard rod mixtures can be derived from the additive one by mapping the former to the latter using $\hat{l}_\alpha = 2l_\alpha$, and the positions of the rods are restricted to lie on the even sites of the lattice (by imposing $\rho_\alpha(i) = 0$ if $i = 2r + 1$ with $r \in \mathbb{Z}$). This yields the following expression for excess free energy functional

$$F_{ex}[\rho_\alpha] = \sum_{i \in Z} \Big[\Phi_0(n_1^{(1)}(i) + \Phi_0(n_0^{(1)}(i)) - \Phi_0(n_0^{(0)}(i)) - \Phi_0(n_0^{(1)}(i)) \Big] \tag{3.39}$$

The zero-dimensional excess free energy functional has the same form as for the additive case. The weighted densities are defined by

$$n_j^{(k)}(i) = \sum_\alpha w_{j,\alpha}^{(k)} * \rho_\alpha(i) \tag{3.40}$$

where $l, k = 0, 1$, and the weight functions are given by

$$w_{j,\alpha}^{(k)}(i) = \begin{cases} w_\alpha^{(j+k(1-j))}(i) & \text{if } l_\alpha \text{ is even} \\ w_\alpha^{(1-j+kj)}(i) & \text{if } l_\alpha \text{ is odd} \end{cases} \tag{3.41}$$

The form in which the free energy functional has been written makes it possible to extend to approximate functional in d dimensions. The quality of this functional has been tested by making a dimensional reduction of the d-dimensional density functional to density functionals of hard cubes, hard squares, and hard hexagons [67, 68].

3.4.2 Dimensional crossover and Cavity theory

As for the continuum FMT, an alternative way to construct the functional in any dimension is the zero-dimensional cavity theory. This important feature states that once we have the exact free energy functional in one dimension, approximate free energy functionals can be constructed in higher dimensions using the dimensional crossover. The inverse transformation called the dimensional reduction is possible as well. This means exact free energy functionals in zero and one dimension can be constructed from the knowledge of the approximate functionals in higher dimensions (if they have the fundamental measure forms). A general diagrammatic procedure for the dimensional crossover on a lattice has been worked out by Lafuente and Cuetsa [62]. Their procedure consists of (i) Identifying the set of all 0D maximum cavities, which are 0D cavities enlarged by one site stop being a 0D cavities. (ii) Write an ansatz for the excess free energy functional as a sum over all excess free energies of the maximum cavities. (iii) Imposing a dimensional reduction to these free energy functional (which is equivalent to inserting the corresponding 0D density profile of any of the maximum cavities in the free energy functional) must yield the exact excess free energy of the 0D cavity. If not, the free energy functional in (i) are not the true one and spurious terms must be appeared in the dimensional reduction. (iv) Eliminating the spurious terms by adding to the free energy functional a new terms correspond to the non maximum cavities. To make ideas clear, let us consider the case of non-additive hard rod mixtures of size $l_1 = 2$ and $l_2 = 3$ [70].

Non-additive hard rod mixtures

Let us consider a mixture of hard rods of size 2 and 3. In this case, because both even and odd diameters are present, two kind of maximum cavities are present and

this can be explained in the following. The weight functions for rods of size $l_1 = 2$ are given by

$$w_1^{(1)}(s) = \begin{cases} 1 & \text{for } -2 < s < 1 \\ 0 & \text{else} \end{cases} \qquad w_1^{(0)}(s) = \begin{cases} 1 & \text{for } -2 < s < 1 \\ 0 & \text{else} \end{cases}$$
$$w_0^{(1)}(s) = \begin{cases} 1 & \text{for } -2 < s < 1 \\ 0 & \text{else} \end{cases} \qquad w_0^{(0)}(s) = \begin{cases} 1 & \text{for } -1 < s < 1 \\ 0 & \text{else} \end{cases} \tag{3.42}$$

and for rods of size $l_2 = 3$,

$$w_1^{(1)}(s) = \begin{cases} 1 & \text{for } -3 < s < 1 \\ 0 & \text{else} \end{cases} \qquad w_1^{(0)}(s) = \begin{cases} 1 & \text{for } -2 < s < 2 \\ 0 & \text{else} \end{cases}$$
$$w_0^{(1)}(s) = \begin{cases} 1 & \text{for } -2 < s < 1 \\ 0 & \text{else} \end{cases} \qquad w_0^{(0)}(s) = \begin{cases} 1 & \text{for } -2 < s < 2 \\ 0 & \text{else} \end{cases} \tag{3.43}$$

The maximum cavity for rods of size 2 is the set of the connected points $-2 < s < 1$ and for rods of size 3 is the set of the connected points $-3 < s < 1$. The two maximum cavities are shown graphically in Fig (3.1).

Merging the two diagrams, we find the set of all possible maximum cavities for

Figure 3.1: Maximum cavities for rods of size $l_1 = 2$ (left), and $l_2 = 3$ (right).

the mixtures which are shown in Fig (3.2).

Figure 3.2: Set of all possible maximum cavities for a mixture of hard rods of size 2 and 3.

Lafuente and Cuesta chose the following notation for the set of maximum cavities

$$C_{max} = \{\overset{s}{\bullet}\!\!-\!\!\bullet\!\!-\!\!\circ, \overset{s}{\circ}\!\!-\!\!\bullet\!\!-\!\!\bullet \mid s \in \mathbb{Z}\} \tag{3.44}$$

The weighted densities corresponding to a maximum cavity can be calculated by placing the maximum cavity at all possible points of the 0D density profiles and choose only densities which result from the overlapping between the points of the maximum cavity and those of 0D density profiles, then add them up and this is

exactly the effect of convolution. A first ansatz for the free energy functional is the following

$$F_{ex1}[\rho_\alpha] = \sum_{s\in Z}\Big[\Phi_0(\overset{s}{\bullet}\!\!-\!\!\bullet\!\!-\!\!\circ) + \Phi_0(\overset{s}{\circ}\!\!-\!\!\bullet\!\!-\!\!\bullet)\Big] \tag{3.45}$$

If we choose ($\eta = \overset{s}{\bullet}\!\!-\!\!\bullet\!\!-\!\!\circ$) as a 0D density profiles (the second choice leads exactly to the same result), the exact dimensional reduction of the free energy functional with respect to this 0D density must lead to excess free energy functional of this cavity $\Phi_0(\bullet\!\!-\!\!\overset{S}{\bullet}\!\!-\!\!\circ)$. Taking the dimensional reduction of the expression (3.45), we find

$$\begin{aligned} F_{ex1}[\rho_{\bullet\!-\!\overset{S}{\bullet}\!-\!\circ}] = \sum_{s\in Z}\Big[&\Phi_0(\bullet\!\!-\!\!\overset{S}{\bullet}\!\!-\!\!\circ) + \Phi_0(\circ\!\!-\!\!\overset{S}{\bullet}\!\!-\!\!\circ) + \Phi_0(\bullet\!\!-\!\!\overset{S}{\circ}) + \Phi_0(\overset{S}{\bullet}\!\!-\!\!\circ) \\ &+\Phi_0(\bullet\!\!-\!\!\overset{S}{\bullet}) + \Phi_0(\overset{S}{\circ}\!\!-\!\!\circ) + \Phi_0(\overset{S-1}{\bullet}) + \Phi_0(\overset{S-1}{\circ}) + 2\Phi_0(\overset{S+1}{\circ})\Big] \end{aligned} \tag{3.46}$$

which doesn't coincide with the exact 0D excess free energy functional. It contains some spurious terms which can be eliminated by adding (or extracting) new terms correspond to a non-maximum cavities, $\circ\!\!-\!\!\overset{S}{\bullet}\!\!-\!\!\circ$ and $\overset{S}{\bullet}\!\!-\!\!\bullet$. This leads to the following expression for the final free energy

$$F_{ex}[\rho] = \sum_{s\in Z}\Big[\Phi_0(\overset{s}{\bullet}\!\!-\!\!\bullet\!\!-\!\!\circ) + \Phi_0(\overset{s}{\circ}\!\!-\!\!\bullet\!\!-\!\!\bullet) - \Phi_0(\circ\!\!-\!\!\overset{S}{\bullet}\!\!-\!\!\circ) - \Phi_0(\overset{S}{\bullet}\!\!-\!\!\bullet)\Big] \tag{3.47}$$

Given that

$$\begin{aligned} n_1^{(1)}(s) &= \overset{s}{\bullet}\!\!-\!\!\bullet\!\!-\!\!\circ = \rho_1(s) + \rho_1(s+1) + \rho_2(s) + \rho_2(s+1) + \rho_2(s+2) \\ n_0^{(1)}(s) &= \overset{s}{\circ}\!\!-\!\!\bullet\!\!-\!\!\bullet = \rho_1(s) + \rho_1(s+2) + \rho_2(s) + \rho_2(s+1) + \rho_2(s+2) \\ n_0^{(0)}(s) &= \circ\!\!-\!\!\overset{S}{\bullet}\!\!-\!\!\circ = rho_1(s+2) + \rho_2(s) + \rho_2(s+1) + \rho_2(s+2) \\ n_0^{(1)}(s) &= \overset{S}{\bullet}\!\!-\!\!\bullet = \rho_1(s) + \rho_1(s+1) + \rho_2(s) + \rho_2(s+1) \end{aligned} \tag{3.48}$$

The expression (3.47) for the free energy functional coincides exactly with those derived previously within the inverse problem approach of Percus.

Hard squares with nearest neighbour interactions on a lattice

As a second example for the dimensional reduction, let us consider another cases, (*i*) hard squares of length $a = 1$ with contact interactions, (*ii*) hard squares of length $a = 2$ and contact interactions. The first case (*i*) is equivalent to standard lattice gas or Ising model with nearest neighbour interactions. The set of all maximum cavities is

$$C_{max} = \left\{\overset{S}{\circ}, \overset{S}{\circ}\!\!-\!\!\circ, \begin{array}{c}{\scriptstyle S}\circ\\ \circ\end{array}\right\} \tag{3.49}$$

where the first diagram represents the 1-particle 0D cavity. The second and the third diagrams represent the 2-particles 0D cavities. The latter contains the horizontal and vertical interactions. The corresponding 0D density profiles of the 0D cavities have these forms

$$\rho_C = \left\{\overset{t}{\bullet}, \overset{t}{\bullet}\!\!-\!\!\bullet, \begin{array}{c}{\scriptstyle t}\bullet\\ \bullet\end{array}\right\} \tag{3.50}$$

It is not difficult to prove that in 2 dimensions, the only combination which reduces to the 0D excess free energy functional under the dimensional reduction with respect to any 0D density profiles is

$$F_{ex}[\rho] = \sum_{s}\Big[\Phi_0(\text{}) + \Phi_0(\text{}) - 3\Phi_0(\text{})\Big] \tag{3.51}$$

In arbitrary dimension, the free energy functional of hard squares of length $a = 1$ have the form (see also [70])

$$F_{ex}[\rho] = \sum_{\text{all nn}\{\mathbf{s},\mathbf{t}\}} F_{\{\mathbf{s},\mathbf{t}\}}[\rho] - \sum_{\mathbf{s}}(q(\mathbf{s}) - 1)F_{\{\mathbf{s}\}}[\rho] \tag{3.52}$$

where the first term is the contribution the 2-particle maximum cavity and the second term is the contribution the 1-particles maximum cavity [70]. $q(s)$ is the coordination number at site $\mathbf{s}$.

In the second case (*ii*), the set of maximum 0D cavities is

$$\rho_C = \left\{\text{ 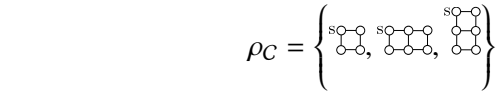 }\right\} \tag{3.53}$$

Where s in this case refers to a two dimensional vector. The first diagram represents the 1-particle 0D cavity and the last two diagrams represent the 2-particle 0D cavities. The latter includes the contact interactions of the hard square with its horizontal and vertical nearest neighbour hard squares. Making use of the dimensional reduction with respect to any density profiles which are outside the 0D cavity yields the following 2D free energy functional

$$F_{exc}[\rho] = \sum_{s}\Big[\Phi_0(\text{}) + \Phi_0(\text{}) - 3\Phi_0(\text{}) + \Phi_0(\text{})\Big] \tag{3.54}$$

The last term represents the contribution of non-maximum cavity. The dimensional reductions of the different terms $F^i_{exc}, i = 1, 2, 3, 4$ in (3.54) with respect to the 0D density profiles of the 1-particle maximum cavity are

$$\begin{aligned} F^1_{exc}[\rho_{\text{}}] =& 2\Phi_0(\text{}) + \Phi_0(\text{}) + \Phi_0(\text{}) + 2\Phi_0(\text{}) + 2\Phi_0(\text{}) \\ &+ \Phi_0(\text{}) + \Phi_0(\text{}) + \Phi_0(\text{}) + \Phi_0(\text{}) \end{aligned} \tag{3.55}$$

$$\begin{aligned} F^2_{exc}[\rho_{\text{}}] =& 2\Phi_0(\text{}) + 2\Phi_0(\text{}) + 2\Phi_0(\text{}) + \Phi_0(\text{}) + \Phi_0(\text{}) \\ &+ \Phi_0(\text{}) + \Phi_0(\text{}) + \Phi_0(\text{}) + \Phi_0(\text{}) \end{aligned} \tag{3.56}$$

$$\begin{aligned} F^3_{exc}[\rho_{\text{}}] =& \Phi_0(\text{}) + \Phi_0(\text{}) + \Phi_0(\text{}) + \Phi_0(\text{}) + \Phi_0(\text{}) \\ &+ \Phi_0(\text{}) + \Phi_0(\text{}) + \Phi_0(\text{}) + \Phi_0(\text{}) \end{aligned} \tag{3.57}$$

$$F^4_{exc}[\rho_{\text{}}] = \Phi_0(\text{}) + \Phi_0(\text{}) + \Phi_0(\text{}) + \Phi_0(\text{}) \tag{3.58}$$

Inserting Eqs. (3.55)-(3.58), in (3.54), the functional reduces neatly to the 0D excess free energy functional.

3.5 Lattice Time Dependent Density Functional Theory

The LTDFT has been developed to account for the dynamics of structure formation and phase transitions in condensed matter systems [45, 49–54, 117, 118, 122]. It is based on the local equilibrium approximation in which the non-equilibrium distribution function is expressed by the Boltzmann distribution with a time dependent external potential. The kinetic equations resulting from this ansatz are nonlinear and yield a significant improvement over ordinary mean field approaches. The theory has been successfully used to kinetics of ordering transitions and time evolution of density profiles in Ising and Potts models [51] as well as the asymmetric exclusion process of interacting stochastic lattice gas [53, 54] and the results were in good agreements with kinetic Monte Carlo simulations. We briefly review the basic idea behind the LTDFT.

Consider a lattice system defined by the Hamiltonian

$$\mathcal{H} = \sum_{i<j} v_{i,j} n_i n_j + \sum_i u_i n_i \tag{3.59}$$

where n_i, $v_{i,j}$ and u_i are the occupation number, the inter-particle interactions and the external potential respectively. The dynamics of this system are defined by the master equation, which describes the time evolution of the probability of any configuration of the system. It reads

$$\frac{dP_i(t)}{dt} = \sum_{j\neq i} \Big[w_{i,j} P_j(t) - w_{j,i} P_j \Big] \tag{3.60}$$

$P_i(t) = P(C_i, t)$ refers to the probability to find the system in a configuration C_i at time t, and $w_{i,j}$ is the transition rate from C_j to C_i. These rates satisfy the so called detailed balance condition,

$$w_{i,j} e^{-\beta \mathcal{H}_j} = w_{j,i} e^{-\beta \mathcal{H}_i} \tag{3.61}$$

$\mathcal{H}_j$ is the energy of configuration C_j and $\beta = 1/k_B T$ is the inverse of temperature. The continuity equation inferred from the master equation reads

$$\frac{d\rho_i(t)}{dt} = \sum_j \langle J_{i,j} \rangle \tag{3.62}$$

where $\rho_i(t)$ here represents the density at site i and at time t, $J_{i,j}$ is the current in the bond $i - j$. $\langle \ldots \rangle$ denotes to the mean with respect to the distribution $P_i(t)$ and the sum include all nearest neighbour sites. The probability distributions can be approximated as

$$P_i(t) = \frac{1}{Z(t)} \exp\left[-\beta \Big(\mathcal{H} - \sum_i h_i(t) n_i - \mu N \Big) \right] \tag{3.63}$$

it describes the equilibrium probability distributions in the presence of a time dependent external potential which needs to be determined self-consistently as follows: The equilibrium grand canonical free energy functional is given by

$$\Omega[\rho] = F[\rho] + \sum_i (u_i - \mu)\rho_i \tag{3.64}$$

Minimizing the grand canonical free energy functional, we find

$$\mu = \frac{\delta F[\rho]}{\delta \rho_i} + u_i + h_i(t) \tag{3.65}$$

Using the fact that the free energy functional $F[\rho]$ is a sum of two contributions, the ideal gas term and the excess term, we get

$$\rho_i(t) = \frac{1}{1 + e^{\beta(u_i - \mu + h_i(t)) - c_i^{(1)}[\rho(t)]}} \tag{3.66}$$

where the 1-point direct correlation function is given by

$$c_i^{(1)}[\rho(t)] = \frac{\delta F_{ex}[\rho]}{\delta \rho_i} \tag{3.67}$$

To evaluate the expression (3.66), we need to know $c_i^{(1)}[\rho(t)]$ in term of the density. For cases where the excess free energy functionals are not explicitly known, this can done by expanding $c_i^{(1)}[\rho(t)]$ as a Taylor series, and truncating the series to its leading terms

$$c_i^{(1)}[\rho(t)] = c_i^{(1)}(\bar{\rho}) + \sum_j c_{i-j}(\rho_j - \bar{\rho}) \tag{3.68}$$

where $\bar{\rho}$ is the density of the uniform system considered as a reference system and c_{i-j} is the two-point direct correlation function of the reference system. Solving eq (3.66) yields a relation for $h_i(t)$ as a functional of the density. Inserting it in (3.60) yields an expression for the non-equilibrium joint probability distributions.

The current from site i to site $i + 1$ is given by

$$J_{i,i+1} = \langle n_i(1 - n_{i+1}) w_{i,i+1} \rangle \tag{3.69}$$

$w_{i,i+1}$ is the transition rate from site i to site $i + 1$. The expression for the current involves n-point correlators which can be decomposed in terms of two-point correlator. In the case that the latter is known, we can use the local equilibrium approximation which states that equilibrium two-point correlator is still valid locally in time for non-equilibrium system. This allows to find an approximate expression for the current as a functional of the density. Inserting the latter in the continuity equation and solving it leads the density profiles of the system. The LTDFT has been used to study kinetics of lattice gas and Ising model and also the kinetics of lattice gas in contact with a wall and it has been extended to systems with internal degree of freedom [52]. Recently it has been applied to the totally asymmetric exclusion process of interacting particles [53, 54]. The results were in good agreements with kinetic Monte Carlo, and this has shown the power of the method for studying the kinetics phase transformations.

Chapter 4

Exact density functional of hard rod mixtures

4.1 Introduction

The extension of density functional theory from continuum to lattice fluids [117] has proven to be useful for treating problems like ordering transitions [117, 118], properties of interfaces separating different phases [119,120,122], phase separation in mixtures [121], or polymer adsorption at solid-liquid interfaces [123]. Time-dependent density functional theory [49] furthermore allows one to describe the kinetics of lattice fluids [45], as emerging in phase ordering phenomena [50], relaxation processes [52], and particle transport in driven lattice gases [53, 54, 124].

In 2002 Lafuente and Cuesta extended Rosenfeld's fundamental measure theory to lattice models based on a derivation of an exact density functional for hard rod mixtures in one dimension [60, 61]. This derivation was carried out following a procedure developed by Vanderlick *et al.* [109] for continuum fluids. Since the excess free energy part of the functional could be expressed in terms of differences between parts that agree in their functional form with the excess free energy functional of a zero-dimensional cavity, approximate functionals in higher dimensions were obtained by dimensional expansion of the corresponding difference operator. By construction these fundamental measure functionals have the property to become exact under dimensional reduction and their impressive power was first shown by determining phase diagrams of hard squares [61, 66] and hard cube mixtures [60, 61, 67] with good quality. The fundamental measure functionals moreover allow one to apply the method of dimensional crossover and the merit of this was demonstrated by deriving functionals for lattice gases with nearest neighbor exclusion for different lattice types (square, triangular, face- and body-centered cubic) from the functional for cubes in $(d + 1)$ dimensions [68]. The structure of the corresponding results led to a suggestion how to construct fundamental measure functionals for hard core lattice gases for any type of lattice, shape of the particles, and arbitrary dimension [62].

In this chapter we rederive the exact density functional for hard rod mixtures in one dimension, that means the starting point of the fundamental measure theory for hard core lattice gases, by applying the Markov chain approach developed by Buschle *et al.* [64]. This approach is conceptually different from the procedure of Vanderlick *et al.* [109] and we believe that it is useful and important on the following reasons: (i) The derivation of the functional becomes surprisingly simple. Making use only of the constraints of mutual rod exclusions, the relevant transition probability in the Markov chain is determined almost without any calculation. (ii) The transition probability is (conditionally) dependent on a spatial region, where at most one particle can be placed, i.e. that of a zero-dimensional cavity. In this respect it reflects a property which turned out to be decisive for the generalized construction of fundamental measure functionals by Lafuente and Cuesta [62]. (iii) The simplicity of the derivation suggests that it can be extended to hard rod mixtures with additional (thermal) interactions. (iv) The derivation yields also an explicit expression for the probability distribution of microstates for a given density profile. This means that in the present case an explicit expression for the "Mermin potential" is obtained, i.e. the unique external potential that would generate the given density profile in thermal equilibrium. In addition to these points we show that it is not necessary to consider non-additive mixtures when mixing parities of rod lengths are present (i.e. rods with both even and odd lengths in units of the lattice spacing).

4.2 Joint probability distribution

The mixture is considered to consist of q types of hard rods with length l_α, $\alpha = 1, \ldots, q$ in the presence of an external potential. It is convenient (although not necessary) to order the lengths according to $l_1 \geq l_2 \geq \ldots l_q$, where different types of rods could have the same lengths due to a different coupling to an external potential. The rods are located on a one-dimensional lattice with L sites and we set the lattice spacing equal to one. The lattice is defined in such a way that the ends of the rods coincide with lattice sites and we introduce occupation numbers n_j^α, $j = 1, \ldots, L$, $\alpha = 1, \ldots, q$, to specify the microstate of the mixture. If the left end of a rod of type α is at site j, then $n_j^\alpha = 1$, else $n_j^\alpha = 0$ (here and in the following Greeks superscripts refer to the type and must not mixed up with exponents). The mutual exclusion of hard rods implies the constraint $n_k^\alpha n_j^\beta = 0$ for $j = k, \ldots, k + l_\alpha - 1$ (and $k = j, \ldots, j + l_\beta - 1$). In a grand-canonical description the chemical potentials μ_α specify the mean numbers of rods of type α.

To set up the Markov chain approach following [64] it is useful to introduce the multicomponent state variables $\hat{n}_j = (n_j^1, \ldots, n_j^q)$ that can assume $(q + 1)$ states $\hat{e}_0, \ldots, \hat{e}_q$, where $\hat{e}_0$ refers to an empty site, i.e. $\hat{e}_0 = (0, \ldots, 0)$, while $\hat{e}_\alpha$, $\alpha = 1, \ldots, q$, refer to a site occupied by rods of type α, i.e. $\hat{e}_\alpha = (0, \ldots, 1, \ldots, 0)$ with the 1 at the $(\alpha + 1)$th entry. The probability $\chi(\hat{n}_1, \ldots, \hat{n}_L)$ of microstates can be

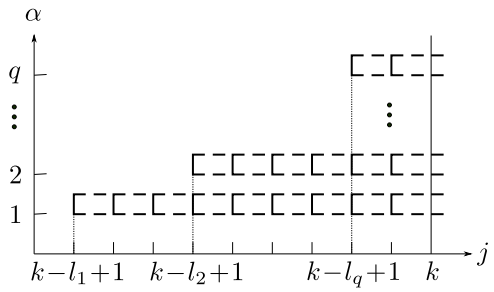

Figure 4.1: Illustration of the set of occupation numbers affecting the occupation of site k. Any placement of the left end of a rod of type α at the sites j with $k - l_\alpha + 1 \leq j \leq k$ means that site k is covered by a part of this rod. This implies (i) that if a left rod end is at site k, all occupation numbers in the set $\{n_j^\alpha\}_{k-1} = \{n_j^\alpha | 1 \leq \alpha \leq q, k - l_\alpha + 1 \leq j \leq k - 1\}$ must be zero, and (ii) that in the set $\{n_j^\alpha\}_k = \{n_j^\alpha | 1 \leq \alpha \leq q, k - l_\alpha + 1 \leq j \leq k\}$ there can be at most one occupation number with value 1.

decomposed as

$$\chi(\hat{n}_1, \ldots, \hat{n}_L) = \prod_{k=1}^{L} \psi(\hat{n}_k | \hat{n}_{k-1}, \ldots, \hat{n}_1) \tag{4.1}$$

where $\psi(.|\ldots)$ denote the corresponding conditional probabilities. To keep the notation simple, we have labeled the starting of the chain, i.e. $\psi(\hat{n}_1)\psi(\hat{n}_2|\hat{n}_1)$ $\times\psi(\hat{n}_3|\hat{n}_2, \hat{n}_1)\ldots$, by the same symbol "$\psi$" (meaning in particular that $\psi(\hat{n}_1)$ is not a conditional probability). By using the Boltzmann expression for the probability of microstates in the grand-canonical equilibrium ensemble, i.e. $\chi \propto \exp[-\beta \sum_{i,\alpha}(u_i^\alpha - \mu_\alpha)n_i^\alpha]$, where $\beta = 1/k_B T$ is the inverse thermal energy and u_i^α the external potential, it can be proven [64] that the conditional probabilities satisfy the following Markov property:

$$\psi(\hat{n}_k | \hat{n}_{k-1}, \ldots, \hat{n}_1) = \psi(\hat{n}_k | \{n_j^\alpha\}_{k-1}) \tag{4.2}$$

where $\{n_j^\alpha\}_{k-1} = \{n_j^\alpha | 1 \leq \alpha \leq q, k - l_\alpha + 1 \leq j \leq k - 1\}$ denotes the set of occupation variables, which have an influence on the occupation of site k, see Fig. 4.1.

In the set $\{n_j^\alpha\}_k = \{n_j^\alpha | 1 \leq \alpha \leq q, k - l_\alpha + 1 \leq j \leq k\}$, i.e. all occupation variables involved in Fig. 4.1, there can be at most one occupation variable $n_j^\alpha = 1$ due to the hard rod constraints, which reflects the corresponding property of a zero-dimensional cavity. In fact this set corresponds exactly to the zero-dimensional cavity for a mixture introduced in [61] as a collection of sets for each rod type. The property to have at most most one occupation variable $n_j^\alpha = 1$ in $\{n_j^\alpha\}_k$ can be utilized to determine the conditional probabilities by simple probabilistic considerations. First let us write for $\alpha = 0, \ldots, q$

$$\psi(\hat{n}_k = \hat{e}_\alpha | \{n_j^\beta\}_{k-1}) = \frac{\text{Prob}(\hat{n}_k = \hat{e}_\alpha, \{n_j^\beta\}_{k-1})}{\text{Prob}(\{n_j^\beta\}_{k-1})} \tag{4.3}$$

where Prob(.) denote joint probabilities. If $\alpha \neq 0$, then all n_j^β in the set $\{n_j^\beta\}_{k-1}$ must be zero. This implies $\text{Prob}(\hat{n}_k = \hat{e}_\alpha, \{n_j^\beta\}_{k-1}) = \text{Prob}(\hat{n}_k = \hat{e}_\alpha, \{n_j^\beta = 0\}_{k-1}) = p_k^\alpha$, where $p_k^\alpha = \langle n_\alpha \rangle$ is the mean occupation of site k ($\langle \ldots \rangle$ denotes an average over the microstate distribution $\chi(\hat{n}_1, \ldots, \hat{n}_L)$). Since with the same reasoning $\text{Prob}(\{n_j^\beta = 1, \text{all other } n_l^\gamma = 0\}_{k-1}) = p_j^\beta$, we further have

$$\text{Prob}(\{n_j^\alpha = 0\}_{k-1}) + \sum_{\beta=1}^{q} \sum_{j=k-l_\beta+1}^{k-1} p_j^\beta = 1 \tag{4.4}$$

due to normalization. Accordingly, we obtain for $\alpha \neq 0$

$$\psi(\hat{n}_k = \hat{e}_\alpha | \{n_j^\beta\}_{k-1}) = \frac{p_k^\alpha}{1 - S_k^{(0)}} \tag{4.5}$$

where we used one of the weighted densities (weighted mean occupations)

$$S_k^{(m)} = \sum_{\alpha=1}^{q} \sum_{j=1-m}^{l_\alpha - 1} p_{k-j}^\alpha \quad m = 0, 1 \tag{4.6}$$

appearing in the lattice fundamental measure theory [60]. If $\hat{n}_k = \hat{e}_0$ there are two possibilities: Either one element in $\{n_j^\beta\}_{k-1}$ is one, or all elements are zero. In the first case, $\hat{n}_k$ must be equal to $\hat{e}_0$, implying that the corresponding conditional probability is one. In the second case we need $\text{Prob}(\hat{n}_k = \hat{e}_0, \{n_j^\beta = 0\}_{k-1}) = \text{Prob}(\{n_j^\beta = 0\}_k)$ in Eq. (4.3), which by utilizing normalization as in Eq. (4.4) (now with inclusion of site k), is given by $\text{Prob}(\{n_j^\beta = 0\}_k) = 1 - \sum_{\beta=1}^{q} \sum_{j=k-l_\beta+1}^{k} p_j^\beta = 1 - S_k^{(1)}$. In summary,

$$\psi(\hat{n}_k = \hat{e}_0 | \{n_j^\beta\}_{k-1}) = \begin{cases} 1\,, & \text{one } n_j^\beta = 1 \text{ in } \{n_j^\beta\}_{k-1} \\ \dfrac{1 - S_k^{(1)}}{1 - S_k^{(0)}}\,, & \text{all } n_j^\beta = 0 \text{ in } \{n_j^\beta\}_{k-1} \end{cases} \tag{4.7}$$

Combining Eqs. (4.5) and (4.7), we can write

$$\psi(\hat{n}_k | \{n_j^\beta\}_{k-1}) = \left(\frac{1 - S_k^{(1)}}{1 - S_k^{(0)}} \right)^{1 - \sum_{\beta=1}^{q} \sum_{j=0}^{k-1} n_j^\beta} \prod_{\alpha=1}^{q} \left(\frac{p_k^\alpha}{1 - S_k^{(0)}} \right)^{n_k^\alpha} \tag{4.8}$$

where the distinction between the possible configurations in the set $\{n_j^\beta\}_k$ is taken into account by the exponents.

Inserting Eq. (4.8) into Eqs. (5.3) and (4.1), the probability distribution of microstates is given by the product of $\psi(\hat{n}_k | \{n_j^\beta\}_{k-1})$ from Eq. (4.8) over all lattice sites, i.e. an explicit expression for $\chi(\mathbf{n})$ as function of the set $\mathbf{n} = \{n_i^\alpha | 1 \leq \alpha \leq q, 1 \leq i \leq L\}$ of occupation numbers is obtained (we define $\chi(\mathbf{n}) = 0$ for all microstates $\mathbf{n}$ violating the hard rod constraints). This means that, for a given density profile $\mathbf{p} = \{p_k^\alpha | 1 \leq \alpha \leq q, 1 \leq k \leq L\}$, the distribution of microstates is uniquely determined if we require it to satisfy the Markov property Eq. (5.3), i.e. $\chi(\mathbf{n}) = \chi_{\mathbf{p}}(\mathbf{n})$.

4.3 Mermin potential and free energy functionals

From the last observation, one could get the impression that this is more general than the uniqueness implied by the Mermin theorem, which states that the prescription of $\mathbf{p}$ fixes the external potential $u_k^\alpha = u_k^\alpha(\mathbf{p})$ in the sense that the Boltzmann distribution yields $\mathbf{p}$ in equilibrium in the presence of $u_k^\alpha(\mathbf{p})$. However, since the Boltzmann distributions satisfy the Markov property Eq. (5.3), and $\chi_{\mathbf{p}}(\mathbf{n})$ is unique, there is in fact no more generality, i.e. the microstate distribution for given $\mathbf{p}$ satisfying the Markov property Eq. (5.3) and the Boltzmann distribution generating $\mathbf{p}$ in equilibrium must be the same [125]. Hence we can identify the "Mermin potential" $U_{\mathbf{p}}(\mathbf{n}) = \sum_{k,\alpha} u_k^\alpha(\mathbf{p}) n_k^\alpha$ by setting $\beta U_{\mathbf{p}}(\mathbf{n}) \propto -\log \chi_{\mathbf{p}}(\mathbf{n})$, which, up to irrelevant constant contributions, yields (after some rearrangement of summations)

$$u_k^\alpha(\mathbf{p}) = \log p_k^\alpha - \log(1 - S_k^{(0)}) + \sum_{j=k}^{k+l_\alpha-1} \log\left(\frac{1 - S_j^{(0)}}{1 - S_j^{(1)}}\right) \tag{4.9}$$

Based on the Gibbs-Bogoliubov inequality the density functional for N_α hard rods of type α in the external potential $U(\mathbf{n}) = \sum_{k,\alpha} u_k^\alpha n_k^\alpha$ is defined as

$$\begin{aligned}\Omega(\mathbf{p}) &= \sum_{\mathbf{n}} \chi_{\mathbf{p}}(\mathbf{n}) \left[k_B T \log \chi_{\mathbf{p}}(\mathbf{n}) + U(\mathbf{n}) - \sum_{\alpha=1}^{q} \mu_\alpha N_\alpha \right] \\ &= F(\mathbf{p}) + \sum_{k=1}^{L} \sum_{\alpha=1}^{q} (u_k^\alpha - \mu_\alpha) p_k^\alpha \end{aligned} \tag{4.10}$$

where $F(\mathbf{p}) = k_B T \sum_{\mathbf{n}} \chi_{\mathbf{p}}(\mathbf{n}) \log \chi_{\mathbf{p}}$ is the free energy functional. Inserting $\chi_{\mathbf{p}}(\mathbf{n})$ one obtains

$$\begin{aligned}\beta F(\mathbf{p}) = \sum_{k=1}^{L} \Big\{ &(1 - S_k^{(1)}) \log(1 - S_k^{(1)}) \\ &- (1 - S_k^{(0)}) \log(1 - S_k^{(0)}) + \sum_{\alpha=1}^{q} p_k^\alpha \log p_k^\alpha \Big\} \end{aligned} \tag{4.11}$$

When minimizing $\Omega(\mathbf{p})$ with respect to the p_j^α, the density profile in equilibrium is obtained.

Following Lafuente and Cuesta [61], one can define an "ideal part" $F_{\mathrm{id}}(\mathbf{p})$ by

$$\beta F_{\mathrm{id}}(\mathbf{p}) = \sum_{k=1}^{L} \sum_{\alpha=1}^{q} p_k^\alpha (\log p_k^\alpha - 1) \tag{4.12}$$

This differs from the expression $\sum_k \{p_k^\alpha \log p_k^\alpha - (1 - \sum_\alpha p_k^\alpha) \log(1 - \sum_\alpha p_k^\alpha)\}$ for a non-interacting multi-component Fermionic lattice gas, but has the advantage to lead to a fundamental measure structure of the excess free energy part $F_{\mathrm{exc}}(\mathbf{p}) =$

$F(\mathbf{p})-F_{\mathrm{id}}(\mathbf{p})$. When using Eqs. (5.16), (4.12), and $\sum_\alpha p_k^\alpha = S_k^{(1)}-S_k^{(0)}$ this becomes

$$\begin{aligned}\beta F_{\mathrm{exc}}[\mathbf{p}] = \sum_{k=1}^{L}\Big\{&\Big[S_k^{(1)} + (1-S_k^{(1)})\log(1-S_k^{(1)})\Big] \\ &- \Big[S_k^{(0)} + (1-S_k^{(0)})\log(1-S_k^{(0)})\Big]\Big\}\end{aligned} \tag{4.13}$$

The terms in the square brackets have the same functional form as the excess free energy $f_{\mathrm{exc}}(\eta) = \eta + (1-\eta)\log(1-\eta)$ of a zero-dimensional cavity with mean occupation η [5, 57]. The free energy functional can be written in a compact form as

$$\beta F_{\mathrm{exc}}[\mathbf{p}] = \sum_{k=1}^{L} D_m f_{\mathrm{exc}}[\tilde{p}_k^{(m)}] \tag{4.14}$$

where $D_m f(m) = f(1) - f(0)$ is the discrete difference operator.

The excess free energy in Eq. (4.13) is equal to that found by Lafuente and Cuesta for an additive mixture. To recover their expressions, occupation numbers $\tilde{n}_k^\alpha = 0, 1$ need to assigned to the rod centers, which amounts to a simple transformation of the site indices, $n_k^\alpha \to \tilde{n}_k^\alpha = n_{k+(l_\alpha-\epsilon)/2}^\alpha$, where $\epsilon = 0$ if all l_α are even and $\epsilon = 1$ if all l_α are odd.

A non-additive mixture appears when considering a setup where the rod centers fall onto lattice sites and both even and odd l_α are present, since in this case rods with even and odd l_α have a minimum separation of half a lattice unit between their ends. For such non-additive mixture one can construct the corresponding functional from that for additive mixtures [61]. This can be done by imposing $\hat{l}_\alpha = 2l_\alpha$, and restrict the positions of the rods to lie on the even sites of the lattice (by imposing $\rho_\alpha(i) = 0$ if $i = 2r+1$ with $r \in \mathbb{Z}$). The resulting free energy functional is

$$\beta F_{\mathrm{exc}}[\mathbf{p}] = \sum_{k=1}^{L} D_m \left[\sum_{j=0,1} f_{\mathrm{exc}}[\tilde{p}_{k,j}^{(m)}]\right] \tag{4.15}$$

where the weight functions $\tilde{p}_{k,j}^{(m)}$ are given by Eq. (3.41). When the rod ends fall onto lattice sites, the mixture is always additive irrespective of having mixed parities of rod lengths.

Approximate fundamental measure functionals in higher dimensions can be constructed by considering the two terms in the square brackets as resulting from applying a one-dimensional difference operator and by generalizing this operator together with the weighted densities to higher dimensions (for details, see [60,61]).

Chapter 5

Simple hard rods with nearest neighbour interactions

5.1 Introduction

Lattice density functional theory is drawing increasing attention on account of its wide range of applicability to phenomena of strong interest in current research [49,117,126]. Its applications include ordering phenomena in metallic alloys, submonolayer adsorbate systems, [45] colloid-polymers mixtures, [69] fluids in porous media, [116] and DNA denaturation [48]. In certain cases, exact density functionals in zero and one dimension can be written in a so-called fundamental measure form, which allows one to construct approximate functionals in higher dimensions that reduce to the exact ones upon dimensional crossover [55,61,62,66–68]. Moreover, the theory can be extended to time-dependent phenomena [51–54].

Particles with shapes that interact solely via hardcore repulsion on a lattice or in a continuum do produce interesting effects including phase transitions, e.g. for hard hexagons [127]. However, the inclusion of attractive or repulsive forces on contact or at some distance is important for more realistic modelling [110, 111, 128–137]. Models with square-well interaction potentials including potentials of the zero-range, stickycore type have proven to exhibit realistic physical features for many systems: colloids suspensions, [138–140] crystallization of polymers, [71, 141] micelles, [72] protein solutions, [73, 142], DNA coated colloids, [74, 75] ionic fluids, [76] and microemulsions. [143, 144]. It is well established that many effects of generic short-range interactions can be reproduced by contact forces of a strength that yields matching second virial coefficients [145].

In this chapter we will used an ideas suggested by Buschle *et al.*, [64, 65] to derive an exact free-energy functional for hard rods with first-neighbor coupling of arbitrary shape.

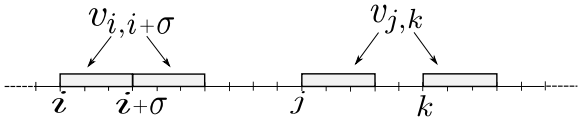

Figure 5.1: Hard rods with size $\sigma = 3$ interacting with a "nearest-neighbor" potential. The rods on the left are in contact. The interaction between the two rods on the right becomes zero for $k > j + \xi$ ($\xi < 2\sigma$).

5.2 Model

We consider rods of size σ on a one-dimensional lattice of L sites, as sketched in Fig. 5.1. Occupation numbers n_i are assigned to the lattice sites, where $n_i = 1$ if the left end of a rod is located at site i, and $n_i = 0$ else. The mutual exclusion of hard rods implies the constraint $n_i n_{i+j} = 0$ for $j = 0, \ldots, \sigma - 1$. A grand-canonical description is used, where the chemical potential μ specifies the mean numbers of rods in the system. A fixed boundary condition is considered where the occupation numbers at the two boundaries are fixed to be one.

In addition to the mutual exclusion, an interaction between neighboring rods is present with range ξ in the interval $\sigma \leq \xi < 2\sigma$. The lattice gas Hamiltonian is

$$\mathcal{H}(\mathbf{n}) = \sum_{i<j} v_{i,j} n_i n_j + \sum_i u_i n_i \tag{5.1}$$

where $v_{i,j}$ is the interaction potential ($v_{i,i+j} = 0$ for $j > \xi$), u_i the external potential, and $\mathbf{n}$ denotes the microstate $\mathbf{n} = \{n_1, \ldots, n_L\}$. The model includes the special case of a square well potential, where a region of constant interaction, $v_{i,j} = const.$ for $\sigma \leq |i - j| \leq \xi$, is added to the hard-core part ($v_{i,j} = \infty$ for $|i - j| \leq \sigma$). If $v_{i,i+\sigma} \neq 0$ and $v_{i,i+j} = 0$ for $j \geq \sigma + 1$, the model corresponds to the so-called sticky core potential introduced by Baxter for continuum systems. [146] In this situation, two rods interact only if they are in contact.

5.3 Distribution of microstates

For given interaction $V(\mathbf{n}) = \sum_{i<j} v_{i,j} n_i n_j$, the external potential $U_{\mathbf{p}}(\mathbf{n}) = \sum_i u_i[\mathbf{p}] n_i$, which yields the set $\mathbf{p} = \{p_1, \ldots, p_L\}$ of mean occupation numbers $p_i = \langle n_i \rangle$ ("density profile") in equilibrium, is a (unique) functional of $\mathbf{p}$. [86] We will derive in this section an explicit expression for the corresponding joint probability $\chi_{\mathbf{p}}(\mathbf{n}) = \exp\{\Omega[\mathbf{p}] - V(\mathbf{n}) - \tilde{U}_{\mathbf{p}}(\mathbf{n})\}$, where $\tilde{U}_{\mathbf{p}}(\mathbf{n}) = \sum_i \tilde{u}_i[\mathbf{p}] n_i$, $\tilde{u}_i[\mathbf{p}] = u_i[\mathbf{p}] - \mu$, and $\Omega[\mathbf{p}]$ is the grand canonical functional. All energies here and in the following are given in units of $k_B T$.

The derivation follows from the method introduced in Ref. [64] and proceeds in three steps. In the first step, a Markov property is utilized to reduce the calculation of $\chi_{\mathbf{p}}(\mathbf{n})$ to the calculation of joint probabilities $\phi(n_i, \ldots, n_{i-\xi})$. In the second step,

these joint probabilities are then expressed in terms of the p_i and correlators $C_{i,j} = \langle n_i n_j \rangle$ by making use of the mutual exclusion constraint, which implies that at most two occupation numbers can be equal to one in the set $\{n_i, \ldots, n_{i-\xi}\}$. In the last step, the $C_{i,j} = C_{i,j}[\mathbf{p}]$ are given as functional of $\mathbf{p}$ by comparing $\chi_{\mathbf{p}}(\mathbf{n})$ with the Boltzmann expression for a few simple configurations $\mathbf{n}$. The knowledge of $C_{i,j}[\mathbf{p}]$ means that we provide an example for the rare cases, where the "Mermin potential" $U_{\mathbf{p}}(\mathbf{n}) = \Omega[\mathbf{p}] - \langle V(\mathbf{n}) \rangle - \ln \chi_{\mathbf{p}}(\mathbf{n})$ can be given. The density functional $\Omega[\mathbf{p}]$ is derived in Sec. 5.4.

5.3.1 Reduction to joint probabilities of finite range

The joint probability distribution can be decomposed as

$$\chi(\mathbf{n}) = \prod_{s=1}^{L} \psi(n_s | n_{s-1}, \ldots, n_1) \,, \tag{5.2}$$

where $\psi(n_s|n_{s-1}, \ldots, n_1)$ is the probability of finding the occupation number n_s at site s under the condition that all occupation numbers left to site s are given. Because of the finite interaction range and because we are dealing with a one-dimensional system, one can prove the following Markov property,

$$\begin{aligned} \psi(n_s|n_{s-1}, \ldots, n_1) &= \psi(n_s|n_{s-1}, \ldots, n_{s-\xi}) \\ &= \frac{\phi(n_s, \ldots, n_{s-\xi})}{\phi(n_{s-1}, \ldots, n_{s-\xi})} \,, \end{aligned} \tag{5.3}$$

where $\phi(n_s, \ldots, n_{s-\xi})$ denotes the joint probability of finding the set $\{n_s, \ldots, n_{s-\xi}\}$ of occupation numbers.

5.3.2 Joint probabilities of finite range

Because of the mutual exclusion of the rods, we can subdivide the range $s, \ldots, s-\xi$ of lattice sites into two ranges $s, \ldots, s-\sigma+1$ and $s-\sigma, \ldots, s-\xi$, where in each of these ranges at most one occupation number can be equal to one. Moreover, if in both ranges appears an occupied site, their distance must be larger than $(\sigma - 1)$. It is convenient to introduce the shortened notation $\phi_s(0,0)$, $\phi_s(0,1_j)$, $\phi_s(1_i,0)$, and $\phi_s(1_i,1_j)$, where the first and second argument refer to the first range $i \in \{s, \ldots, s-\sigma+1\}$ and second range $j \in \{s-\sigma \ldots, s-\xi\}$, respectively. A zero in one argument means that all occupation numbers in the corresponding range are zero, and a 1_k in an argument means that $n_k = 1$ in the corresponding range, while all other occupation numbers are zero. For example, $\phi_s(1_i,0) = \phi(n_s = 0, \ldots, n_{i+1} = 0, n_i = 1, n_{i-1} = 0, \ldots, n_{s-\xi} = 0)$.

The joint probability $\phi(n_s, \ldots, n_{s-\xi})$ can then be written as

$$\begin{aligned}\phi(n_s, \ldots, n_{s-\xi}) =& \phi_s(0,0)^{\left(1-\sum_{(i)_1} n_i\right)\left(1-\sum_{(j)_2} n_j\right)} \\ &\times \prod_{(i)_1} \phi_s(1_i, 0)^{n_i\left(1-\sum_{(j)_2} n_j\right)} \\ &\times \prod_{(j)_2} \phi_s(0, 1_j)^{n_j\left(1-\sum_{(i)_1} n_i\right)} \\ &\times \prod_{(i,j)} \phi_s(1_i, 1_j)^{n_i n_j}\,, \end{aligned} \tag{5.4}$$

where $(i)_1$ and $(j)_2$ refer to indices running over the first and second range, respectively. The specification (i, j) means that the two indices run over the set $i = s, \ldots, s-\xi+\sigma$, $j = i-\sigma, \ldots, s-\xi$. Equation (5.4) amounts to expressing the joint probability in terms of the $\phi_s(.,.)$ by selecting all possible configurations via the exponents. For example, for the configuration $(1_i, 0)$, the associated exponent $n_i(1-\sum_{(j)_2} n_j)$ is one for $n_i = 1$ and all $n_j = 0$ in the second range, while otherwise it is zero and thus giving an (irrelevant) factor one in Eq. (5.4). Note that, different from a case selection by products in the exponents, e.g.. by $n_i \prod_{(j)_2}(1-n_j)$ for the configuration $(1_i, 0)$, we have written sums. This is allowed because at most one occupation number can be one in the two ranges and $\prod_{(j)_2}(1-n_j) = 1-\sum_{(j)_2} n_j$.

The joint probability $\phi(n_{s-1}, \ldots, n_{s-\xi})$ in the denominator appearing in Eq. (5.3) can be expressed in the same way with the only difference that now the range of indices indicated by $(i)_1$ refers to $s-1, \ldots, s-\sigma+1$ and the range of indices indicated by (i, j) refers to $i = s-1, \ldots, s-\sigma-1$, $j = i-\sigma, \ldots, s-\xi$. The range indicated by $(j)_2$ remains unchanged. The corresponding shortened notation is indicated by a tilde, i.e. $\tilde{\phi}_s(0,0)$, $\tilde{\phi}_s(1_i, 0)$ etc. For example, $\tilde{\phi}_s(1_i, 0) = \phi(n_{s-1} = 0, \ldots, n_{i+1} = 0, n_i = 1, n_{i-1} = 0, \ldots, n_{s-\xi} = 0)$.

The $\phi_s(.,.)$ can be written in terms of the mean occupation numbers p_i and correlators $C_{i,j}$ based on their definition and by utilizing the normalization condition. It holds

$$C_{i,j} = \langle n_i n_j \rangle = \sum_{(k,l)} n_i n_j \phi_s(n_k, n_l) = \phi_s(1_i, 1_j) \tag{5.5a}$$

$$\begin{aligned} p_i = \langle n_i \rangle &= \sum_{\{\mathbf{n}\}_s} n_i \phi_s(n_k, n_j) \\ &= \phi_s(1_i, 0) + \sum_{(j)_2} \phi_s(1_i, 1_j)\,, \end{aligned} \tag{5.5b}$$

$$\begin{aligned} 1 = \sum_{\{\mathbf{n}\}_s} \phi_s(n_i, n_j) &= \phi_s(0,0) + \sum_{(i)_1} \phi_s(1_i, 0) \\ &\quad + \sum_{(j)_2} \phi_s(0, 1_j) + \sum_{(i,j)} \phi_s(1_i, 1_j)\,, \end{aligned} \tag{5.5c}$$

where $\{\mathbf{n}\}_s = \{n_s, \ldots, n_{s-\xi}\}$. From this follows

$$\phi_s(0,0) = 1 - \sum_{k=s-\xi}^{s} p_k + \sum_{i=s-\xi+\sigma}^{s} \sum_{j=s-\xi}^{i-\sigma} C_{i,j} \tag{5.6a}$$

$$\phi_s(1_i,0) = p_i - \sum_{j=s-\xi}^{i-\sigma} C_{i,j} \tag{5.6b}$$

$$\phi_s(0,1_j) = p_j - \sum_{i=j+\sigma}^{s} C_{i,j} \tag{5.6c}$$

$$\phi_s(1_i,1_j) = C_{i,j} \tag{5.6d}$$

The equations for the $\tilde{\phi}_s(.,.)$ are the same except that in the upper limit of the sums s has to be replaced by $(s-1)$.

Equations (5.3), (5.4), and (5.6) yield the joint probabilities $\chi(\mathbf{n})$ in Eq. (5.2) as functionals of the p_i and $C_{i,j}$.

5.3.3 Correlators as functionals of densities

To express the $C_{i,j}$ as functionals of the p_i joint probabilities $\chi(\mathbf{n})$ calculated from the approach described above are now compared with the Boltzmann probability for a few simple configurations $\mathbf{n}$:

$$\chi(0_1,\ldots,0_L) = \frac{1}{Z}\,, \tag{5.7a}$$

$$\chi(0_1,\ldots,1_i,\ldots,0_L) = \frac{e^{-\tilde{u}_i}}{Z}\,, \tag{5.7b}$$

$$\chi(0_1,\ldots,1_j,\ldots,1_i,\ldots,0_L) = \frac{1}{Z} e^{-(\tilde{u}_i+\tilde{u}_j+v_{i,j})}\,, \tag{5.7c}$$

where $\tilde{u}_i = u_i - \mu$, and in Eq. (5.7c) the expression is valid for $i - j \geq \sigma$. This gives the following relation:

$$\begin{aligned}&\chi(0_1,\ldots,0_L)\chi(0_1,\ldots,1_i,\ldots,1_j,\ldots,0_L)\\ &\quad = e^{-v_{i,j}}\chi(0_1,\ldots,1_i,\ldots,0_L)\chi(0_1,\ldots,1_j,\ldots,0_L)\end{aligned} \tag{5.8}$$

One can now insert into this relation the results for $\chi(\mathbf{n})$ from the previous Secs. 5.3.2 and 5.3.3. For example, for a configuration with two rods at site i and j with

$\sigma \le (i-j) \le \xi$ we have

$$\begin{aligned}\chi(0_1,\ldots,1_i,\ldots,1_j,\ldots,0_L) = \\ &\left[\prod_{s=1}^{j-1}\frac{\phi_s(0,0)}{\tilde{\phi}_s(0,0)}\right]\frac{\phi_j(1_j,0)}{\tilde{\phi}_j(0,0)}\left[\prod_{s=j+1}^{i-1}\frac{\phi_s(1_j,0)}{\tilde{\phi}_s(1_j,0)}\right]\frac{\phi_i(1_i,1_j)}{\tilde{\phi}_j(0_i,1_j)} \\ &\times\left[\prod_{s=i+1}^{j+\xi}\frac{\phi_s(1_i,1_j)}{\tilde{\phi}_s(1_i,1_j)}\right]\left[\prod_{s=j+\xi+1}^{i+\sigma-1}\frac{\phi_s(1_i,0)}{\tilde{\phi}_s(1_i,0)}\right] \\ &\times\left[\prod_{s=i+\sigma}^{i+\xi}\frac{\phi_s(0,1_i)}{\tilde{\phi}_s(0,1_i)}\right]\left[\prod_{s=i+l+1}^{L}\frac{\phi_s(0,0)}{\tilde{\phi}_s(0,0)}\right].\end{aligned} \tag{5.9}$$

The different terms in this equation are a consequence of the Markov chain in Eq. (5.3) with progressing s index: The first four factors arise from successively capturing the rods located at sites j and i. The next four terms are associated with the following specific s-values: If $s = j+\xi+1$, the rod at site j falls out of the interaction range, and if $s = i+\sigma$, the rod at site i is no longer in the first range (see above) with respect to site s. If $s = i+\xi+1$, the rod at site i eventually falls out of the interaction range.

Decomposing the other joint probabilities in Eq. (5.7) in an analogous way and inserting the $\phi(.,.)$, $\tilde{\phi}(.,.)$ from Eq. (5.6), yields, after elementary algebra,

$$C_{i,j} = \frac{\phi_i(1_i,0)\phi_i(0,1_j)}{\phi_i(0,0)}\left[\prod_{s=i+1}^{j+\xi}\frac{\phi_s(0,1_j)}{\tilde{\phi}_s(0,1_j)}\frac{\tilde{\phi}_s(0,0)}{\phi_s(0,0)}\right]e^{-v_{i,j}} \tag{5.10}$$

for $\sigma \le |i-j| \le \xi$. With the $C_{i,j}$ determined from Eqs. (5.10) as functional of $\mathbf{p}$, the distribution of microstates becomes also a functional of $\mathbf{p}$ using Eqs. (5.6), (5.4), (5.3), and (5.2), i.e. $\chi = \chi_{\mathbf{p}}(\mathbf{n})$.

For general interactions $v_{i,j}$, Eqs. (5.10) needs to be solved numerically. In the special case of (spatially homogeneous) contact interaction $v_c \equiv v_{i,i+m}$, Eq. (5.10) gives

$$C_{i-\sigma,i} = \frac{[p_i - C_{i-\sigma,i}][p_{i-\sigma} - C_{i-\sigma,i}]}{[1 - \sum_{k=i-\sigma}^{i} p_k + C_{i-\sigma,i}]}e^{-v_c}, \tag{5.11}$$

with explicit solution

$$C_{i-\sigma,i} = \frac{A_i - \left[A_i^2 - 4e^{-v_c}(e^{-v_c}-1)p_{i-\sigma}p_i\right]^{1/2}}{2(e^{-v_c}-1)}, \tag{5.12}$$

where

$$A_i = 1 + e^{-v_c}(p_{i-\sigma} + p_i) - \sum_{k=i}^{i-\sigma} p_k\,. \tag{5.13}$$

Figure 5.2 shows, as an example, the contact correlators $C_c \equiv C_{i-\sigma,i}$ for a spatially homogeneous bulk system ($u_i = 0$) with mean occupation numbers $p_i = p$. The

C_c are plotted as functions of the coverage (or "mass density") $\rho = p\sigma$ for two fixed rod lengths $\sigma = 1$ and 5, and repulsive ($v_c > 0$) as well as attractive ($v_c < 0$) interactions. For comparison, the results for the non-interacting case ($v_c = 0$) are also shown.

In the non-interacting case for $\sigma = 1$, $C_c = p^2 = \rho^2$, because of absence of correlation effects in the simple Fermi lattice gas, while for larger rod size $\sigma = 5$, $C_c \geq p^2 = \rho^2/\sigma^2$, meaning that neighboring rods have some tendency to come into contact. This is a consequence of the well-known entropy effect in systems with athermal (exclusion) interactions: Bringing neighboring rods closer to each other gives the remaining rods more configurational freedom and in total the system more configurational space.

For repulsive interactions, C_c decreases with increasing v_c and for $v_c \to \infty$ approaches zero for $\rho \leq [\sigma/(\sigma+1)]$, because $\sigma/(\sigma+1)$ is the maximal coverage where all rods can avoid to come into contact. For $\rho > [\sigma/(\sigma+1)]$, as less as possible rods want to get into contact, leading to a linear increase of C_c with ρ until $C_c = p = \rho/\sigma$ is reached at $\rho = 1$. For attractive interactions, C_c increases with increasing interaction strength $|v_c|$, and for $v_c \to -\infty$ approaches the line $C_c = p = \rho/\sigma$, because all rods want to come into contact.

5.4 Density functionals

Based on the Gibbs-Bogoliubov inequality the following functional is defined in density functional theory,

$$\Omega[\mathbf{p}] = \sum_{\mathbf{n}} \chi_{\mathbf{p}}(\mathbf{n}) \Big[\ln \chi_{\mathbf{p}}(\mathbf{n}) + V(\mathbf{n}) + U(\mathbf{n}) - \mu N \Big] \tag{5.14}$$

$$= F[\mathbf{p}] + \sum_{k=1}^{L} (u_k - \mu) p_k \,, \tag{5.15}$$

where $F[\mathbf{p}] = \sum_{\mathbf{n}} \chi_{\mathbf{p}}(\mathbf{n})[\ln \chi_{\mathbf{p}}(\mathbf{n}) + V(\mathbf{n})]$ is the free energy functional. Minimizing $\Omega[\mathbf{p}]$ yields the equilibrium density profile $\mathbf{p}^{eq} = \{p_i^{eq}\}$.

Inserting $\chi_{\mathbf{p}}(\mathbf{n})$ from the previous Sec. 5.3 and setting $\Phi(x) := x \ln x$ one obtains

$$\begin{aligned} F[\mathbf{p}] = \sum_{i,j} v_{i,j} C_{i,j} + \sum_{s=1}^{L} \Bigg\{ & \Phi\Big(p_s - \sum_{i=s-\xi}^{s-\sigma} C_{s,i}\Big) + \Phi\Big(1 - \sum_{i=s-\xi}^{s} p_i + \sum_{i=s-\xi+\sigma}^{s} \sum_{j=s-\xi}^{i-\sigma} C_{i,j}\Big) \\ & - \Phi\Big(1 - \sum_{i=s-\xi}^{s-1} p_i + \sum_{i=s-\xi+\sigma}^{s-1} \sum_{j=s-\xi}^{i-\sigma-1} C_{i,j}\Big) + \sum_{i=s-\xi}^{s-\sigma} \Big\{ \Phi\Big(C_{s,i}\Big) + \Phi\Big(p_i - \sum_{j=i+\sigma}^{s} C_{j,i}\Big) \\ & - \Phi\Big(p_i - \sum_{j=i+\sigma}^{s-1} C_{j,i}\Big) \Big\} \Bigg\}, \end{aligned} \tag{5.16}$$

where $C_{i,j} = C_{i,j}[\mathbf{p}]$ from Eq. (5.10). In the case of contact interaction in particular,

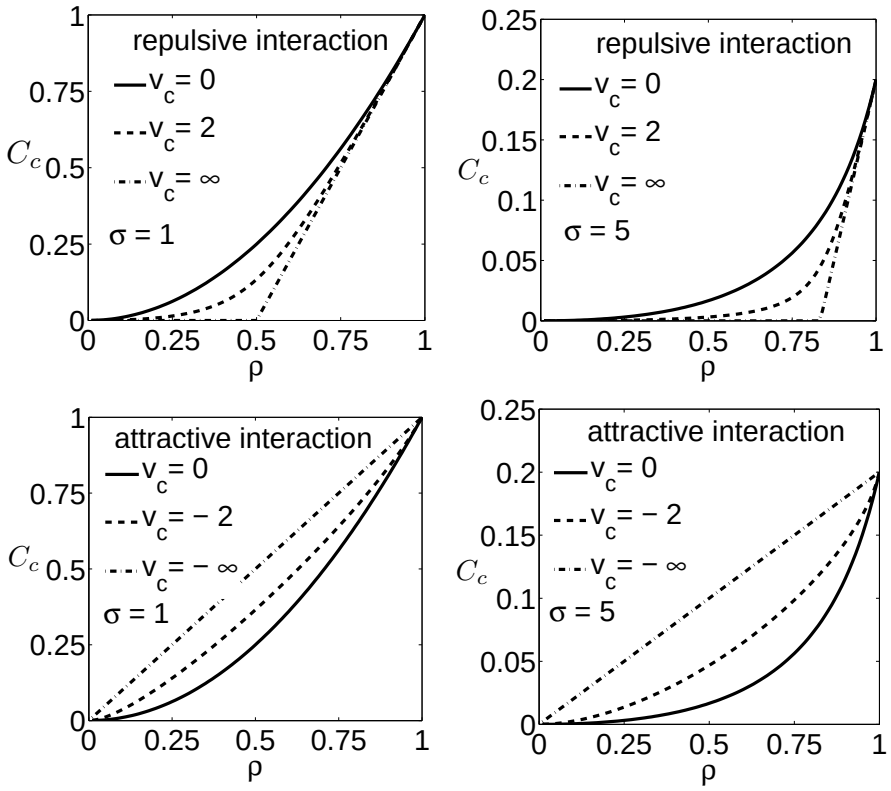

Figure 5.2: Contact correlators $C_c = C_{i-\sigma,i}$ for spatially homogeneous systems of hard rods of sizes $\sigma = 1$ and 5, and different strength of repulsive and attractive contact interactions $v_c = v_{i-\sigma,i}$.

we obtain

$$
\begin{aligned}
F[\mathbf{p}] = \sum_s \Big\{ & C_{s-\sigma,s} v_{s-\sigma,s} + \Phi\Big(p_s - C_{s-\sigma,s}\Big) \\
& + \Phi\Big(1 - \sum_{k=s-\sigma}^{s} p_k + C_{s-\sigma,s}\Big) - \Phi\Big(1 - \sum_{k=s-\sigma}^{s-1} p_k\Big) \\
& + \Phi\Big(C_{s-\sigma,s}\Big) + \Phi\Big(p_{s-\sigma} - C_{s-\sigma,s}\Big) - \Phi\Big(p_{s-\sigma}\Big) \Big\}
\end{aligned}
\tag{5.17}
$$

For the Ising model, $\sigma = 1$, one can proof that this functional agrees with the one previously determined in Ref. [64], for which Lafuente and Cuesta [70] derived a fundamental measure form also.

In fact, eliminating $v_{i,i+\sigma} C_{i,i+\sigma}$ in Eq. (5.17) in favor of correlators and densities via Eq. (5.10), a fundamental measure form is readily obtained also for extended

hard rods ($\sigma > 1$) with contact interaction,

$$F[\mathbf{p}] = \sum_{s=1}^{L} (\mathcal{F}_2[p_{s-\sigma}, \ldots, p_s] - \mathcal{F}_1[p_{s-\sigma}, \ldots, p_{s-1}]) \tag{5.18}$$

where

$$\mathcal{F}_1[p_{s-\sigma}, \ldots, p_{s-1}] = p_{s-\sigma} \ln p_{s-\sigma} + (1 - \sum_{i=s-\sigma}^{s-1} p_i) \ln(1 - \sum_{i=s-\sigma}^{s-1} p_i) \tag{5.19}$$

and

$$\begin{aligned} \mathcal{F}_2[p_{s-\sigma}, \ldots, p_s] =& p_s \ln(p_s - C_{s-\sigma,s}) + p_{s-\sigma} \ln(p_{s-\sigma} - C_{s-\sigma,s}) \\ &+ (1 - \sum_{i=s-\sigma}^{s} p_i) \ln(1 - \sum_{i=s-\sigma}^{s} p_i + C_{s-\sigma,s}) \end{aligned} \tag{5.20}$$

are the free energy functionals of one-particle and two-particle cavities, respectively. A one-particle cavity refers to a range of successive lattice sites, where at most one occupation number can be one, in analogy to the zero-dimensional cavity in Rosenfeld's fundamental measure theory in continuous space. For discrete lattice gas systems, following Lafuente and Cuesta, [70] an m-particle cavity refers to a range of successive lattice sites, where at most m occupation numbers can be one. Notice that the size of an m-particle cavity can vary between $m\sigma$ (minimal m-particle cavity) and $(m + 1)\sigma - 1$ (maximal m-particle cavity). In this respect, $\mathcal{F}_1$ in Eq. (5.19) refers to a maximal one-particle cavity and $\mathcal{F}_2$ in Eq. (5.20) to a minimal two-particle cavity. Fundamental measure forms allow for a straighforward extension to approximate functionals in higher dimensions that become exact under dimensional reduction. [55, 70]

5.5 Thermodynamics of homogeneous systems

The contact correlator C_c in Eq. (5.12) readily gives the internal energy $u(p) = U/L = v_c C_c$ per lattice site, and accordingly $u(p)$ exhibits the same behavior as that shown in Fig. 5.2, except that the curves have to be multiplied by their v_c. The free energy $f(p) = F/L$ per lattice site, given by Eq. (5.17), reduces to

$$\begin{aligned} f(p) =& 2p \ln(p - C) + (1 - (\sigma + 1)p) \ln(1 - (\sigma + 1)p + C) \\ &- (1 - \sigma p) \ln(1 - \sigma p) - p \ln p \end{aligned} \tag{5.21}$$

for a homogeneous system.

The entropy $s = S/L = u - f$ per lattice site is shown in Fig. 5.3 as function of the coverage $\rho = p\sigma$ for the same set of rod lengths and interactions as in Fig. 5.2. The entropy always becomes smaller with increasing interaction strength, but the change of its functional form is different for attractive and repulsive interactions.

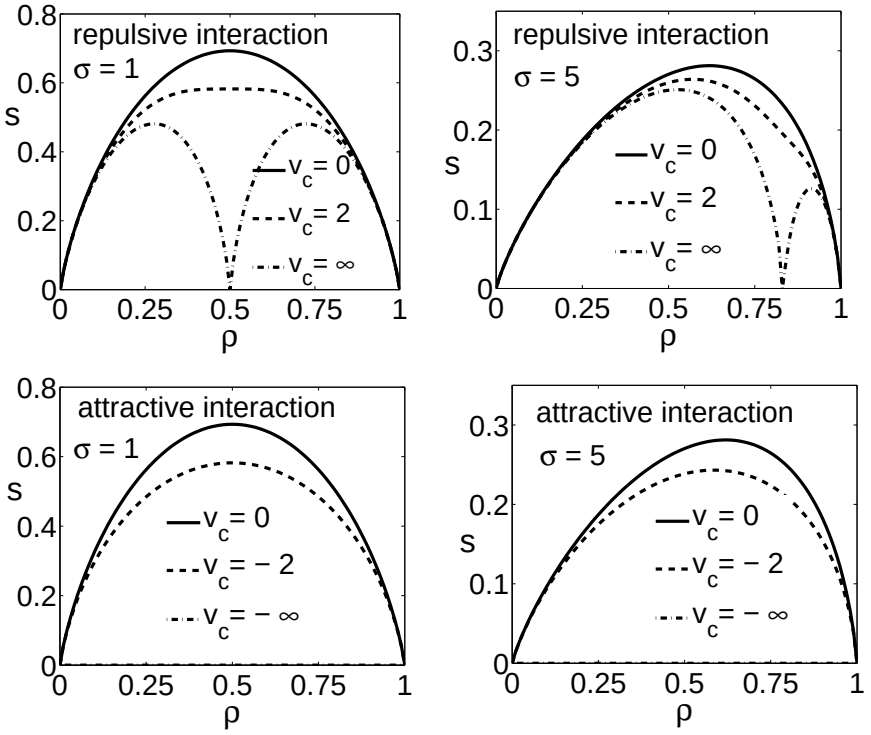

Figure 5.3: Entropy s per lattice site as a function of the coverage ρ for a homogeneous system of hard rods of sizes $\sigma = 1$ and 5, and various contact interactions v_c.

In the case of attractive interactions, there is only one maximum for all v_c, and s approaches zero in the limit $v_c \to -\infty$ for all coverages, because the rods are forming one cluster. This implies that the number of possible configurations becomes $(1-\rho)L$, so that s vanishes in the thermodynamic limit. By contrast, in the case of repulsive interactions, a double hump structure develops with two maxima below a certain interaction strength $v_c^\star = v_c^\star(\sigma)$. The behavior is caused by the fact that close to $\rho = \sigma/(\sigma+1)$ the rods have almost no freedom to avoid contacts. In the limit $v_c \to \infty$ this leads to vanishing entropy at $\rho = \sigma/(\sigma+1)$. At densities $\rho \neq \sigma/(\sigma+1)$ the number of configurations with contact avoidance grows still exponentially with L, leading to a non-vanishing s.
Interestingly, the coverage of maximal entropy is on one hand increasing with σ in the non-interacting case, and decreasing with the interaction strength for $\sigma > 1$. This holds true for both attractive and repulsive interactions. This behavior can be understood intuitively by viewing rods and vacancies as two species with numbers $N_{rod} = pL = \rho L/\sigma$ and $N_v = (1-\rho)L$, respectively. Neglecting entropy related correlation effects in the non-interacting case, the number e^s of possible configurations could then be estimated by $(N_{rod}+N_v)!/(N_{rod}!N_v!)$. For $\sigma = 1$, this is

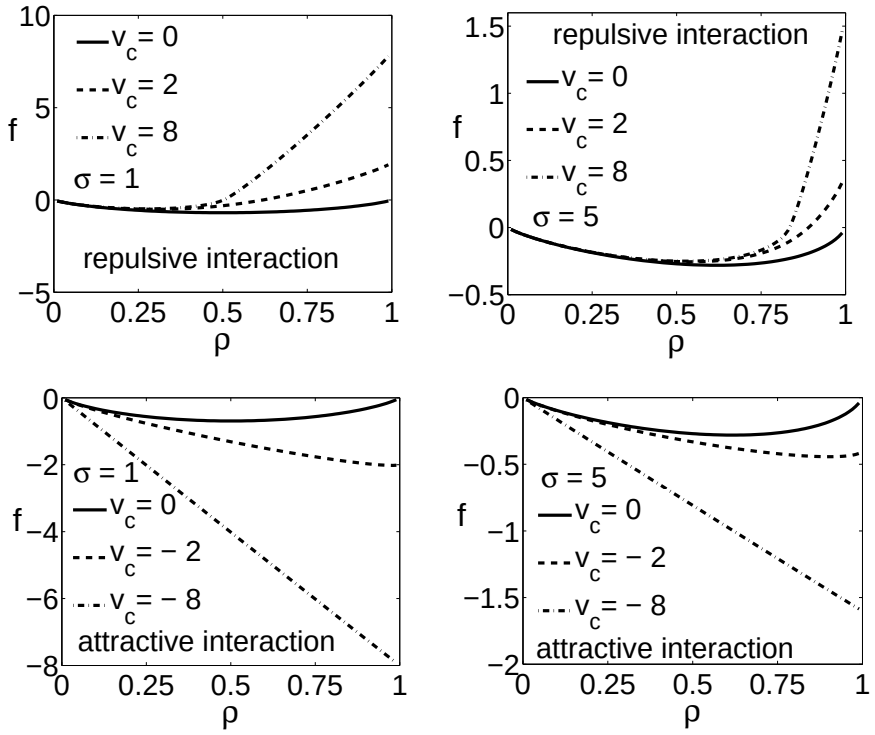

Figure 5.4: Free energy f per lattice site as a function of the coverage ρ for a homogeneous system of hard rods of sizes $\sigma = 1$ and 5, and various contact interactions v_c.

clearly maximal for equal number of particles and vacancies ($\rho = 1/2$), while for $\sigma > 1$, one has to take into account that $(N_{rod} + N_v)$ decreases with increasing ρ. Accordingly, the location of the entropy maximum occurs left to $\rho = \sigma/(\sigma + 1)$, where $N_{rod} = N_v$. In the interacting case, the coverage of maximum entropy moves to the left for increasing interaction strength, because the enhanced configurational restrictions for larger $|v_c|$ can be partly compensated by lowering ρ.

Because of absence of phase transitions in one dimension (if not considering "exotic" cases of interaction with particular long-range behavior [147]) the free energy shown in Fig. 5.4 does not show any peculiarities as a function of ρ. In the case of attractive interaction, it approaches the line $f \sim -|v_c|\rho/\sigma$ for large $|v_c|$ due to the aggregation of the rods into one cluster. For strong repulsive interactions, i.e. for v_c significantly larger than $v_c^\star$, the free energy essentially follows the (negative) entropy for $\rho \lesssim \sigma/(\sigma + 1)$, increases linearly for $\rho \gtrsim \sigma/(\sigma + 1)$ due to the linear increase of non-avoidable contacts until reaching $C_c v_c \simeq v_c/\sigma$ for $\rho \to 1$. In the case of repulsive interactions, the density $\rho = \sigma/(\sigma + 1)$ should also show up as a particular value in the behavior of the chemical potential, because the free energy amount to add a rod to the system is expected to increase strongly around this point.

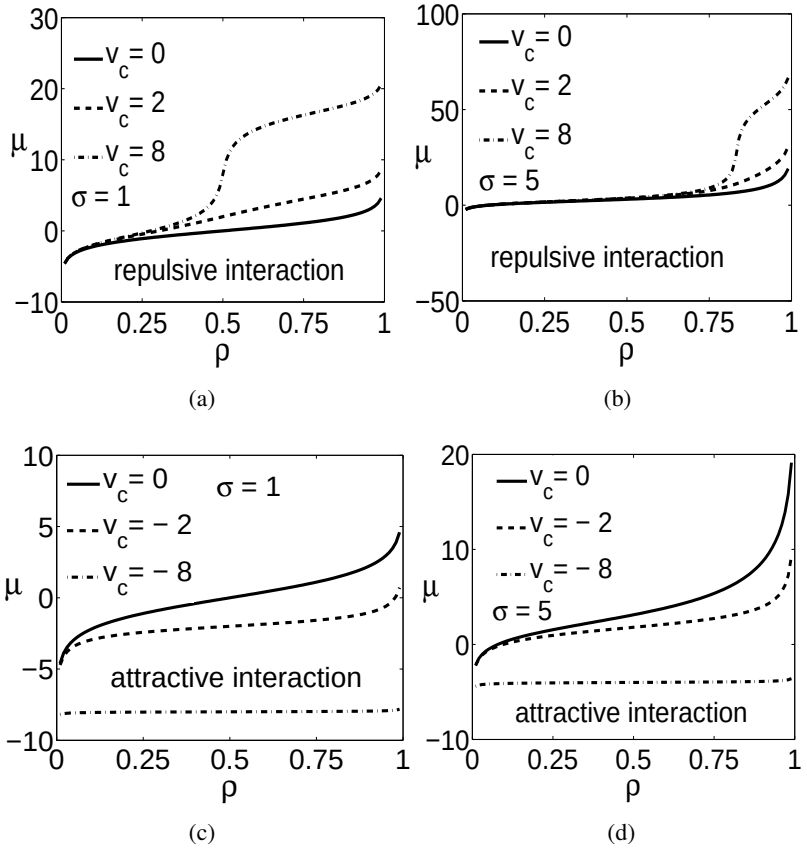

Figure 5.5: Chemical potential μ as a function of the coverage ρ for a homogeneous system of hard rods of sizes $\sigma = 1$ and 5, and various contact interactions v_c.

The chemical potential $\mu = \partial f / \partial \rho$ is given by

$$\mu = \ln\left\{\frac{\sigma C}{\rho e^{-v} e^{1-\sigma}}\right\} + \sigma \ln\left\{\left[\frac{1-\rho}{1-(\sigma+1)\rho/\sigma + C}\right]\right\} \tag{5.22}$$

and plotted in Fig. 5.5 as function of ρ. It indeed shows a step-like change around $\rho = \sigma/(\sigma+1)$ for strong repulsive interactions. For comparison the behavior for attractive interaction is also displayed in Fig. 5.5.

5.6 Conclusions

Our solution for the distribution of microstates of hard rod lattice gases with a general nearest-neighbor-range interaction potential provides a promising basis for future studies related to applications. For example, the results can be utilized to describe formation of molecular nanowires on surfaces, where molecules interact via van der Waals interactions and form hydrogen bonds when coming into contact.

In the model, such situation could be accounted for by an interaction profile $v_{i,j}$ with strong attractive interaction $v_{i,i+\sigma} < 0$ at contact distance σ and a smoothly decreasing, weaker attractive part for $\sigma < |i - j| < 2\sigma$. Also, based on experiences in other contexts, [53, 54] the explicit exact expressions for the density functionals should allow one to faithfully study the kinetics of wire formation by employing time-dependent density functional theory. Similarly, our results may be helpful in the future to treat diffusion of molecules through nanopores or membrane channels.

Our derivation of a fundamental measure form of the hard rod lattice gas with contact interaction enables a straightforward extension to higher dimensions. This should be useful to account for transitions between different phases in corresponding systems, which generally resemble nematic (and other) phases of liquid crystals. [148–150] It has been shown [61, 67] for athermal hard rod lattice gases ($v_{i,j} = 0$) that extensions to higher dimensions are a powerful means to treat corresponding phase transitions. Up to now, we did not succeed to identify fundamental measure forms for general nearest-neighbor-range interactions $v_{i,j}$. However, there seem to be other possibilities of extensions, which become exact under dimensional reduction. These will be explored elsewhere.

Considering the core in the derivation of the distribution of microstates, it is important to realize that the procedure can in principle be extended to interactions of longer range covering several rod lengths. For a given range ξ, the exclusion constraint leads to a natural decomposition of the set $\{\mathbf{n}\}_s = \{n_s, \ldots, n_{s-\xi}\}$ into ranges covering the lattice sites $s - \sigma + 1, \ldots, s$ (first range), $s - 2\sigma + 1, \ldots, s - \sigma$ (second range), and so on. In each of these ranges at most one occupation number can be equal to one. The total number of ranges that need to be taken into account is $\lceil \xi/\sigma \rceil$, where $\lceil x \rceil$ denotes the integer ceiling division, i.e. the smallest integer larger than x. Accordingly, we would need to consider higher-order correlators $C(1_{i_1}, 1_{i_2}, 1_{i_3}, \ldots, ...)$, where 1_{i_k}, specifies the location of the occupied site in the kth range as in Sec. 5.3.2. The distribution of microstates can then be expressed in term of these correlators $C(1_{i_1}, 1_{i_2}, 1_{i_3}, \ldots, ...)$ and the densities p_i. By equating with the Boltzmann formula for simple configurations, relations between the $C(1_{i_1}, 1_{i_2}, 1_{i_3}, \ldots, ...)$ and the p_i eventually can be obtained, which need to be solved for expressing the $C(1_{i_1}, 1_{i_2}, 1_{i_3}, \ldots, ...)$ in terms of the p_i.

Let us finally note that the rod length defines a length scale independent of the lattice spacing, which implies that a continuum limit of the results should be accessible. This and the possible extension to larger interaction ranges open new and challenging possibilities for further investigations.

Chapter 6

Hard rod mixtures with contact interactions

6.1 Introduction

In this chapter, we extend the results obtained for a simple hard rods with arbitrary nearest neighbour interactions [78,79] to the case of hard rod mixtures with contact interactions. The derivation is based on the strategy developed in chap. (4) for hard rod mixtures [77], where a sets of multi-component random variables were introduced to represent the different species of the rods. It was shown that these sets are very helpful in establishing a connection with the 0D cavity of the FMT.

Due to the finite range of the interactions and because of the one dimensional nature of the system, the latter fulfills the Markov chain property which allows to an exact derivation of the probability distributions of the microstates for a given density profiles. In analogy with the simple hard rods with contact interactions, we made a connection of our approach to the LFMT. The free energy functional contains two different contributions. One is due to the hard core exclusion encoded in the 1-particle cavity. The second is due to the contribution of the 2-particle cavity and it contains the effect of interactions. For rods of size one, previously derived results for Potts model were recovered [65]. Once we have the free energy functional, equilibrium thermodynamics can be derived using the DFT formalism. Some of the thermodynamic functions are presented at the end of the chapter.

6.2 Joint probability distributions

The mixture is considered to consist of q types of hard rods with length l_α, $\alpha = 1, \ldots, q$ in the presence of an external potential, where different types of rods could have the same lengths due to a different coupling to an external potential. The rods are located on a one-dimensional lattice with L sites and we set the lattice spacing equal to one. The lattice is defined in such a way that the ends of the rods coincide with lattice sites, Fig. 6.1. We introduce occupation numbers n_j^α, $j = 1, \ldots, L$,

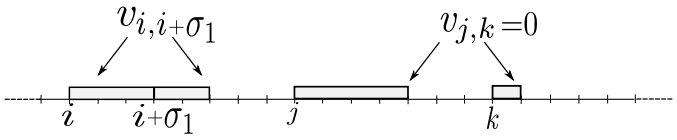

Figure 6.1: hard rods mixture of rods with different sizes interacting with a contact interaction.

$\alpha = 1, \ldots, q$, to specify the microstates of the mixture. If the left end of a rod of type α is at site j then $n_j^\alpha = 1$, while $n_j^\alpha = 0$ otherwise. The mutual exclusion of hard rods implies the constraint $n_k^\alpha n_j^\beta = 0$ for $j = k, \ldots, k + l_\alpha - 1$. A grand-canonical description is used, where the chemical potential μ specifies the mean numbers of rods in the system. The nearest neighbour rods interact through an interaction potential given by

$$v_{i,j}^{\alpha\beta} = \begin{cases} \infty & \text{for } i - j < l_\alpha \\ v^{\alpha\beta} & \text{for } i - j = l_\alpha \\ 0 & \text{for } i - j > l_\alpha \end{cases} \tag{6.1}$$

two rods interact only if they are in contact and the interaction strength $v^{\alpha\beta}$ depends on temperature and the type of the rods. In general $v^{\alpha\beta}$ depends as well on the positions of the two interacting rods and they are allowed to have positive or negative values. The Hamiltonian of the system is given by

$$\mathcal{H} = \sum_{\alpha,\beta} \sum_{i<j} v_{i,j}^{\alpha\beta} n_i^\alpha n_j^\beta + \sum_\alpha \sum_i u_i^\alpha n_i^\alpha \,, \tag{6.2}$$

To set up the Markov chain approach following [64], let us define as in chap. (4) a set multi-component state variables $\hat{n}_j = (n_j^1, \ldots, n_j^q)$ that can assume $q + 1$ basic states $\hat{e}_0, \ldots, \hat{e}_q$, where $\hat{e}_0$ refers to an empty site, i.e. $\hat{e}_0 = (0, \ldots, 0)$ and $\hat{e}_\alpha$, $\alpha = 1, \ldots, q$, refers to a site occupied by the rod of type α, i.e. $\hat{e}_\alpha = (0, \ldots, 1, \ldots, 0)$ with the 1 at the αth entry. The joint probability distributions $\chi(\hat{n}_1, \ldots, \hat{n}_L)$ of the microstates can be decomposed as

$$\chi(\hat{n}_1, \ldots, \hat{n}_L) = \prod_{k=1}^{L} \psi(\hat{n}_k | \hat{n}_{k-1}, \ldots, \hat{n}_1) \tag{6.3}$$

where $\psi(.|\ldots)$ denotes the corresponding conditional probabilities. Because of the finite range of the interactions and because we are dealing with a one dimensional system, the joint probabilities of microstates are simplified to

$$\chi(\hat{n}_1, \ldots, \hat{n}_L) = \prod_{k=1}^{L} \psi(\hat{n}_k | \hat{n}_{k-1}, \ldots, \hat{n}_{k-l_\alpha}) \tag{6.4}$$

To make the notation easier, we use the following notation $\{n_j^\alpha\}_k = \{n_j^\alpha | 1 \le \alpha \le q, k - l_\alpha + 1 \le j \le k\}$. In the set $\{\hat{n}_j\}_k$, at most two occupation numbers can be

one. In analogy with the FMT, the set $\{\hat{n}_j\}_k$ with one occupation number is equal to one and all others are 0 corresponds to the 1-particle cavity, and the set $\{\hat{n}_j\}_k$ with two occupation numbers are one is the 2-particle cavity. The 1-particle cavity results from the hard core exclusion however, the 2-particle cavity includes the effect of interactions. The previous properties of 1-particle and 2-particle cavities can be used to determine the conditional probabilities $\psi(n_k, \ldots, n_{k-l_\alpha})$ based on a simple probability considerations. This can be done as follows: the total conditional probabilities can be written as

$$\psi(\hat{n}_k = \hat{e}_\alpha | \{n_j^\beta\}_{k-1}) = \frac{\phi(\hat{n}_k = \hat{e}_\alpha, \{n_j^\beta\}_{k-1})}{\phi(\{n_j^\beta\}_{k-1})} \tag{6.5}$$

The joint probabilities can be decomposed as

$$\begin{aligned}
\phi(\hat{n}_k, \{n_j^\beta\}_{k-1}) = \phi(\hat{n}_k = \hat{e}_0, \{n_j^\beta = 0\}_{k-1}\})^{\left(1-\sum_\alpha \sum_{i=k-l_\alpha}^{k} n_i^\alpha + \sum_{\alpha,\beta} n_{k-l_\alpha}^\alpha n_k^\beta\right)} \\
\times \phi(\hat{n}_k = \hat{e}_\alpha, \{n_j^\beta = 0\}_{k-1}\})^{\left(n_k^\alpha - \sum_{\alpha,\beta} n_{k-l_\alpha}^\alpha n_k^\beta\right)} \\
\times \phi(\hat{n}_k = \hat{e}_0, \{n_j^\beta = 0/n_{k-l_\alpha}^\beta = 1\}_{k-1}\})^{\left(n_{k-l_\alpha}^\beta - \sum_{\alpha,\beta} n_{k-l_\alpha}^\alpha n_k^\beta\right)} \\
\times \phi(\hat{n}_k = \hat{e}_\alpha, \{n_j^\beta = 0/n_{k-l_\alpha}^\beta = 1\}_{k-1}\})^{n_k^\alpha n_{k-l_\beta}^\beta},
\end{aligned} \tag{6.6}$$

The notation $\{n_j^\beta = 0/n_i^\beta = 1\}_{k-1}$ means that all occupation numbers in the set $\{n_j^\beta\}_{k-1}$ are 0 except the one at site i ($n_i^\beta = 1$). The joint probabilities $\phi(n_{k-1}, \ldots, n_{k-l_\alpha})$ in the denominator appearing in Eq. (6.5) can be expressed in the same way with the only difference that the region of consideration now is $k-1, \ldots, k-l_\alpha$.
The joint probabilities of the decomposition of Eq. (6.6) can be written in terms of the mean occupation numbers p_i^α and correlators $C_{i,j}^{\alpha\beta}$ based on their definitions. The latter is defined by

$$C_{k-l_\alpha,k}^{\alpha\beta} = \langle n_{k-l_\alpha}^\alpha n_k^\beta \rangle = \phi(\hat{n}_k = \hat{e}_\alpha, \{n_j^\beta = 0/n_{k-l_\alpha}^\beta = 1\}_{k-1}) \tag{6.7}$$

and the former is given by

$$p_k^\alpha = \langle n_k^\alpha \rangle = \phi(\hat{n}_k = \hat{e}_\alpha, \{n_j^\beta = 0\}_{k-1}) + \sum_{\beta=1}^{q} C_{k-l_\alpha,k}^{\alpha\beta} \tag{6.8}$$

From the normalization condition, we have

$$\phi(\{n_j^\alpha = 0\}_k) + \sum_{\alpha=1}^{q} \sum_{j=k-l_\alpha}^{k} p_j^\alpha - \sum_{\alpha,\beta=1}^{q} C_{k-l_\alpha,k}^{\alpha\beta} = 1 \tag{6.9}$$

From Eqs. (6.8) , (6.7) and (6.9), we get the following expressions for the joint probabilities

$$\phi(\{n_j^\beta = 0\}_k) = 1 - \sum_{\alpha=1}^{q} \sum_{j=k-l_\alpha}^{k} p_j^\alpha + \sum_{\alpha,\beta=1}^{q} C_{k-l_\alpha,k}^{\alpha\beta} \tag{6.10a}$$

$$\phi(\hat{n}_k = \hat{e}_\alpha, \{n_j^\beta = 0\}_{k-1}) = p_k^\alpha - \sum_{\beta=1}^{q} C_{k-l_\alpha,k}^{\alpha\beta} \tag{6.10b}$$

$$\phi(\hat{n}_k = \hat{e}_0, \{n_j^\beta = 0/n_{k-l_\alpha}^\beta = 1\}_{k-1}) = p_{k-l_\alpha}^\beta - \sum_{\alpha=1}^{q} C_{k-l_\alpha,k}^{\alpha\beta} \tag{6.10c}$$

$$\phi(\hat{n}_k = \hat{e}_\alpha, \{n_j^\beta = 0/n_{k-l_\alpha}^\beta = 1\}_{k-1}) = C_{k-l_\alpha,k}^{\alpha\beta} \tag{6.10d}$$

Equations for the denominator are exactly the same, except that the upper limit of the sums k in Eq. (6.10a) has to be replaced by $(k-1)$. From the previous equations we get for the total conditional probabilities

$$\begin{aligned}\psi(\hat{n}_k|\{n_j^\beta\}_{k-1}) = &\left[p_k^\alpha - \sum_\beta C_{k-l_\alpha,k}^{\alpha\beta}\right]^{n_k^\alpha - \sum_\beta n_{k-l_\alpha}^\alpha n_k^\beta} \left[p_{k-l_\alpha}^\alpha - \sum_\beta C_{k-l_\alpha,k}^{\alpha\beta}\right]^{n_{k-l_\alpha}^\alpha - \sum_\beta n_{k-l_\alpha}^\alpha n_k^\beta} \\ &\times \left[C_{k-l_\alpha,k}^{\alpha\beta}\right]^{n_{k-l_\alpha}^\alpha n_k^\beta} \frac{\left[1 - \sum_\alpha \sum_{i=k-l_\alpha}^{k} p_i^\alpha + \sum_{\alpha,\beta} C_{k-l_\alpha,k}^{\alpha\beta}\right]^{1-\sum_\alpha \sum_{i=k-l_\alpha}^{k} n_i^\alpha + \sum_\beta n_{k-l_\alpha}^\alpha n_k^\beta}}{\left[\rho_{k-l_\alpha}^\alpha\right]^{n_{k-l_\alpha}^\alpha} \left[1 - \sum_\alpha \sum_{i=k-l_\alpha}^{k-1} p_i^\alpha\right]^{1-\sum_\alpha \sum_{i=k-l_\alpha}^{k-1} n_i^\alpha}}\end{aligned} \tag{6.11}$$

6.3 Correlators and density functionals

As a last step in determining the total joint probability distributions, we need to express the $C_{i,j}$ as functional of the p_i. This can be done by comparing joint probabilities $\chi(\mathbf{n})$ calculated from the approach described above with the Boltzmann probability for a few simple configurations $\mathbf{n}$

$$\chi(0_1, \ldots, 0_L) = \frac{1}{Z}, \tag{6.12a}$$

$$\chi(0_1, \ldots, 1_i^\alpha, \ldots, 0_L) = \frac{e^{-\tilde{u}_i^\alpha}}{Z}, \tag{6.12b}$$

$$\chi(0_1, \ldots, 1_j^\beta, \ldots, 1_i^\alpha, \ldots, 0_L) = \frac{1}{Z} e^{-(\tilde{u}_i^\alpha + \tilde{u}_j^\beta + v_{i,j}^{\alpha\beta})}, \tag{6.12c}$$

where $\tilde{u}_i^\alpha = u_i^\alpha - \mu^\alpha$. The expression (6.12c) is valid for $j - i = l_\alpha$. Inserting the joint probability distribution for each cases we get

$$C_{i,j}^{\alpha\beta} = \frac{[p_i^\alpha - \sum_\gamma C_{i,j}^{\alpha\gamma}][p_j^\beta - \sum_\gamma C_{i,j}^{\gamma\beta}]}{[1 - \sum_\gamma \sum_{k=i-l_\gamma}^{i} p_k^\gamma + \sum_{\delta,\gamma} C_{i,j}^{\delta\gamma}]} e^{-\beta v_{i,j}^{\alpha\beta}} \tag{6.13}$$

Based on the Gibbs-Bogoliubov inequality the density functional for N_α hard rods of type α in the external potential $U(\mathbf{n}) = \sum_{k,\alpha} u_k^\alpha n_k^\alpha$ is defined as

$$\begin{aligned}\Omega(\mathbf{p}) &= \sum_{\mathbf{n}} \chi_{\mathbf{p}}(\mathbf{n}) \left[k_B T \log \chi_{\mathbf{p}}(\mathbf{n}) + V(\mathbf{n}) + U(\mathbf{n}) - \sum_{\alpha=1}^{q} \mu_\alpha N_\alpha \right] \\ &= F(\mathbf{p}) + \sum_{k=1}^{L} \sum_{\alpha=1}^{q} (u_k^\alpha - \mu_\alpha) p_k^\alpha \end{aligned} \tag{6.14}$$

where $F(\mathbf{p}) = k_B T \sum_{\mathbf{n}} \chi_{\mathbf{p}}(\mathbf{n}) \log \chi_{\mathbf{p}}$ is the free energy functional and $V(\mathbf{n})$ is the interaction potential. Inserting $\chi_{\mathbf{p}}(\mathbf{n})$, one obtains

$$\begin{aligned} F[\rho^\alpha] = \sum_{\alpha,\beta} \sum_{i,j} v_{i,j}^{\alpha\beta} C_{i,j}^{\alpha\beta} + \sum_{s=1}^{L} \Bigg\{ & \sum_\alpha \Phi\Big(p_s^\alpha - \sum_\beta C_{s-l_\alpha,s}^{\alpha\beta}\Big) + \sum_{\alpha,\beta} \Phi\Big(C_{s-l_\alpha,s}^{\alpha\beta}\Big) \\ & + \Phi\Big(1 - \sum_\alpha \sum_{i=s-l_\alpha}^{s} p_i^\alpha + \sum_{\alpha,\beta} C_{s-l_\alpha,s}^{\alpha\beta}\Big) + \sum_\alpha \Phi\Big(p_{s-l_\alpha}^\alpha - \sum_\beta C_{s-l_\alpha,s}^{\alpha\beta}\Big) \\ & - \sum_\alpha \Phi(p_i^\alpha) - \Phi\Big(1 - \sum_\alpha \sum_{i=s-l_\alpha}^{s-1} p_i^\alpha\Big) \Bigg\} \end{aligned} \tag{6.15}$$

where $\Phi(x) := x \ln x$ Using the expression (6.13) to express the first term in the free energy functional as a functional of the density and the pair density, the free energy reduces to

$$\begin{aligned} F[\rho^\alpha] = \sum_{s=1}^{L} \Bigg\{ & \sum_\alpha p_s^\alpha \ln\Big(p_s^\alpha - \sum_\beta C_{s-l_\alpha,s}^{\alpha\beta}\Big) + \sum_\alpha p_{s-l_\alpha}^\alpha \ln\Big(p_{s-l_\alpha}^\alpha - \sum_\beta C_{s-l_\alpha,s}^{\alpha\beta}\Big) \\ & - \sum_\alpha p_{s-l_\alpha}^\alpha \ln p_{s-l_\alpha}^\alpha - \Big(1 - \sum_\alpha \sum_{i=s-l_\alpha}^{s-1} p_i^\alpha\Big) \ln\Big(1 - \sum_\alpha \sum_{i=s-l_\alpha}^{s-1} p_i^\alpha\Big) \\ & + \Big(1 - \sum_\alpha \sum_{i=s-l_\alpha}^{s} p_i^\alpha\Big) \ln\Big(1 - \sum_\alpha \sum_{i=s-l_\alpha}^{s} p_i^\alpha + \sum_{\alpha,\beta} C_{s-l_\alpha,s}^{\alpha\beta}\Big) \Bigg\} \end{aligned} \tag{6.16}$$

As for the mono-component case, the free energy functional has a clear interpretation in term of the lattice cavity theory. Let us construct the free energy functional of binary mixture of hard rods with length $l_1 = 3$ and $l_2 = 5$ and with contact

interactions diagrammatically. The set of maximum 0D cavities of this system is given by

$$\mathcal{W}_{max} = \left\{ \overset{\text{S}}{\circ}\!\!-\!\!\bullet\!\!-\!\!\bullet\!\!-\!\!\bullet\!\!-\!\!\bullet\!\!-\!\!\circ,\ \overset{\text{S}}{\circ}\!\!-\!\!\bullet\!\!-\!\!\bullet\!\!-\!\!\bullet\!\!-\!\!\bullet\!\!-\!\!\circ \right\} \tag{6.17}$$

The first diagram represents the 1-particle 0D cavity where rods of length 5 can be placed at any site of the cavity, whereas rods of length 3 can be placed only on the black sites, because placing a rod of length 3 at the white circle at one end of the cavity does not prevent a second rod to be placed at the white circle at the other end and this in contradiction with the definition of the 1-particle 0D cavity. The second diagram in (6.17) represents the 2-particles 0D cavity. The only combination which fulfills the dimensional reduction to 0D is

$$F_{1d}[\rho] = \sum_s \Big[\Phi_0(\overset{\text{S}}{\circ}\!\!-\!\!\bullet\!\!-\!\!\bullet\!\!-\!\!\bullet\!\!-\!\!\bullet\!\!-\!\!\circ) - \Phi_0(\overset{\text{S}}{\circ}\!\!-\!\!\bullet\!\!-\!\!\bullet\!\!-\!\!\bullet\!\!-\!\!\circ) \Big] \tag{6.18}$$

This can be understood in the following way; We denote the first and second term in (6.18) respectively by $F_{1d}^{(i)}, i = 1, 2$. Consider a 0D density profile which correspond to the 2-particle maximum cavity $\circ\!\!-\!\!\bullet\overset{t}{\bullet}\!\!-\!\!\bullet\!\!-\!\!\circ$ (choosing those of the 1-particle maximum cavity yields exactly the same results). Inserting this density in the first term of rhs of (6.18) yields

$$\begin{aligned} F_{1d}^{(1)}[\rho_{\circ\!-\!\bullet\overset{t}{\bullet}\!-\!\bullet\!-\!\circ}] = \sum_s \Big[& \Phi_0(\circ\!\!-\!\!\bullet\overset{t}{\bullet}\!\!-\!\!\bullet\!\!-\!\!\circ) + \Phi_0(\circ\!\!-\!\!\bullet\overset{t}{\bullet}\!\!-\!\!\bullet) + \Phi_0(\circ\!\!-\!\!\bullet\overset{t}{\bullet}\!\!-\!\!\circ) + \Phi_0(\circ\!\!-\!\!\bullet\!\!-\!\!\overset{t}{\circ}) \\ & + \Phi_0(\circ\overset{t-1}{\circ}) + \Phi_0(\overset{t-2}{\circ}) + \Phi_0(\circ\overset{t}{\bullet}\!\!-\!\!\bullet\!\!-\!\!\circ) + \Phi_0(\overset{t}{\circ}\!\!-\!\!\bullet\!\!-\!\!\bullet\!\!-\!\!\circ) \\ & + \Phi_0(\overset{t+1}{\circ}\!\!-\!\!\bullet\!\!-\!\!\circ) + \Phi_0(\overset{t+2}{\circ}\!\!-\!\!\circ) + \Phi_0(\overset{t+3}{\circ}) \Big] \end{aligned} \tag{6.19}$$

Inserting in the second term we find

$$\begin{aligned} F_{1d}^{(2)}[\rho_{\circ\!-\!\bullet\overset{t}{\bullet}\!-\!\bullet\!-\!\circ}] = \sum_s \Big[& \Phi_0(\Phi_0(\circ\!\!-\!\!\bullet\overset{t}{\bullet}\!\!-\!\!\bullet\!\!-\!\!\circ) + \Phi_0(\circ\overset{t}{\bullet}\!\!-\!\!\bullet\!\!-\!\!\bullet\!\!-\!\!\circ) + \Phi_0(\overset{t}{\circ}\!\!-\!\!\bullet\!\!-\!\!\bullet\!\!-\!\!\circ) + \Phi_0(\overset{t+1}{\circ}\!\!-\!\!\bullet\!\!-\!\!\circ) \\ & + \Phi_0(\overset{t+2}{\circ}\!\!-\!\!\circ) + \Phi_0(\overset{t+3}{\circ}) + \Phi_0(\circ\!\!-\!\!\bullet\!\!-\!\!\overset{t}{\circ}) + \Phi_0(\circ\overset{t-1}{\circ}) + \Phi_0(\overset{t-2}{\circ}) \Big] \end{aligned} \tag{6.20}$$

Subtracting the two equations (6.19) and (6.20) we get

$$\mathcal{F}_{1d}[\rho_{\circ\!-\!\bullet\overset{t}{\bullet}\!-\!\bullet\!-\!\circ}] = \Phi_0(\eta = \circ\!\!-\!\!\bullet\overset{t}{\bullet}\!\!-\!\!\bullet\!\!-\!\!\circ) \tag{6.21}$$

which is the exact excess free energy functional of the 0D cavity. We identify each part of the functionals as

$$\Phi_0(\overset{\text{s}}{\circ}\!\!-\!\!\bullet\!\!-\!\!\bullet\!\!-\!\!\bullet\!\!-\!\!\circ) = \sum_\alpha p^\alpha_{s-l_\alpha} \ln p^\alpha_{s-l_\alpha} + \Big(1 - \sum_\alpha \sum_{i=s-l_\alpha}^{s-1} p_i^\alpha\Big) \ln\Big(1 - \sum_\alpha \sum_{i=s-l_\alpha}^{s-1} p_i^\alpha\Big) \tag{6.22}$$

represents the contribution of the hard core interactions, and

$$\begin{aligned} \Phi_0(\overset{\text{s}}{\circ}\!\!-\!\!\bullet\!\!-\!\!\bullet\!\!-\!\!\bullet\!\!-\!\!\bullet\!\!-\!\!\circ) = & \sum_\alpha p_s^\alpha \ln\Big(p_s^\alpha - \sum_\beta C^{\alpha\beta}_{s-l_\alpha,s}\Big) + \sum_\alpha p^\alpha_{s-l_\alpha} \ln\Big(p^\alpha_{s-l_\alpha} - \sum_\beta C^{\alpha\beta}_{s-l_\alpha,s}\Big) \\ & + \Big(1 - \sum_\alpha \sum_{i=s-l_\alpha}^{s} p_i^\alpha\Big) \ln\Big(1 - \sum_\alpha \sum_{i=s-l_\alpha}^{s} p_i^\alpha + \sum_{\alpha,\beta} C^{\alpha\beta}_{s-l_\alpha,s}\Big) \end{aligned} \tag{6.23}$$

represents the contribution of the contact interactions.

The limit of the Potts model can be recovered from the hard rod mixtures with contact interactions by imposing $j - i = l_\alpha = 1$ in eqs (6.13) and (6.16) and we find

$$C_{i,j}^{\alpha\beta} = \frac{\left[\rho_i^\alpha - \sum_\gamma C_{i,j}^{\alpha\gamma}\right]\left[p_j^\beta - \sum_\gamma C_{i,j}^{\gamma\beta}\right]}{\left[1 - \sum_\gamma p_i^\gamma - \sum_\gamma p_j^\gamma + \sum_{\delta,\gamma} C_{i,j}^{\delta\gamma}\right]} e^{-\beta v_{i,j}^{\alpha\beta}} \tag{6.24}$$

For this case, the free energy functional reduces to

$$\begin{aligned} F[\rho^\alpha] = \sum_{s=1}^{L} \Bigg\{ & \sum_\alpha p_s^\alpha \ln\Big(p_s^\alpha - \sum_\beta C_{s-1,s}^{\alpha\beta}\Big) + \sum_\alpha p_{s-1}^\alpha \ln\Big(p_{s-1}^\alpha - \sum_\beta C_{s-1,s}^{\alpha\beta}\Big) \\ & + \Big(1 - \sum_\alpha p_{s-1}^\alpha - \sum_\alpha p_s^\alpha\Big) \ln\Big(1 - \sum_\alpha p_{s-1}^\alpha - \sum_\alpha p_s^\alpha + \sum_{\alpha,\beta} C_{s-1,s}^{\alpha\beta}\Big) \\ & - \sum_\alpha p_{s-1}^\alpha \ln p_{s-1}^\alpha - \Big(1 - \sum_\alpha p_{s-1}^\alpha\Big) \ln\Big(1 - \sum_\alpha p_{s-1}^\alpha\Big) \Bigg\} \end{aligned} \tag{6.25}$$

Eqs (6.24) and (6.25) coincide exactly with the results obtained by Buschle *et al* [65].

6.4 Thermodynamics of the system

Once we have the free energy functional, we can derive in principle all the thermodynamics of the system, using functional differentiation. The grand canonical free energy functional is given by

$$\Omega[\rho] = F[\rho] + \sum_{\alpha=1}^{q} \sum_{s=1}^{L} (u_s^\alpha - \mu^\alpha) p_s^\alpha \tag{6.26}$$

where $F[\rho]$ is given by the expression (6.25). A unique relation between the external potential and the density can be derived from the minimization of the grand canonical free energy functional ($\partial\Omega/\partial\rho = 0$). For the case of homogeneous hard rods we get

$$e^{-\beta(u^\alpha - \mu^\alpha)} = \frac{C^{\alpha\alpha}}{e^{-\beta v^{\alpha\alpha}} p^\alpha} \left[\frac{1 - \sum_\alpha l_\alpha p^\alpha}{1 - \sum_\alpha (l_\alpha + 1) p^\alpha + \sum_{\alpha,\beta} C^{\alpha\beta}}\right]^{l_\alpha} \tag{6.27}$$

For the in-homogeneous system, an equivalent relation needs to be derived numerically. The internal energy is

$$U = \langle \mathcal{H} \rangle = \sum_{\alpha,\beta} \sum_{s=1}^{L} C_{s,s-l_\alpha}^{\alpha\beta} v_{s,s-l_\alpha}^{\alpha\beta} + \sum_{\alpha=1}^{q} \sum_{s=1}^{L} u_s^\alpha p_s^\alpha \tag{6.28}$$

The entropy of the system is given by

$$S = -\sum_{\eta} \chi(\eta) \ln \chi(\eta) \tag{6.29}$$

where the sum extends over all possible configurations η. From the Boltzmann formula, we have

$$S[\rho] = -F[\rho] + \beta \langle \mathcal{H} \rangle \tag{6.30}$$

we get for the entropy

$$\begin{aligned} S[\rho^\alpha] = \sum_{s=1}^{L} \Bigg\{ & \sum_{\alpha,\beta} C^{\alpha\beta}_{s,s-l_\alpha} v^{\alpha\beta}_{s,s-l_\alpha} + \sum_{\alpha=1}^{q} u^\alpha_s p^\alpha_s - \sum_{\alpha} p^\alpha_s \ln\Big(p^\alpha_s - \sum_{\beta} C^{\alpha\beta}_{s-l_\alpha,s}\Big) \\ & - \Big(1 - \sum_{\alpha} \sum_{i=s-l_\alpha}^{s} p^\alpha_i\Big) \ln\Big(1 - \sum_{\alpha} \sum_{i=s-l_\alpha}^{s} p^\alpha_i + \sum_{\alpha,\beta} C^{\alpha\beta}_{s-l_\alpha,s}\Big) \\ & - \sum_{\alpha} p^\alpha_{s-l_\alpha} \ln\Big(p^\alpha_{s-l_\alpha} - \sum_{\beta} C^{\alpha\beta}_{s-l_\alpha,s}\Big) + \sum_{\alpha} p^\alpha_{s-l_\alpha} \ln p^\alpha_{s-l_\alpha} \\ & + \Big(1 - \sum_{\alpha} \sum_{i=s-l_\alpha}^{s-1} p^\alpha_i\Big) \ln\Big(1 - \sum_{\alpha} \sum_{i=s-l_\alpha}^{s-1} p^\alpha_i\Big) \Bigg\} \end{aligned} \tag{6.31}$$

A more detailed thermodynamical studies of the system need some numerical treatments. The extension of the free energy functional to higher dimensions will be very useful for studying phase transitions in colloidal systems and liquid crystals. It is well known that in higher dimensions, the hard rod mixtures exhibit an ordering transition even in the case where only athermal hard core interaction is present. This is due separately on the entropic effect and also on the demixing of the mixture (entropic demixing mechanism). The latter results from the depletion effect, where for a mixture of large and small rods, two large rods attract each other effectively due to the presence of a smaller ones. The entropic demixing mechanism can, e.g., drive a gas liquid transition in colloid-polymer mixtures [151, 152]. We are planning to go beyond these two effects, and looking for the case where a very short repulsive or attractive (contact) interactions are present. The latter is proven to be realistic for many condensed matter systems. Our density functionals for hard rod mixtures fulfill the requirement of the dimensional crossover namely that they are exact and they have been written in a fundamental measure form. This will permit us to construct an approximate density functionals in two and three dimensions and then use this functionals to study phase transformations in the previously mentioned systems. In addition, we believe that our method can be generalize to the case of hard rod mixtures with arbitrary nearest neighbour interactions.

Chapter 7

Pair density functional Theory

7.1 Introduction

There has been recently an enormous growth of research in studying the particles correlations in many body systems using the pair density matrix functional theory [153–166]. As for the standard DFT, a functional relation can be established between the density functionals and the pair particles density profiles. This has been done by generalizing the Hohenbeg-Kohn [84] and the Kohn-Sham theory [85] to the pair density [155, 156]. An extensive work is still going on to determine the exchange and correlations functionals as a functionals of the pair density. Since this theory has been developed for systems at zero temperature, we present in this chapter an extension of the theory to finite temperature systems. The reason is that for systems where the thermal fluctuation is equal or larger than the quantum fluctuation, the systems need or must be studied with finite temperature statistical models, depending on the strength of the thermal fluctuation [154, 167, 168]. Due to this, in this chapter we extend the lattice DFT to the pair level. Our proof is based on the Mermin recipe [86] in his extension of the Hohenberg-Kohn theory for an electron gas at finite temperature. We use a procedure suggested by Gonis *et al* [155, 156]. This procedure makes use of the invariance of the Hamiltonian under the two bodies partition. We will consider an in-homogeneous electron gas, but the prove is general and can be applied to any type of particles, bosonic or fermionic. The aim is to prove that there exists a free energy functional which depends uniquely on the pair particles density, independent of any external potential and fulfills the minimization requirement with respect to the pair density at thermal equilibrium. Next we will use the same approach to prove that the same theory holds for lattice systems. At the end of this chapter, we illustrate the general formalism for the case of a simple hard rods.

7.2 Generalization of the Mermin theory to the pair density

Let us consider an equilibrium in-homogeneous electrons gas at a finite temperature T, chemical potential μ, and external potential u_i. To simplify the demonstration, we consider the non-relativistic case. The same prove can be used for the generalization to spin dependent Hamiltonian.

The Hamiltonian of the system is given by

$$\mathcal{H} = -\sum_{i=1}^{M} \frac{1}{2}\nabla_i^2 + \frac{1}{2}\sum_{i<j} v_{i,j} + \sum_{i=1}^{M} u_i \tag{7.1}$$

the first term represents the kinetic energy. The Laplacian operator is defined in 3-dimensional space by

$$\nabla_i^2 = \frac{\partial^2}{\partial x_i^2} + \frac{\partial^2}{\partial y_i^2} + \frac{\partial^2}{\partial z_i^2} \tag{7.2}$$

$v_{i,j} = 1/|\mathbf{r}_i - \mathbf{r}_j|$ is the interaction potential between electrons located at position i and j. M is the total number of electrons. For avoiding problems with the partition of the system, consider that M is either even or infinite number. We block the electrons to non-overlapping pairs in such a way that each electron belong only to one pair. The new Hamiltonian $\mathcal{H}_p$ is

$$\mathcal{H}_p = -\sum_{I=1}^{N} \frac{1}{2}\nabla_I^2 + \frac{1}{2}\sum_{I<J} V_{I,J} + \sum_{I=1}^{N} U_I \tag{7.3}$$

$N = M/2$ is the number of pairs of electrons. The electron pairs in 3-dimensional space can be seen as an effective single particles in 6-dimensional space spanned by the coordinate $\mathbf{x}_I = (\mathbf{r}_{i_1}, \mathbf{r}_{i_2})$. The kinetic energy of the single effective particles is defined via the 6-dimensional Laplacian operator

$$\nabla_I^2 = \nabla_{\mathbf{x}}^2 = \nabla_{i_1}^2 + \nabla_{i_2}^2 \tag{7.4}$$

The inter-particle potential becomes

$$\begin{aligned} V_{IJ} &= V(\mathbf{x}_I, \mathbf{x}_J) = V(\mathbf{r}_{i_1}, \mathbf{r}_{i_2}, \mathbf{r}_{j_1}, \mathbf{r}_{j_2}) \\ &= \frac{1}{|\mathbf{r}_{i_1} - \mathbf{r}_{j_1}|} + \frac{1}{|\mathbf{r}_{i_1} - \mathbf{r}_{j_2}|} + \frac{1}{|\mathbf{r}_{i_2} - \mathbf{r}_{j_1}|} + \frac{1}{|\mathbf{r}_{i_2} - \mathbf{r}_{j_2}|} \end{aligned} \tag{7.5}$$

and the external potential applied on a pair of particles is

$$U_I = U(\mathbf{x}_I) = U(\mathbf{r}_{i_1}, \mathbf{r}_{i_2}) = v(\mathbf{r}_{i_1}) + v(\mathbf{r}_{i_2}) + \frac{1}{|\mathbf{r}_{i_2} - \mathbf{r}_{i_1}|} \tag{7.6}$$

The pair electrons density is defined by

$$\rho(\mathbf{x}_I) = \rho(\mathbf{r}_{i_1}, \mathbf{r}_{i_2}) = \mathrm{Tr}\left[\Gamma \psi_p^{\star}(\mathbf{x}_I)\psi_p(\mathbf{x}_I)\right] \tag{7.7}$$

where the wave functions $\psi_p(\mathbf{x}_I)$ are a solutions of the effective single particle Schrödinger equation [155, 156]

$$\mathcal{H}_p\psi_p(\mathbf{x}_1,\ldots,\mathbf{x}_N) = E_p\psi_p(\mathbf{x}_1,\ldots,\mathbf{x}_N) \tag{7.8}$$

Γ is the reduced density matrix operator. It is defined by

$$\Gamma = \psi_p^\star(\mathbf{x}_I)\psi_p(\mathbf{x}_I) \tag{7.9}$$

and fulfills the normalization condition

$$\mathrm{Tr}\Gamma = 1 \tag{7.10}$$

At equilibrium, the grand canonical density matrix operator is given by

$$\Gamma = e^{-(\mathcal{H}_p-\bar{\mu}N)}/\mathrm{Tr}e^{-(\mathcal{H}_p-\bar{\mu}N)} \tag{7.11}$$

$\bar{\mu} = \mu/2$ is the chemical potential of the effective system. Using the same logic of Mermin (chap. 2) we arrive to the results that for arbitrary Γ, we have

$$\Omega[\Gamma^0] \leq \Omega[\Gamma] \tag{7.12}$$

Γ^0 is the equilibrium density matrix. A second result is that there is a unique relation between the pair density and external potential

$$\rho(\mathbf{r}_{i_1},\mathbf{r}_{i_2}) \longleftrightarrow U(\mathbf{r}_{i_1},\mathbf{r}_{i_2}) \tag{7.13}$$

The same formalism holds in classical statistical mechanics. The equivalence of the thermal equilibrium density matrix, the joint probability distributions

$$f^0(\mathbf{x},\ldots,\mathbf{x}_N,\mathbf{p}_1,\ldots,\mathbf{p}_N) = \frac{e^{-(\mathcal{H}_p-\bar{\mu}N)}}{Z} \tag{7.14}$$

where the partition function is given by

$$Z = \mathrm{Tr}_{cl}\left[exp(-(\mathcal{H}_p-\bar{\mu}N))\right] \tag{7.15}$$

The trace here denotes an integration over phase space coordinates (positions and momenta). The quantities f^0, $\mathcal{H}_p$ and N in the last formula are c-number, whereas in the quantum case they represent quantum operators and the trace is defined as a sum over the diagonal elements of the matrix. A similar relation can be derived for the grand potential

$$\begin{aligned}\Omega[f^0] &= \mathrm{Tr}_{cl}\left[f^0\left(\mathcal{H}_p-\bar{\mu}N+\frac{1}{\beta}\log f^0\right)\right]\\ &= F[\rho(\mathbf{x}_I)] + \int d\mathbf{x}\rho(\mathbf{x}_I)(U(\mathbf{x}_I)-\bar{\mu})\end{aligned} \tag{7.16}$$

Using the Gibbs-Bogoliubov for the grand functional (7.16), we arrive to the minimization principle.

$$\Omega[f^0] \leq \Omega[f] \tag{7.17}$$

where f is probability densities such that

$$\mathrm{Tr}_{cl}f = 1 \tag{7.18}$$

7.3 Lattice pair density functional Theory

To construct a pair DFT for lattice systems, let us for simplicity consider a one dimensional lattice gas with finite range nearest neighbour interactions. The proof presented here is general and can be applied for other systems and in higher dimensions. The system consists of M particles distributed on one dimensional lattice of L sites. The microstates are described by a set of occupation numbers $n_i, i = 1, \ldots, L$ which can be either 0 if the site is empty or 1 if the site is occupied. The lattice Hamiltonian of this system is given by

$$\mathcal{H} = \sum_{i<j} v_{i,j} n_i n_j + \sum_{i=1}^{L} u_i n_i \tag{7.19}$$

where u_i is the external potential at site i and $v_{i,j}$ is the interaction potential between particle located at site i and particle located at site j. We use the invariance of the Hamiltonian of the system under the partitioning into subsystems of two particles. If we partition our system into pair of successive particles (In order to avoid problem of partition, consider that we have an even or infinite number of particles) and re-write the Hamiltonian in terms of these pairs, we get

$$\mathcal{H}_p = \sum_{I<J} V_{IJ} n_I n_J + \sum_{I=1}^{L/2} U_I n_I \tag{7.20}$$

The inter-particle potential becomes

$$V_{IJ} = V_{i,j,k,l} = v_{i,k} + v_{i,l} + v_{j,k} + v_{j,l} \tag{7.21}$$

because we have a system with nearest neighbour interactions, the effective inter-particle potential reduces to

$$V_{IJ} = v_{j,k} \tag{7.22}$$

the external potential for the new effective system is given by

$$U_I = U_{i,j} = u_i + u_j + v_{i,j} \tag{7.23}$$

n_I is a random variable of two components characterizing the occupation numbers of the pair of sites. $n_I = n_{i,j} = (n_i, n_j)$ can be seen as single random variable, with i and j is coordinate of the effective single particle. It is equal to one if an effective particle is located at (i, j) and zero else. The equilibrium state of the system in a finite temperature grand canonical ensemble is described by the probability distribution function

$$P_0(n_{\mathbf{1}}, \ldots, n_{\mathbf{L}}) = \frac{\exp(-\beta(\mathcal{H}_p - \bar{\mu}N))}{Z} \tag{7.24}$$

where the numbers $(\mathbf{1}, \ldots, \mathbf{L})$ refer to all possible pair of sites. $\beta = 1/kT$, k_B is the Boltzmann constant and T is the temperature. $\bar{\mu} = \mu/2$ is chemical potential of the

effective system and the index 0 denotes the equilibrium state. The grand canonical partition function is given by

$$Z = \mathrm{Tr}\left[exp(-\beta(\mathcal{H}_p - \bar{\mu}N))\right] \tag{7.25}$$

The trace is a summation over all possible configurations of the system. The grand potential is given by

$$\Omega = \mathrm{Tr}\left[P\left(\mathcal{H}_p - \bar{\mu}N + \frac{1}{\beta}\log P\right)\right] \tag{7.26}$$

which can be written as

$$\Omega[\rho] = F[\rho] - \sum_I \rho_I(U_I - \bar{\mu}) \tag{7.27}$$

P is probability density of trace equals to unit and

$$F[\rho] = \mathrm{Tr}\left[P_0\left(\sum_{I<J} V_{IJ}n_I n_J + \frac{1}{\beta}\log P_0\right)\right] \tag{7.28}$$

Now with the previous definition and the Mermin theory, it is straightforward to prove the two conditions (*i*) that $\Omega[\rho]$ fulfills the minimization principle with respect to the pair density

$$\Omega[P_0] < \Omega[P] \tag{7.29}$$

and (*ii*) that the pair density ρ_I is uniquely determines the effective external potential U_I.

$$\rho_{i,j} \longleftrightarrow U_{i,j} \tag{7.30}$$

We shown that for a lattice system at finite temperature, the free energy functional can be set up as a unique functional of the pair density. At equilibrium, this free energy functional is minimum and equals to the grand canonical free energy functional.

7.4 Pair density functional theory for hard rods

We consider here as an example the simple hard rods. The lattice is defined in such a way that the ends of the rods coincide with lattice sites. A set of occupation numbers n_j, $j = 1, \ldots, L$, are introduced to specify the microstates of the system. If the left end of a rod is at site j then $n_j = 1$, while $n_j = 0$ otherwise. The mutual exclusion of hard rods implies the constraint $n_k n_j = 0$ for $j = k, \ldots, k + l - 1$. In a grand-canonical description the chemical potentials μ specify the mean numbers of rods. Fixed boundary conditions are considered here where site 0 and $L + 1$ are supposed to be occupied by a rod. Here we assume that $\beta = 1/k_B T = 1$ where T is the temperature and k_B is the Boltzmann constant. The invariance of

the Hamiltonian under the partition of the system into pair of rods permits us to use the method outlined in [64, 65, 77].

Let us calculate the joint probability distributions of the effective system associated with the Hamiltonian (7.19). Because we are dealing with a Markov process of order l, the joint probabilities distribution can be decomposed as

$$\chi(n_1, \ldots, n_L) = \prod_{k=1}^{L} \psi(n_k | n_{k-1}, \ldots, n_{k-l+1}) \tag{7.31}$$

where the conditional probabilities are defined by $\psi(a|b) = \phi(a, b)/\phi(b)$, and $\phi()$ is the joint probabilities.

For our effective system, the Markov chain property implies that if there is an effective single particle in a position (i, j) of a two-dimensional lattice (which means that a pair of rods are located at positions i and j on one dimensional lattice), no other particle can be at sites located on rectangular lattice of length $i - j$ and width l where (i, j) is the bottom-left corner of the square. The expression (7.31) becomes

$$\chi(n_{\mathbf{1}}, \ldots, n_{\mathbf{L}}) = \prod_{(k,m)=(1,1)}^{(L,L)} \psi(n_{k,m} | n_{k-1,m}, \ldots, n_{k-l+1,m}, n_{k,m-1}, \ldots, n_{k-l+1,m-l+1}) \tag{7.32}$$

The joint probabilities can be calculated based on the following considerations. By definition, the pair density $C_{i,j}$ is given by

$$C_{i,j} = \langle n_i n_j \rangle \tag{7.33}$$

The normalization condition reads

$$\phi(0_{k,m}, \ldots, 0_{k-l+1,m-l+1}) + \sum_{(i,j)=(k-l+1,m-l+1)}^{(k,m)} C_{i,j} = 1 \tag{7.34}$$

From eqs (7.33) and (7.34) we get

$$\psi(n_{k,m} | n_{k-1,m} = 0, \ldots, n_{k-l+1,m-l+1} = 0) = \begin{cases} \frac{1 - \sum_{(i,j)=(k-l+1,m-l+1)}^{(k,m)} C_{i,j}}{1 - \sum_{(i,j)=(k-l+1,m-l+1)}^{(k-1,m)} C_{i,j}} & \text{if } n_{k,m} = 0 \\ \\ \frac{C_{k,m}}{\sum_{(j=k-l+1,m-l+1)}^{k-1,m} C_{i,j}} & \text{if } n_{k,m} = 1 \end{cases} \tag{7.35}$$

and we get for the total conditional probabilities

$$\psi(n_{k,l} | x_{k-1,1}, \ldots, x_{k-l+1,m-l+1}) = (C_{k,m})^{n_{k,m}} \frac{\left[1 - \sum_{(i,j)=(k-l+1,m-l+1)}^{(k,m)} C_{i,j}\right]^{1 - \sum_{(i,j)=(k-l+1,m-l+1)}^{(k,m)} C_{i,j}}}{\left[1 - \sum_{(i,j)=(k-l+1,m-l+1)}^{(k-1,m)} C_{i,j}\right]^{1 - \sum_{(i,j)=(k-l+1,m-l+1)}^{(k-1,m)} C_{i,j}}} \tag{7.36}$$

Based on the Gibbs-Bogoliubov inequality the density functional for N hard rods in an external potential $U(\mathbf{n}) = \sum_k u_k n_k$ is defined as

$$\begin{aligned}\Omega[\mathbf{C}] &= \sum_{\mathbf{n}} \chi_{\mathbf{C}}(\mathbf{n}) \left[k_{\mathrm{B}} T \log \chi_{\mathbf{C}}(\mathbf{n}) + U(\mathbf{n}) - \mu N\right] \\ &= F[\mathbf{C}] + \sum_{I=\mathbf{1}}^{\mathbf{L}} \tilde{U}_I C_I \end{aligned} \tag{7.37}$$

where $F[\mathbf{C}] = k_{\mathrm{B}} T \sum_{\mathbf{n}} \chi_{\mathbf{C}}(\mathbf{n}) \log \chi_{\mathbf{C}}$ is the free energy functional and $\tilde{U}_I = U_I - \bar{\mu}$. Inserting the expression for the joint probabilities in eq (7.37) we get for the pair free energy functional

$$\begin{aligned}F[C] = \sum_{(k,m)=\mathbf{1}}^{\mathbf{L}} \Big\{ & C_{k,m} \left(\log C_{k,m} - 1\right) + \tilde{C}^{(1)}_{k,m} + \left(1 - \tilde{C}^{(1)}_{k,m}\right) \log\left(1 - \tilde{C}^{(1)}_{k,l}\right) \\ & - \tilde{C}^{(0)}_{k,m} - \left(1 - \tilde{C}^{(0)}_{k,m}\right) \log\left(1 - \tilde{C}^{(0)}_{k,m}\right) \Big\} \end{aligned} \tag{7.38}$$

where the weighted pair densities are given by

$$\tilde{C}^{(0)}_{k,l} = \sum_{(i,j)=(k-l+1,m-l+1)}^{(k-1,m)} C_{i,j} \tag{7.39}$$

and

$$\tilde{C}^{(1)}_{k,m} = \sum_{(i,j)=(k-l+1,m-l+1)}^{(k,m)} C_{i,j} \tag{7.40}$$

In eq (7.38) we made use the following relation

$$\sum_{(i,j)=(k-l+1,m-l+1)}^{(k,m)} C_{i,j} = \sum_{(i,j)=(k-l+1,m-l+1)}^{(k-1,m)} C_{i,j} + \sum_{j=m-l+1}^{l} C_{i,j} \tag{7.41}$$

The same as for the standard DFT, the pair free energy functional is composed of an effective ideal gas part

$$F_{id}[C] = \sum_{(k,m)=\mathbf{1}}^{\mathbf{L}} C_{k,m} \left(\log C_{k,m} - 1\right) \tag{7.42}$$

and an excess part

$$\begin{aligned}F_{exc}[C] = \sum_{(k,m)=\mathbf{1}}^{\mathbf{L}} \Big\{ & \tilde{C}^{(1)}_{k,m} + \left(1 - \tilde{C}^{(1)}_{k,m}\right) \log\left(1 - \tilde{C}^{(1)}_{k,m}\right) \\ & - \tilde{C}^{(0)}_{k,m} - \left(1 - \tilde{C}^{(0)}_{k,m}\right) \log\left(1 - \tilde{C}^{(0)}_{k,m}\right) \Big\} \end{aligned} \tag{7.43}$$

The pair excess free energy functional has the same form as the fundamental measure functionals and hence can be extended to higher dimensions by the procedure

suggested by Lafuente and Cuesta [61, 62, 67, 68]. To do this, let us re-write the excess pair free energy functionals (7.43) in the following form

$$F_{exc}[C] = \sum_{k,m} \mathcal{D}_j \left[\omega^{(j)}_{k,m} * C_{k,m} + \left(1 - \omega^{(j)}_{k,m} * C_{k,m}\right) \log\left(1 - \omega^{(j)}_{k,m} * C_{k,m}\right)\right] \quad (7.44)$$

the weight functions are defined by $\omega^{(j)}_{k,m} = \omega^{(j)}_{k} \omega_m$ with

$$\omega^{(j)}_{k} = \begin{cases} 1 & \text{if } l-1 \leq k \leq 1-j \\ 0 & \text{else} \end{cases} \quad (7.45)$$

and

$$\omega_{m} = \begin{cases} 1 & \text{if } l-1 \leq m \leq 1 \\ 0 & \text{else} \end{cases} \quad (7.46)$$

the approximate pair excess free energy functional in d-dimensional lattice are given by

$$F_{exc}[C_{\mathbf{k},\mathbf{m}}] = \quad (7.47)$$
$$\sum_{\mathbf{k},\mathbf{m}} \mathcal{D}_{\mathbf{j}} \left[\omega^{(\mathbf{j})}_{\mathbf{k},\mathbf{m}} * C_{\mathbf{k},\mathbf{m}} + \left(1 - \omega^{(\mathbf{j})}_{\mathbf{k},\mathbf{m}} * C_{\mathbf{k},\mathbf{m}}\right) \log\left(1 - \omega^{(\mathbf{j})}_{\mathbf{k},\mathbf{m}} * C_{\mathbf{k},\mathbf{m}}\right)\right]$$

where $j \in \{0,1\}^d$, $\mathbf{k} = (k_1, \ldots, k_d)$ and $\mathbf{m} = (m_1, \ldots, m_d)$. The d-dimensional difference operator is given by $\mathcal{D}_{\mathbf{j}} \equiv \prod_{i=1}^{d} \mathcal{D}_{j_i}$ and the d-dimensional weight functions are defined by $\omega^{(\mathbf{j})}_{\mathbf{k},\mathbf{m}} \equiv \prod_{i=1}^{d} \omega^{(j_i)}_{k_i} \omega_{m_i}$. The approximate functionals in higher dimension fulfill the requirement that an exact functionals are recovered under the dimensional reduction to 0 or 1 dimension [61, 62, 67, 68].
This complete the extension of the Markov DFT to the pair level. Our results shown that the lattice free energy functional can be written uniquely as functional of the pair particles density profiles and that it has the same form as fundamental measure functionals and this makes it possible to extend the free energy functional to higher dimensions.

Chapter 8

Steady state dynamics of hard rods with contact interactions

8.1 Introduction

Driven transport of rods in one-dimensional lattice have attracted recently much interest because of its applications in condensed matter and biophysics. It has been introduced as a model for protein synthesis, where the RNA is modeled as a one dimensional lattice and the ribosomes as rods (because the ribosome covers several codons considered here as lattice sites). It can describe also the diffusion of ions (rods of size one) or large molecules such DNA through nano-channels [169, 170]. An important model in this field is the asymmetric simple exclusion process (ASEP) which constitutes one of the few models in non-equilibrium statistical mechanics that can be solved exactly [171–174] and it provides insight to a wide range of complex physical phenomena. It describes the diffusion of particles along one-dimensional lattice. An interesting aspect of the ASEP is that it can be mapped onto a problem of spin dynamics [175, 176]. This implies that a variety of powerful methods developed in the field of spin dynamics can be applied also to study, the driven transport phenomena. Utilizing this connection, it was possible to trait the dynamics of simple and hard rod mixture with periodic boundary conditions via the matrix product algebra [177, 178] and the Bethe ansatz [179, 180]. In appropriate limits, the corresponding results reproduce those of the standard ASEP earlier obtained by other methods. These methods include mean-field and Monte Carlo simulation [181–184]. However, exact solutions are lacking for open systems.

Despite that the pure hard core exclusion is proved to be very useful, there are still many physical situations where the molecules interact with an additive (attractive or repulsive) short range interactions [74, 185]. An example is the transport of DNA or protein through nanofluidic channels where it has been proved that these molecules have sticky ends [186]. In this chapter, we study the steady state dynamics of hard rods with contact interactions on a periodic and open lattice within the

lattice time dependent density functional theory (LTDFT).

8.2 ASEP and its generalizations

The ASEP is one of the simplest non-equilibrium statistical mechanics models which is known to be exactly solvable [171, 187–189]. It describes the asymmetric diffusion of hard core particles in a one-dimensional lattice of L sites. The microstates of the system are described by a set of random variables $n_i, i = 1, \ldots, L$ which specify the occupation at site i. It is one ($n_i = 1$) if site i is occupied by a particle and zero ($n_i = 0$) else. The particles jump to the left with probability p and to the right with probability q, providing that the target site is empty. The hard core constraint prevents two particles to be at the same site. In general the transition rates p and q are different and sites dependent. For the case where $p = 0$, particles jump only in one direction and the model is named the totally asymmetric simple exclusion process (TASEP). For a system with periodic boundary condition Fig (8.1(a)), the particles number is conserved, and the steady state of the ASEP is particularly simple [172]. However for the case of open boundaries, the system is connected to two reservoirs at the left and right ends. The dynamics at the two boundaries is defined as fellow: Particles can enter the lattice at the first site with rate α if the latter is empty and exit with rate δ if it is occupied. The same dynamics holds at the last site L, where particles can exit the lattice with rate β if site L is occupied and enter the lattice with rate γ if it is empty Fig (8.1(b)). The steady state dynamics can be investigated by solving the master equation of the system

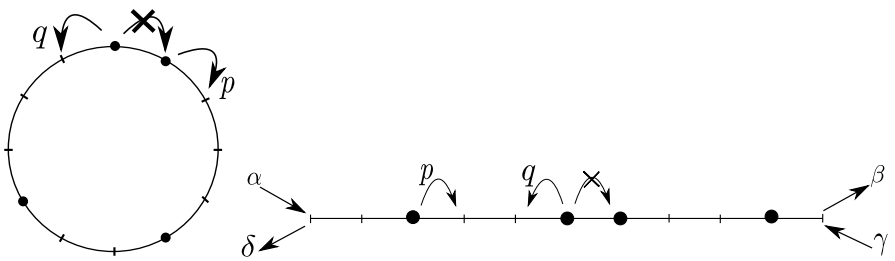

Figure 8.1: Asymmetric simple exclusion process, (*a*): periodic system, (*b*) open system.

which describes the time evolution of the probability distributions of microstates. It is given by

$$\frac{\mathrm{d}P_C}{\mathrm{d}t} = \sum_{C'} \left[W_{C'C} P_{C'} - W_{CC'} P_C \right] \tag{8.1}$$

P_C is the joint probability of configuration C and $W_{CC'}$ is the transition rate from C to C' which fulfills $\sum_{C'} W_{CC'} = 1$. In the steady states, the probability distributions P_C is independent of the time, and the corresponding steady states properties of the

system have to be determined from the equation:

$$\sum_{C'} W_{C'C} P_{C'} = \sum_{C} W_{CC'} P_C \tag{8.2}$$

which is named the detailed balance condition and it means that the probabilities of entering and leaving any configuration at a time interval dt are equal.
Different methods have been used to investigate the steady states properties of this model such as the matrix product algebra [171, 190], Bethe Ansatz [175], mean field theory and Monte Carlo simulations [189]. All of them are based on solving eq (8.1) to find the steady state distributions $P_{steady}(C)$ from which the steady state properties can be calculated in similar way to equilibrium properties, namely by averaging over $P_{steady}(C)$ [172]. An interesting aspect in the results for the exclusion process is the boundary induced phase transitions [191]. It has been shown that by varying the boundaries parameters, the system undergoes a phase transitions from one to another of the following phases

$$\begin{array}{ll}
\textit{Phase I} : \textit{MC} & \\
\quad j = \frac{1}{4}, \quad \rho = \frac{1}{2}, & \text{for } \alpha, \beta > \frac{1}{2} \\
\textit{Phase II} : \textit{HD} & \\
\quad j = \beta(1-\beta), \quad \rho = 1-\beta, & \text{for } \beta < \alpha < \frac{1}{2} \\
\textit{Phase III} : \textit{LD} & \\
\quad j = \alpha(1-\alpha), \quad \rho = \alpha, & \text{for } \alpha < \beta < \frac{1}{2}
\end{array} \tag{8.3}$$

As it is shown in Fig (8.2), the phase diagram consists of three phases: maximum

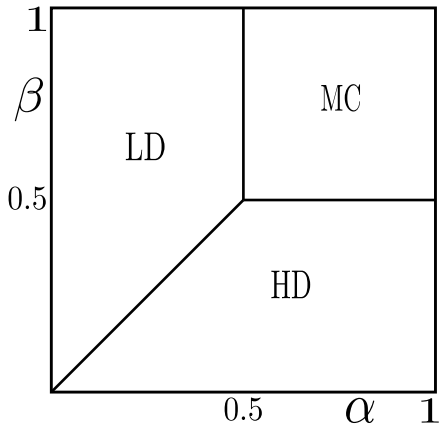

Figure 8.2: Phase diagram of the totally asymmetric simple exclusion process.

current (MC), high density (HD) and low density (LD). The lines $\alpha = 1/2, \beta > 1/2$ and $\beta = 1/2$, $\alpha > 1/2$ are second order phase transitions lines (ρ is continuous) and the line $\alpha = \beta < 1/2$ is first order phase transitions (ρ is discontinuous). The exclusion process with the most general boundaries conditions where the particles are allowed to enter and exit the lattice at the two ends with arbitrary transition rates has been investigated exactly using the Bethe ansatz [175, 192].

The ASEP has been generalized to the case of particles with different species. The case of two species has been treated with mean field and Monte Carlo simulation [193, 194]. An exact solution for this model based on the matrix product algebra has been done by Kolomeisky [195]. The case of N species ASEP was solved exactly using the matrix product algebra [196, 197].

Another interesting generalization of the ASEP is the case where particles have size l greater than one (hard rods). This model has been extensively studied recently because of potential applications in biophysics such as the translation process in protein synthesis. The model consists of particles which cover l lattice sites and move by one lattice site. The totally asymmetric case of this model (which is the more realistic case for many biophysical applications) has been studied using mean field theory and Monte Carlo simulation for open and periodic boundary conditions [181–184]. An exact solution is available for the case of periodic system using the Bethe ansatz and the matrix product ansatz [177–180], however non exact solutions are available for the case of open boundaries.
The phase diagram Fig. (8.4) has qualitatively the same form as the standard TASEP except that the critical point $(1/2, 1/2)$ is shifted to $(1/(1+\sqrt{l}), 1/(1+\sqrt{l}))$. Of particular interest is the case of ASEP with short ranged interactions. This model has been studied using the extremal principle by Hager *et al* [198] and within lattice LTDFT by Dierl *et al* [53, 54] for general open boundaries, and the results were in good agreements with kinetic Monte Carlo simulations. The current-density relation is shown to have two maxima and these leads to an interesting structure for the phase diagram which has seven different phases: two maximum current phases, two high density phases, two low density phases and a new minimal current phase.

8.3 Steady state dynamics of hard rods

8.3.1 Lattice Time Dependent Density Functional Theory

In this section, we will employ the lattice LTDFT to investigate the steady state dynamics of hard rods with contact interactions. The LTDFT is based on the local equilibrium approximation which states that the equilibrium properties of the system still valid locally in time for non-equilibrium system. This allows us to approximate the non-equilibrium two-point correlator by the corresponding equilibrium one. This approximation has been widely used in many applications for time dependent phenomena and the results were in good agreements with kinetic Monte Carlo simulations [53, 54].

As mentioned in the introduction of this chapter, our system is considered to consist of N rods of length l, distributed on a one dimensional lattice of L sites. We will focus here on the case of TASEP with both periodic and open and boundary conditions. For periodic system, the density of rods is uniform through the lattice, however, for open system, the time evolution of the density profiles is described by

the continuity equation inferred from the master equation (8.1), and it is given by

$$\frac{d\rho_i(t)}{dt} = j_{i-1}(t) - j_i(t) \tag{8.4}$$

where j_i is the current from site i to site $i+1$. It is given by

$$j_i = \langle n_i(1-n_{i+1})w_{i,i+1}\rangle \tag{8.5}$$

$w_{i,i+1} = \exp(-\Delta E/2)$ is the hopping rate from site i to $i+1$ and ΔE is the energy difference between the two configurations before and after the jump. Inserting the hopping rate in the expression (8.5), we find the following relation for the current

$$\begin{aligned} j_{i,i+l} = &\langle \tilde{n}_{i-l-1}n_i\tilde{n}_{i+l+1}\tilde{n}_{i+l+2}\rangle \\ &+e^{v/2}\langle n_{i-l-1}n_i\tilde{n}_{i+l+1}\tilde{n}_{i+l+2}\rangle \\ &+e^{-v/2}\langle \tilde{n}_{i-l-1}n_i\tilde{n}_{i+l+1}n_{i+l+2}\rangle \\ &+\langle n_{i-l-1}n_i\tilde{n}_{i+l+1}\tilde{n}_{i+l+2}\rangle \end{aligned} \tag{8.6}$$

where $\tilde{n}_i = 1 - n_i$. Eq (8.6) contains correlators of order four which can be decomposed as a product of two points correlator as fellow

$$\phi(n_i, n_j, n_k, n_l) = \phi(n_i)\psi(n_j|n_i)\psi(n_k|n_j)\psi(n_l|n_k). \tag{8.7}$$

$\psi(a|b) = \phi(a,b)/\phi(b)$ is the conditional probability for a to happen given that b is happened and $\phi()$ is the probability distributions. Inserting expression (8.7) for the case of rods of size l, and using the density of rods $\rho = lp$ where $p_i = \langle n_i\rangle$ is the mean occupation number at site i, we get

$$\begin{aligned} j_i = &\frac{\rho_i - lC_i}{\rho_i(1-\rho_{i+l+1})}\left[(\frac{\rho_{i+l+2}}{l} - C_{i+l+1,2})e^{-v/2} + 1 - \rho_{i+l+1} - \frac{\rho_{i+l+2}}{l} + C_{i+l+1,2}\right] \\ &\times\left[\frac{\rho_i}{l} - C_{i-l-1} + e^{v/2}C_{i-l-1}\right] \end{aligned} \tag{8.8}$$

where the pair density $C_{i,i+l}$ has been worked out exactly in [78]. In term of mean occupation numbers p_i, the pair density is given by

$$C_{i,i+l} = \frac{A - \sqrt{A^2 - 4e^{-\beta v}(e^{-\beta v}-1)p_i p_{i+l}}}{2(e^{-\beta v}-1)} \tag{8.9}$$

and A is given by

$$A = 1 + e^{-\beta v}(p_i + p_{i+l}) - \sum_{k=i}^{i+l} p_k \tag{8.10}$$

In eq (8.8), we have used the notation $C_i = C_{i,i+l+1}$ and $C_{i+l+1,2} = C_{i+l+1,i+l+2}$.

8.3.2 Periodic boundary conditions

Let us consider first a system with periodic boundary conditions. In this case the density is uniform through the lattice. The current becomes

$$j = \frac{(\rho/l - C)^2 e^{-v/2}}{(\rho/l)(1-\rho)} \left[1 + \frac{(\rho/l - C)e^{-v/2}}{C}\right]\left[\frac{\rho}{l} - C + e^{v/2}C\right] \tag{8.11}$$

and the pair density is given by

$$C = \frac{1}{2\xi}\left[1 + 2(\xi+1)p - (l+1)p - \sqrt{(1 + 2(\xi+1)p - (l+1)p)^2 - 4\xi(\xi+1)p^2}\right] \tag{8.12}$$

where $\xi = e^{-\beta v} - 1$. Eqs (8.11) and (8.12) give the current for hard rods with arbitrary size and arbitrary contact interactions. By switching of the interactions, we recover the earlier results of rods with hard core interactions. In this case, the pair density reduces to

$$C = \frac{p^2}{1 - (l-1)p} \tag{8.13}$$

or in term of the density of rods ρ,

$$C = \frac{\rho^2}{l^2}\frac{1}{1 - \rho + \rho/l} \tag{8.14}$$

and the current becomes

$$j = \frac{\rho}{l}\frac{1-\rho}{1 - \rho + \rho/l} \tag{8.15}$$

which coincides with the earlier result derived in [182] with a completely different approach. The variation of the current (8.15) versus the density for hard rods of sizes $l = 1$ and 5 without interactions are shown in Fig (8.3). For rods of size l and low density, the current is an increasing function of the density. It reaches it maximum value at the density $\rho = l/(l+1)$. Below this point which corresponds to the half filling, the rods have more freedom to diffuse through the lattice. Beyond this point, more and more rods come into contact and hence from clusters of longer size which play a role of defect for moving rods. This results in strong suppression of the current at high densities.

The maximum density can be found from the relation $\delta j/\delta\rho = 0$. It is given by

$$\rho_{max} = \frac{1}{\sqrt{l}+1} \tag{8.16}$$

and it corresponds the maximum current

$$j_{max} = \frac{1}{(\sqrt{l}+1)^2} \tag{8.17}$$

For hard rods on an open lattice, the phase diagram Fig (8.4) is proved to have qualitatively the same form as those of the standard exclusion process except that

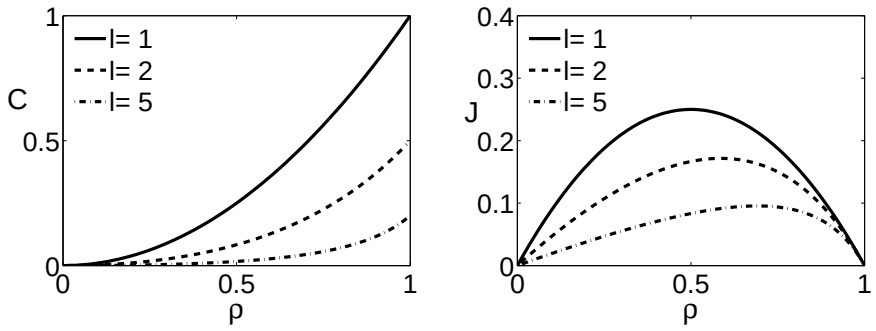

(a) (b)

Figure 8.3: Correlator (*a*) and current (*b*) of hard rods with sizes $l = 1, 2$ and 5 for vanishing coupling constant v.

the critical point $(1/2, 1/2)$ is shifted to $(1/(\sqrt{l}+1), 1/(\sqrt{l}+1))$ [181, 182]. The phase diagram consists of three phases: maximum current (MC), high density (HD) and low density (LD) phases

$$\begin{aligned}
&\textit{Phase I} : \textit{MC} \\
&\qquad j = \tfrac{1}{(\sqrt{l}+1)^2}, \quad \rho = \tfrac{1}{(\sqrt{l}+1)}, \qquad \text{for } \alpha, \beta > \rho_c \\
&\textit{Phase II} : \textit{HD} \\
&\qquad j = \tfrac{\beta(1-\beta)}{1+\beta(l-1)}, \quad \rho = 1-\beta, \qquad \text{for } \beta < \alpha < \rho_c \\
&\textit{Phase III} : \textit{LD} \\
&\qquad j = \tfrac{\alpha(1-\alpha)}{1+\alpha(l-1)}, \quad \rho = \tfrac{\alpha}{1+\alpha(l-1)}, \quad \text{for } \alpha < \beta < \rho_c
\end{aligned} \tag{8.18}$$

where $\rho_c = 1/(\sqrt{l}+1)$ is the critical density.

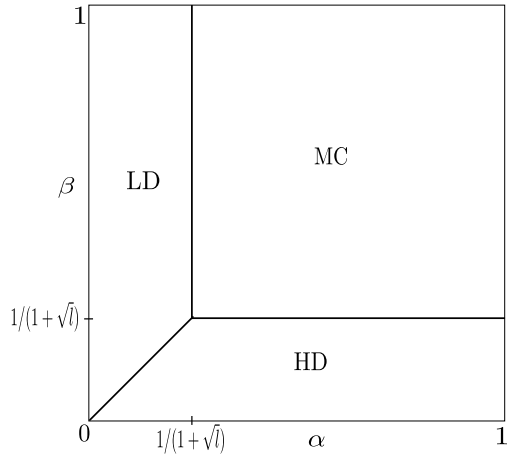

Figure 8.4: Phase diagram of hard rods with size l.

The effects of attractive and repulsive interactions on the current of hard rods

of size $l = 1$ and 5 are shown in Fig. (8.5).

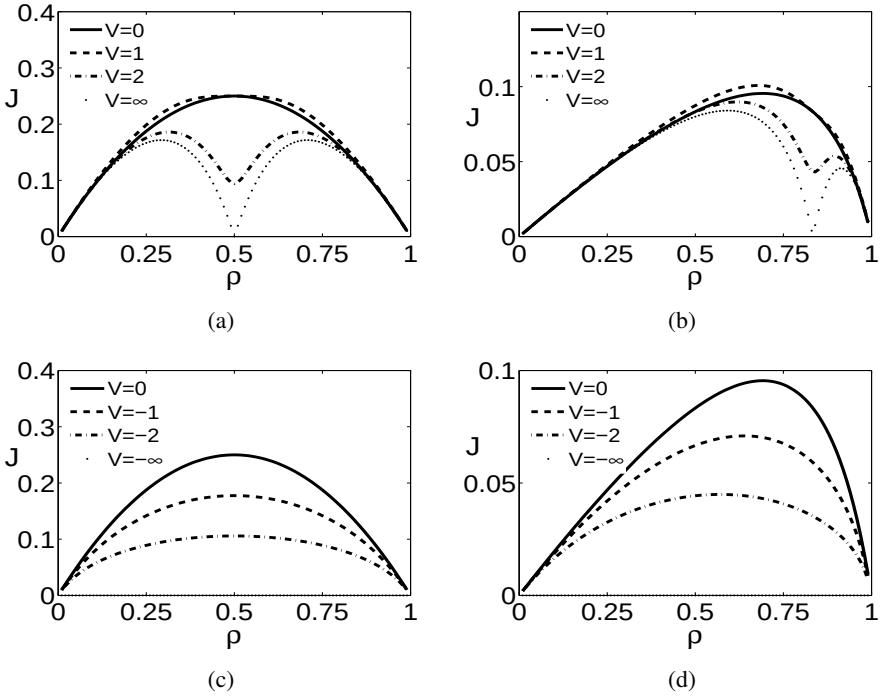

Figure 8.5: Current of hard rods with sizes $l = 1$ (a, c) and $l = 5$ (b, d) for repulsive $(V > 0)$ and atrractive $(V < 0)$ interactions.

For the case of particles of size one interacting via nearest neighbour repulsive interactions, the expression (8.11) reduced neatly to those results previously derived by Dierl *et al* [53,54]. In this case and at half filling, the current is suppressed for a very strong repulsive interactions which leads to a double hump structure in the current-density relation. For the case of particles of size l greater than one, the point $1/2$ where the current is suppressed is shifted to $l/(l+1)$ and the current is not symmetric with respect to this point due to the particle-hole symmetry breaking. For the case of attractive interactions, the current decreases when increasing the attractive interaction between rods which due to the tendency of rods to clustering forming together leading to a zero current for a very strong attractive interactions.

8.3.3 Open boundary conditions

For hard rods on a lattice with open boundaries, we fellow idea suggested in Ref. [182] to calculate the current at the left and right boundaries. Let suppose now that our system is coupled to two reservoirs, one to the left end with density ρ_L and one to right end with density ρ_R. Our concern here is to calculate ρ_L and ρ_R as functions of the injection and extraction rates α and β respectively.

The left reservoir density can be calculated as follows: consider two sites $k-1$

and k in the bulk and let us ask what is the probability for site $k-1$ to be filled given that site k is empty? we denote this probability by R_k and it is given by

$$R_k = \frac{\langle n_{k-1}(1-n_k)\rangle}{\langle 1-n_k\rangle} = \frac{\rho_{k-1} - C_{k-1,k}}{1-\rho_k} \tag{8.19}$$

Inserting the relation of C for homogeneous system in R_k, we find

$$R = \frac{-1+(l-1)\rho + \sqrt{(1-(l-1)\rho)^2 + 4(e^{-\beta v}-1)\rho - 4l\rho^2(e^{-\beta v}-1)}}{2(e^{-\beta v}-1)(1-\rho)} \tag{8.20}$$

If we consider now that sites $k-1$ and k represent respectively the reservoir and the first site of our system, and because the first site will be filled with probability α than we have the equality

$$\alpha = \frac{-1+(l-1)\rho_L + \sqrt{(1-(l-1)\rho_L)^2 + 4(e^{-v}-1)\rho_L - 4l\rho_L^2(e^{-v}-1)}}{2(e^{-\beta v}-1)(1-\rho_L)} \tag{8.21}$$

Solving eq (8.21) for ρ_L we find

$$\rho_L = \frac{\alpha(1-\alpha+\alpha e^{-v})}{1+(l-1)\alpha - \alpha^2(e^{-v}-1)} \tag{8.22}$$

and the corresponding current is given by

$$j_L = \frac{\alpha(1-\alpha)(1-\alpha+\alpha e^{-v})}{1+(l-1)\alpha - \alpha^2(e^{-v}-1)} \tag{8.23}$$

At the right boundary, the current j_R is

$$j_R = \frac{\beta(1-\beta)(1-\beta+\beta e^{-v})}{1+(l-1)\beta - \beta^2(e^{-v}-1)} \tag{8.24}$$

and the density ρ_R is given by

$$\rho_R = 1-\beta \tag{8.25}$$

Eqs. (8.22)-(8.25) represent an explicit equations for the currents and densities at the two boundaries for rods of arbitrary sizes and arbitrary contact interactions. Let us consider some limits of the expressions (8.22)-(8.25). The case of rods with size $l=1$ and vanishing interactions $v=0$, corresponds to the standard totally simple asymmetric process [171–173]. The density and current of the ASEP at left and right boundaries are given by

$$\begin{aligned} \rho_L &= \alpha \\ j_L &= \alpha(1-\alpha) \end{aligned} \tag{8.26}$$

and

$$\rho_R = 1-\beta \tag{8.27}$$

$$j_R = \beta(1-\beta) \tag{8.28}$$

The densities at the two boundaries vary linearly with the injection and extraction rates.

For rods with size l and vanishing interactions $v = 0$ (driven hard rods), we recover the results previously derived for this system [181, 182]. Many properties of the driven hard rods are qualitatively similar to the case of $l = 1$. The density and the current at the left boundary are given respectively by

$$\rho_L = \frac{\alpha}{1 + \alpha(l-1)} \tag{8.29}$$

$$j_L = \frac{\alpha(1-\alpha)}{1 + \alpha(l-1)} \tag{8.30}$$

Their variations are shown on Fig. (8.6). Both density and current decrease with increasing the rod size. The current reaches it maximum at $\alpha = 1/(1+l)$ or in term of coverage at $l\alpha = l/(1+l)$.

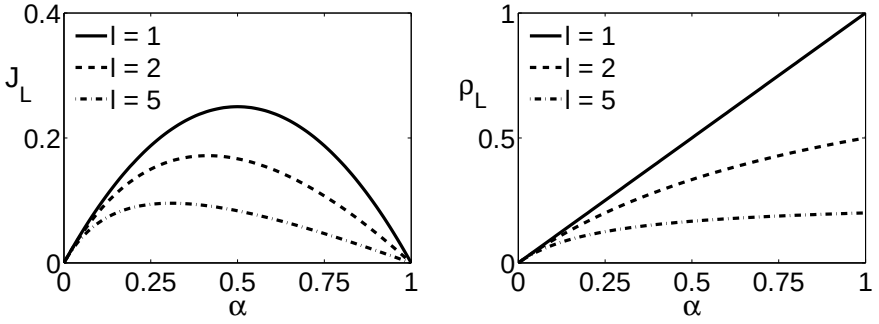

(a) (b)

Figure 8.6: Density (a) and current (b) at the left boundary of driven hard rods.

At the right boundary, the density and current are given respectively by

$$\begin{aligned} \rho_R &= 1 - \beta \\ j_R &= \frac{\beta(1-\beta)}{1 + \beta(l-1)} \end{aligned} \tag{8.31}$$

The current has the same form as for the entry current at the left boundary. The size of the rod has no effect on the density at the right boundary.

Finally for the case of standard TASEP ($l = 1$) with next neighbour interactions, we find

$$\begin{aligned} \rho_L &= \frac{\alpha(1 - \alpha + \alpha e^{-v})}{1 - \alpha^2(e^{-v} - 1)} \\ j_L &= \frac{\alpha(1-\alpha)(1 - \alpha + \alpha e^{-v})}{1 - \alpha^2(e^{-v} - 1)} \end{aligned} \tag{8.32}$$

and at the right boundary

$$\begin{aligned} \rho_R &= 1-\beta \\ j_R &= \frac{\beta(1-\beta)(1-\beta+\beta e^{-v})}{1-\beta^2(e^{-v}-1)} \end{aligned} \tag{8.33}$$

Apart form the quadratic terms for α and β in the denominator, the expressions (8.32) and (8.33) coincide with the expressions derived in [53,54] for the boundary current.

Eqs (8.22)-(8.25) represent a general expressions for the variation of the current and density at the boundaries of rods of any sizes and at different values of interactions potential. The density and current of rods of size $l = 1$ and 5 at the left boundary for different values of the interactions strength are shown in Fig 8.7.

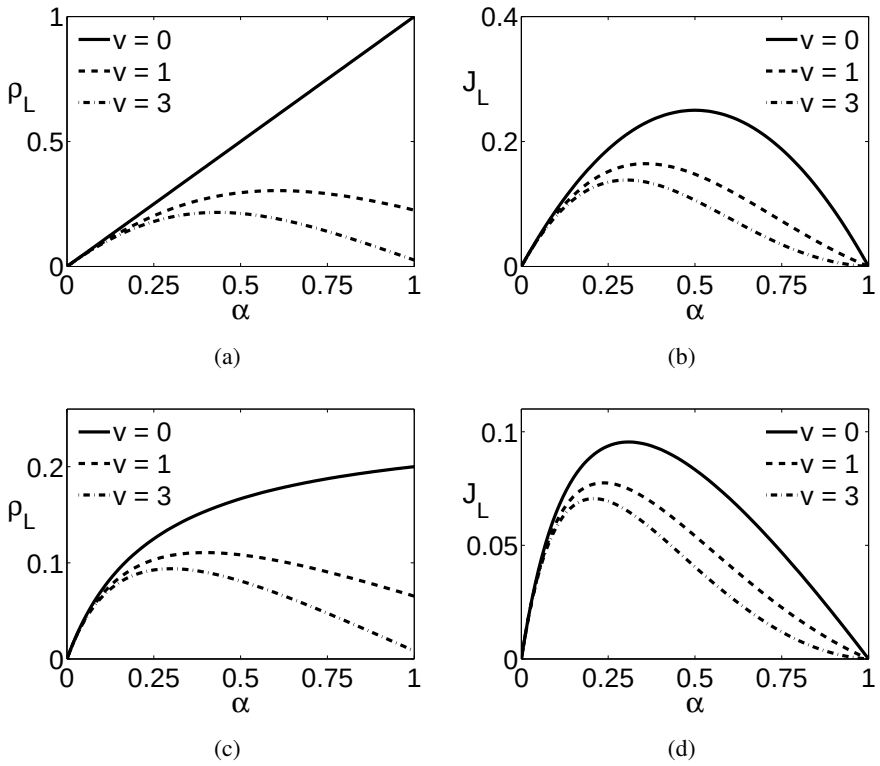

Figure 8.7: Density and current at the left boundary of driven hard rods with contact interactions of rods with sizes 1 (a, c) and 5 (b, d), for different values of the contact interactions.

For the case of vanishing interactions, the density at the left boundary is just the left injection rate. Repulsion causes a decreasing of the density at the left boundary. This effect is more pronounce for higher injection rate due to the increasing of correlation. Increasing the size of the rods results also in a decreasing of the density at the left boundary. For sizes $l > 1$ and in the absence of interactions, the density

is no longer linear. This is due to the mechanism of injection of rods, where the first site is partially covered by a rod. We can distinguish two possible mechanisms for injection: first the case where the rod is injected completely in the lattice at the left boundary (which is our case). The second mechanism is the case where the rod enter the lattice site by site. For low injection rate, the density of rods approaches the limit where no interactions are present.

When increasing the injection rate and/or the interactions, the current at the left boundary has qualitatively a similar form for all sizes. It increases with increasing the injection rate. Then attends a maximum value at $\alpha = 1/(l+1)$. Beyond this value it decreases again to reach the value 0. This is due to the fact that at $\alpha = 1/(l+1)$, the system is at half filling where all rods are repulsing each other, which suppresses the current in the bulk and in at the boundary.

8.4 Conclusion

In this chapter, we have carried out an analysis based on the time-dependent density functional theory of the steady state dynamics of the totally asymmetric simple exclusion process of particles with size l which interact through a contact interactions. We have shown that the steady state properties are qualitatively the same as the standard TASEP of interacting particles of size 1. Current-density relations present the double hump structure for rod of any sizes and hence the phase diagram for a driven hard rods with contact interactions has a similar structure to the stochastic interacting lattice gas. In some appropriate limits, results of the latter have been recovered as well as for the driven hard rods with hard core exclusion. Our results for the hard rod mixtures with contact interactions presented in the Chap. (4) can be utilize to generalize the current results of driven hard rods to the case of mixtures.

Chapter 9

Summary and Conclusion

This thesis deals principally with one dimensional exactly solvable models in condensed matter and statistical physics using the density functional theory. These models have been proved to be very useful in the development of the DFT, as many approximate methods in 2D and 3D have been inspired in their constructions by the exact results in one dimension, and also because of the discovery of dimensional crossover of the fundamental measure theory. The exact density functionals in one dimension contains information on the density functionals in higher dimensions and the recipes to set up the latter from the former have been well established.

Our second interest is in the effects of thermal interactions which have been proved to have an important roles in the phase transformations of condensed matter systems. We have shown that it has a dramatic effects on equilibrium and non-equilibrium properties of statistical models even in one dimension.

To derive exact density functionals in one dimension, we employed the method of the Markov chain, proposed by Buschle *et al*. First we generalized it to the case of hard rod mixtures with athermal hard core exclusion. The results were reduced to those derived previously within a discrete version of Percus's inverse problem approach. As a second step, we considered hard rods with arbitrary nearest neighbour interactions extending over two rod lengths. The strategies employed in the investigations of the two previous models were combined to set up an exact density functionals for hard rod mixtures with contact interactions.

Considering the core in the derivation of the distribution of microstates, it is important to realize that the procedure can in principle be extended to interactions of longer range covering several rod lengths. For a given range ξ, the exclusion constraint leads to a natural decomposition of the set $\{n_s, \ldots, n_{s-\xi}\}$ into ranges covering the lattice sites $s-\sigma+1, \ldots, s$ (first range), $s-2\sigma+1, \ldots, s-\sigma$ (second range), and so on. In each of these ranges at most one occupation number can be equal to one. The total number of ranges that need to be taken into account is $\lceil \xi/\sigma \rceil$, where $\lceil x \rceil$ denotes the integer ceiling division, i.e. the smallest integer larger than x. Accordingly we would need to consider higher-order correlators $C(1_{i_1}, 1_{i_2}, 1_{i_3}, \ldots, ...)$, where 1_{i_k}, specifies the location of the occupied

site in the kth range as in Chap. 5. The distribution of microstates can then be expressed in term of these correlators $C(1_{i_1}, 1_{i_2}, 1_{i_3}, \ldots, ...)$ (and the densities p_i, which in this general language, correspond to the "one-point correlators"). By equating with the Boltzmann formula for simple configurations, relations between the $C(1_{i_1}, 1_{i_2}, 1_{i_3}, \ldots, ...)$ and the p_i eventually can be obtained, which need to be solved for expressing the $C(1_{i_1}, 1_{i_2}, 1_{i_3}, \ldots, ...)$ in terms of the p_i. An interesting aspect of the Markov chain approach is that its density functionals have the same form as the fundamental measure functionals, which means that the density functionals have been written as a lattice sum over density functionals of a 0D cavity. In this respect we have identified two sorts of cavities, the 1-particle cavity which is a cavity that cannot hold more than one particle (in our language, at most one occupation number can be one in the range of the cavity) and a 2-particle cavity which cannot hold more than two particles (two occupation numbers can be one in the range of the cavity at most) This feature permitted us to construct an approximate density functionals in 2D and 3D from the exact ones using the dimensional crossover.

The Markov chain approach offers an alternative to the dimensional crossover which is independent of any reference to the zero-dimensional excess free energy functional. The idea is to simplify conditional probabilities appearing in the Markov chains by only taking into account memory over a limited spatial range comparable to the range of interactions. Preliminary results for the two-dimensional Ising model show that with such procedure, bulk phase diagrams are described with a quality comparable to the Kikuchi's cluster variation method. This big advantage of the DFT approach is that the influence of arbitrary external fields can be considered to be on the same footing without any reconstruction of the underlying functional.

To account for the dynamics of our system, we have employed the TDFT to investigate the steady state dynamics of hard rods with contact interactions. By taking an appropriate limits, results previously derived for the standard totally asymmetric simple exclusion process as well as the driven hard rods have been recovered. In principle, the TDFT is general to arbitrary dimension and can be used to study, as an example, diffusion and phase transformations of binary alloys and colloidal particles with contact interactions where their density functionals can be inferred from our exact results by dimensional crossover.

Erklärung

Hiermit versichere ich, dass ich die vorliegende Arbeit selbständig verfasst und keine anderen als die angegebenen Quellen und Hilfsmittel benutzt habe, dass alle Stellen der Arbeit, die wörtlich oder sinngemäßaus anderen Quellen übernommen wurden, als solche kenntlich gemacht worden sind, und dass die Arbeit in gleicher oder ähnlicher Form noch keiner anderen Prüfungsbehörde vorgelegt wurde.

I hereby confirm that I accomplished this work independently and did not use other sources or resources than mentioned. I confirm that all passages of this work which have been taken from other sources literally or in meaning have been indicated. This work has not been presented in a same or similar form to another commission.

Acknowledgment

First, I would sincerely like to thank my supervisor, Prof. Dr. Philipp Maaß, for all the support he has shown by admitting me as a PhD student and for giving me the opportunity to work in his group. I am also grateful to him for helping me to get the DAAD award. He has always encouraged me to strive for independence and excellence in my scientific research, as well as providing his personal support in my endeavors. In addition, I am thankful to him for giving me the opportunity to visit the University of Rhode Island in the USA.

I wish to express my sincere gratitude to Prof. Dr. Gerhard Müller from the University of Rhode Island and his wife Christine Müller for their very kindness and hospitality and their help during my stay in their house. I am grateful to him for having had the opportunity to collaborate on the fascinating field of fractional exclusion statistics. His helpful discussions and suggestions are particularly acknowledged.

I am very grateful to the official reviewers Prof. Dr. Michael Rohlfing, Prof. Dr. Joachim Wollschläger, and to Dr. Mario Einax for reviewing the thesis manuscript and for their useful suggestions. I am thankful to Prof. Dr. Michael Rohlfing for many help during my PhD.

Special thanks to Prof. Dr. Petr Chvosta and to Prof. Dr. Mohammad Reza Rahimi Tabar for all fruitful discussions and suggestions.

Grateful thanks to my parent Meriem and Abdelkader, my wife Hanane, my brothers Mohammed and Habib and my sisters Mlouka, Fatiha, Yamina and Kheira, and also to all my family for their continuous encouragement and support over the course of my PhD.

I use this opportunity to thank my friends Mohammed Reda Chellali, Ahmed Abdel Fattah, Djamal Gaffor, Abdellah Khodja, Houari Bouchikhaoui, and Ferdinand Schulz for their help.

I also really want to thank my friends from the Statistical Physics group: Sandra Nostheide, Tayebeh Jadidi, Marcel Dierl, Susanne Hahne, Michael Schuch, Mohamad Elhamad and Yvonne Richter.

Appreciation is also extended to my friends at the University of Rhode Island, Sarah Brent, Amer Hodzic, Mohammad Mokim and Christopher Moore.

Finally I would like to express my deep thanks to the *Deutscher Akademischer Austauschdienst* (DAAD) for financial support of my PhD and also for supporting my stay at the University of Rhode Island

List of Figures

Bibliography

[1] Löwen, H. (1994) *Phys. Rep.* **237(5)**, 249–324.

[2] Evans, R. (1992) Fundamentals of Inhomogeneous Fluids*, D. Henderson, ed, Marcel Dekker, NY* p. 85.

[3] Tarazona, P., Cuesta, J. A., and Martínez-Ratón, Y. (2008) *in* Theory and Simulation of Hard-Sphere Fluids and Related Systems*, A. Mulero, ed, Lect. Notes Phys. Springer* p. 249.

[4] Lutsko, J. F. Recent Developments in Classical Density Functional Theory volume **144**, pp. 1–92 John Wiley & Sons, Inc. (2010).

[5] Rosenfeld, Y., Schmidt, M., Löwen, H., and Tarazona, P. (1996) *J. Phys.: Condens. Matter* **8(40)**, L577.

[6] Dietrich, S. (1987) in Phase Transitions and Critical Phenomena, volume **12**, Academic Press, London, .

[7] Schmidt, M. (2002) *Phys. Rev. E* **66**, 041108.

[8] Lafuente, L. and Cuesta, J. A. (2006) *Phys. Rev. E* **74**, 041502.

[9] Pilania, G. and Ramprasad, R. (2010) *Surf. Sci.* **604**, 1889.

[10] Pilania, G., Zhu, H., and Ramprasad, R. (2012) *in* The Density of Matter: Exploring the Electron Density Concept in the Chemical, Biological, and Materials Sciences*, N. Sukumar, ed, Wiley* pp. 271–312.

[11] Cardona Quintero, Y., Zhu, H., and Ramprasad, R. (2013) *J. Mater. Sci.* **48**, 2277.

[12] Schmidt, M. and Löwen, H. (1997) *Phys. Rev. E* **55**, 7228.

[13] Götzelmann, B. and Dietrich, S. (1997) *Phys. Rev. E* **55**, 2993.

[14] Rosenfeld, Y. (1994) *Phys. Rev. E* **50**, R3318.

[15] Martínez-Ratón, Y. (1994) *Phys. Rev. E* **69**, 061712.

[16] Cuesta, J. A. and Martínez-Ratón, Y. (1997) *Phys. Rev. Lett* **78**, 3681.

[17] Cuesta, J. A. and Martínez-Ratón, Y. (1997) *J. Chem. Phys* **107**, 6379.

[18] Schmidt, M. (2001) *Phys. Rev. E* **63**, 050201.

[19] Hansen-Goos, H. and Mecke, K. (2009) *Phys. Rev. Lett* **102**, 018302.

[20] Munakata, T. (1989) *J. Phys Soc. Jap* **58(7)**, 2434.

[21] Talanquer, V. and Oxtoby, D. W. (1994) *J. Chem. Phys.* **100(7)**, 5190.

[22] Penna, F. and Tarazona, P. (2003) *J. Chem. Phys.* **119**, 1766.

[23] Marconi, U. M. B. and Tarazona, P. (1999) *J. Chem. Phys.* **110**, 8032.

[24] Fuchizaki, K. and Kawasaki, K. (1999) *Physica A* **266**, 400.

[25] Marconi, U. M. B. and Tarazona, P. (2000) *J. Phys.: Condens. Matter* **12**, A413.

[26] Fuchizaki, K. and Kawasaki, K. (2002) *J. Phys.: Condens. Matter* **14**, 12203.

[27] Dzubiella, J. and Likos, C. N. (2003) *J. Phys.: Condens. Matter* **15**, L147.

[28] Archer, A. J. and Evans, R. (2004) *J. Chem. Phys.* **121**, 4246.

[29] Archer, A. J. (2005) *J. Phys.: Condens. Matter* **17**, 1405.

[30] Marconi, U. M. B. and Tarazona, P. (2006) *J. Chem. Phys.* **124**, 160901.

[31] Archer, A. J. (2006) *J. Phys.: Condens. Matter* **18**, 5617.

[32] Chou, C. Y., Eng, B. C., and Robert, M. (2006) *J. Chem. Phys.* **124**, 044902.

[33] Rex, M., Wensink, H. H., and Löwen, H. (2007) *Phys. Rev. E* **76**, 021403.

[34] Rex, M. and Löwen, H. (2008) *Phys. Rev. Lett* **101**, 148302.

[35] Marconi, U. M. B., Tarazona, P., Cecconi, F., and Melchionna, S. (2008) *J. Phys.: Condens. Matter* **20**, 494233.

[36] Tarazona, P. and Marconi, U. M. B. (2008) *J. Chem. Phys.* **128**, 164704.

[37] Archer, A. J. (2009) *J. Chem. Phys.* **130**, 014509.

[38] Español, P. and Löwen, H. (2009) *J. Chem. Phys.* **131**, 244101.

[39] Rex, M. and Löwen, H. (2009) *Euro. Phys. J. E* **28**, 139.

[40] Archer, A. J., Robbins, M. J., and Thiele, U. (2010) *Phys. Rev. E* **81**, 021602.

[41] Robbins, M. J., Archer, A. J., and Thiele, U. (2011) *J. Phys.: Condens. Matter* **23**, 415102.

[42] Wittkowski, R. and Löwen, H. (2011) *Mol. Phys* **109(23-24)**, 2935.

[43] Wittkowski, R., Löwen, H., and Brand, H. R. (2012) *J. Chem. Phys.* **137**, 224904.

[44] Goddard, B. D., Nold, A., Savva, N., Pavliotis, G. A., and Kalliadasis, S. (2012) *Phys. Rev. Lett* **109**, 120603.

[45] Gouyet, J.-F., Plapp, M., Dieterich, W., and Maass, P. (2003) *Adv. Phys.* **52(7)**, 523.

[46] Biroli, G. and Mézard, M. (2001) *Phys. Rev. Lett.* **88**, 025501.

[47] Chui, S. T. and Weeks, J. D. (1981) *Phys. Rev. B* **23**, 2438.

[48] Azbel, M. Y. (1979) *Phys. Rev. A* **20**, 1671–1684.

[49] Reinel, D. and Dieterich, W. (1996) *J. Chem. Phys.* **104(13)**, 5234–5239.

[50] Fischer, H. P., Reinhard, J., Dieterich, W., Gouyet, J. F., Maass, P., Majhofer, A., and Reinel, D. (1998) *J. Chem. Phys.* **108(7)**, 3028–3037.

[51] Kessler, M., Dieterich, W., Frisch, H. L., Gouyet, J. F., and Maass, P. (2002) *Phys. Rev. E* **65**, 066112.

[52] Heinrichs, S., Dieterich, W., Frisch, H. L., and Maass, P. (2004) *J. Stat. Phys.* **114(3-4)**, 1115–1125.

[53] Dierl, M., Maass, P., and Einax, M. (2011) *Europhys. Lett.* **93(5)**, 50003.

[54] Dierl, M., Maass, P., and Einax, M. (2012) *Phys. Rev. Lett.* **108**, 060603.

[55] Rosenfeld, Y. (1989) *Phys. Rev. Lett.* **63**, 980–983.

[56] Tarazona, P. and Rosenfeld, Y. (1997) *Phys. Rev. E* **55**, R4873–R4876.

[57] Rosenfeld, Y., Schmidt, M., Löwen, H., and Tarazona, P. (1997) *Phys. Rev. E* **55**, 4245–4263.

[58] Tarazona, P. (2000) *Phys. Rev. Lett.* **84**, 694–697.

[59] Tarazona, P. (2002) *Physica A* **306**, 243.

[60] Lafuente, L. and Cuesta, J. A. (2002) *Phys. Rev. Lett.* **89(14)**, 145701.

[61] Lafuente, L. and Cuesta, J. A. (2002) *J. Phys.: Condens. Matter* **14(46)**, 12079–12097.

[62] Lafuente, L. and Cuesta, J. A. (2004) *Phys. Rev. Lett.* **93(13)**, 130603.

[63] Robledo, A. and Varea, C. *J. Stat. Phys* **26(3)**, 513–525.

[64] Buschle, J., Maass, P., and Dieterich, W. (2000) *J. Phys. A* **33**, L41.

[65] Buschle, J., Maass, P., and Dieterich, W. (2000) *J. Stat. Phys.* **99(1-2)**, 273–312.

[66] Schmidt, M., Lafuente, L., and Cuesta, J. A. (2003) *J. Phys.: Condens. Matter* **15(27)**, 4695–4708.

[67] Lafuente, L. and Cuesta, J. A. (2003) *J. Chem. Phys.* **119(20)**, 10832–10843.

[68] Lafuente, L. and Cuesta, J. A. (2003) *Phys. Rev. E* **68(6)**, 066120.

[69] Cuesta, J. A., Lafuente, L., and Schmidt, M. (2005) *Phys. Rev. E* **72(3)**, 031405.

[70] Lafuente, L. and Cuesta, J. A. (2005) *J. Phys A: Math. Gen.* **38(34)**, 7461.

[71] Hoy, R. S. and O'Hern, C. S. (2010) *Phys. Rev. Lett.* **105**, 068001.

[72] Amokrane, S. and Regnaut, C. (1997) *J. Chem. Phys.* **106(1)**, 376–387.

[73] Braun, F. N. (2002) *J. Chem. Phys.* **116(15)**, 6826–6830.

[74] Xu, Q., Feng, L., Sha, R., Seeman, N. C., and Chaikin, P. M. (2011) *Phys. Rev. Lett.* **106**, 228102.

[75] Dreyfus, R., Leunissen, M. E., Sha, R., Tkachenko, A. V., Seeman, N. C., Pine, D. J., and Chaikin, P. M. (2009) *Phys. Rev. Lett.* **102**, 048301.

[76] Stell, G. (1995) *J. Stat. Phys* **78(1-2)**, 197–238.

[77] Bakhti, B., Schott, S., and Maass, P. (2012) *Phys. Rev. E* **85**, 042107.

[78] Bakhti, B., Müller, G., and Maass, P. (2013) *J. Chem. Phys* **139**, 054113.

[79] Bakhti, B., Karbach, M., Maass, P., Mokim, M., and Müller, G. *(submited)*.

[80] Parr, R. G. and Yang, W. (1994) Density Functional Theory of Atomes and Molecules, volume **16**, Oxford University Press, .

[81] Dreizler, R. M. and Gross, E. K. U. (1990) Density Functional Theory, Springer Verlag, Berlin, .

[82] Gross, E. K. U., Dobson, J. F., and Persilka, M. (1996) Density Functional Theory II, Topics in Current Chemistry, volume **181**, Springer, Berlin, .

[83] Fulde, P. (2002) Electron Correlations in Molecules and Solids, Springer Verlag, Berlin, Heidelberg, New York, .

[84] Hohenberg, P. and Kohn, W. (1964) *Phys. Rev.* **136**, B864–B871.

[85] Kohn, W. and Sham, L. J. (1965) *Phy. Rev.* **140**, A1133.

[86] Mermin, N. D. (1965) *Phys. Rev.* **137**, A1441–A1443.

[87] Ebner, C., Saam, W. F., and Stroud, D. (1976) *Phys. Rev. A* **14**, 2264–2273.

[88] Saam, W. F. and Ebner, C. (1977) *Phys. Rev. A* **15**, 2566–2568.

[89] Ornstein, L. S. and Zernike, F. (1914) *Proc. acad. Sci. Amsterdam* p. 793.

[90] Percus, J. K. and Yevick, G. (1958) *Phys. Rev.* **110**, 1–13.

[91] van Leeuwen, J. M. J., Groeneveld, J., and de Boer, J. (1959) *Physica* **25(7–12)**, 792–808.

[92] Rosenfeld, Y. and Ashcroft, N. W. (1979) *Phys. Rev. A* **20**, 1208–1235.

[93] Born, M. and Green, H. S. (1946) *Proc. Roy. Soc. A* **188**, 10.

[94] Lebowitz, J. L. and k.Percus, J. (1966) *Phys. Rev.* **144**, 251–258.

[95] Ramakrishnan, T. V. and Yussouff, M. (1979) *Phys. Rev. B* **19**, 2775–2794.

[96] Baus, M. and Colot, J. (1985) *Mol. Phys.* **55(3)**, 653–677.

[97] Baus, M. (1989) *J. Phys. Condens. Matter* **1(19)**, 3131.

[98] Lutsko, J. F. and Baus, M. (1990) *Phys. Rev. A* **41**, 6647–6661.

[99] Lutsko, J. F. and Baus, M. (1990) *Phys. Rev. Lett.* **64**, 761–763.

[100] Nordholm, S., Johnson, M., and Freasier, B. C. (1980) *Aust. J. Chem.* **33**, 2139.

[101] Rowlinson, J. S. *J. Stat. Phys.* **20(2)**, 197–200.

[102] van der Waals, J. D. (1894) *Z. Phys. Chem.* **13**, 657.

[103] Tarazona, P. (1985) *Phys. Rev. A* **31**, 2672–2679.

[104] Curtin, W. A. and Ashcroft, N. W. (1985) *Phys. Rev. A* **32**, 2909–2919.

[105] Denton, A. R. and Ashcroft, N. W. (1989) *Phys. Rev. A* **39**, 4701–4708.

[106] Percus, J. K. (1976) *J. Stat. Phys.* **15(6)**, 505–511.

[107] Reiss, H., Frisch, H. L., and Lebowitz, J. L. (1959) *J. Chem. Phys.* **31(2)**, 369–380.

[108] Reiss, H., Frish, H. L., and Lebowitz, J. L. (1960) *J. Chem. Phys.* **32(1)**, 119–124.

[109] Vanderlick, T. K., Davis, H. T., and Percus, J. K. (1989) *J. Chem. Phys.* **91(11)**, 7136–7145.

[110] Percus, J. K. (1982) *J. Stat. Phys.* **28(1)**, 67–81.

[111] Brannock, G. R. and Percus, J. K. (1996) *J. Chem. Phys.* **105(2)**, 614–627.

[112] Wertheim, M. S. (1984) *J. Stat. Phys* **35(1-2)**, 19–34.

[113] Wertheim, M. S. (1986) *J. Stat. Phys* **42(3-4)**, 459–476.

[114] Percus, J. K. (1997) *J. Stat. Phys* **89(1-2)**, 249–272.

[115] Tutschka, C. and Cuesta, J. A. (2003) *J. Stat. Phys* **111(5-6)**, 1125–1148.

[116] Kierlik, E., Monson, P. A., Rosinderg, M. L., Sarkisov, L., and Tarjus, G. (2001) *Phys. Rev. Lett.* **87**, 055701.

[117] Nieswand, M., Dieterich, W., and Majhofer, A. (1993) *Phys. Rev. E* **47(1)**, 718–720.

[118] Nieswand, M., Majhofer, A., and Dieterich, W. (1993) *Phys. Rev. E* **48(4)**, 2521–2527.

[119] Prestipino, S. and Giaquinta, P. V. (2003) *J. Phys.: Condens. Matter* **15(23)**, 3931–3956.

[120] Prestipino, S. (2003) *J. Phys.: Condens. Matter* **15**, 8065–8080.

[121] Woywod, D. and Schoen, M. (2006) *Phys. Rev. E* **73(1, Part 1)**, 011201.

[122] Reinel, D., Dieterich, W., and Majhofer, A. (1994) *Phys. Rev. E* **50(6)**, 4744–4749.

[123] Chen, X., Sun, L., Liu, H., Hu, Y., and Jiang, J. (2009) *J. Chem. Phys.* **131(4)**, 044710.

[124] Brams Dwandaru, W. S. and Schmidt, M. (2007) *J. Phys. A: Math. Theor.* **40(44)**, 13209–13215.

[125] The Mermin theorem does not ensure that to each **p** a corresponding external potential exists (it ensure only that, if it exists, it is unique), but this more academic question seems to be irrelevant for physical applications.

[126] Reinhard, J., W.Dieterich, Maass, P., and Frisch, H. L. (2000) *Phys. Rev. E* **61**, 422–428.

[127] Baxter, R. J. (1980) *J. Phys. A: Math. Gen.* **13(3)**, L61.

[128] Choudhury, N. and Ghosh, S. K. (1997) *J. Chem. Phys.* **106(4)**, 1576–1584.

[129] Acedo, L. and Santos, A. (2001) *J. Chem. Phys.* **115(6)**, 2805–2817.

[130] Gazzillo, D. and Giacometti, A. (2004) *J. Chem. Phys.* **120(10)**, 4742–4754.

[131] Miller, M. A. and Frenkel, D. (2004) *J. Chem. Phys.* **121(1)**, 535–545.

[132] Miller, M. A. and Frenkel, D. (2004) *J. Phys.:Condens. Matter* **16(42)**, S4901.

[133] Rickayzen, G. and Heyes, D. M. (2007) *J. Chem. Phys.* **126(11)**, 114504.

[134] Buzzaccaro, S., Rusconi, R., and Piazza, R. (2007) *Phys. Rev. Lett.* **99**, 098301.

[135] Santos, A., Fantoni, R., and Giacometti, A. (2008) *Phys. Rev. E* **77**, 051206.

[136] Hansen-Goos, H. and Wettlaufer, J. S. (2011) *J. Chem. Phys.* **134(1)**, 014506.

[137] Hansen-Goos, H., Miller, M. A., and Wettlaufer, J. S. (2012) *Phys. Rev. Lett.* **108**, 047801.

[138] Jamnik, A. (1998) *J. Chem. Phys.* **109(24)**, 11085–11093.

[139] Pontoni, D., Finet, S., Narayanan, T., and Rennie, A. R. (2003) *J. Chem. Phys.* **119(12)**, 6157–6165.

[140] Lajovic, A., Tomsic, M., and Jamnik, A. (2009) *J. Chem. Phys.* **130(10)**, 104101.

[141] Dasmahapatra, A. K., Nanavati, H., and Kumaraswamy, G. (2009) *J. Chem. Phys.* **131(7)**, 074905.

[142] Lomakin, A., Asherie, N., and Benedek, G. B. (1996) *J. Chem. Phys.* **104(4)**, 1646–1656.

[143] Seto, H., Okuhara, D., Kawabata, Y., Takeda, T., Nagao, M., Suzuki, J., Kamikubo, H., and Amemiya, Y. (2000) *J. Chem. Phys.* **112(23)**, 10608–10614.

[144] Robertus, C., Philipse, W. H., Joosten, J. G. H., and Levine, Y. K. (1989) *J. Chem. Phys.* **90(8)**, 4482–4490.

[145] Gazzillo, D., Giacometti, A., Fantoni, R., and Sollich, P. (2006) *Phys. Rev. E* **74**, 051407.

[146] Baxter, R. J. (1968) *J. Chem. Phys.* **49(6)**, 2770–2774.

[147] Berlin, T. H. and Kac., M. (1952) *Phys. Rev.* **86**, 821–835.

[148] Martínez-Ratón, Y. (2007) *Phys. Rev. E* **75**, 051708.

[149] Martínez-Ratón, Y., Varga, S., and Velasco, E. (2008) *Phys. Rev. E* **78**, 031705.

[150] de las Heras, D., Martínez-Ratón, Y., and Velasco, E. (2010) *Phys. Rev. E* **81**, 021706.

[151] Dijkstra, M., Brader, J. M., and Evans, R. (1999) *J. Phys.: Conden. Matter* **11(50)**, 10079.

[152] Shundyak, K. and vanR. Roij (2002) *Phys. Rev. Lett.* **88**, 205501.

[153] Brack, M. (1984) *Phys. Rev. Lett.* **53**, 119–122.

[154] Li, S. and Percus, J. K. (1990) *J. Stat. Phys* **59(1-2)**, 323–332.

[155] Gonis, A., Schulthess, T. C., vanEk, J., and Turchi, P. E. A. (1996) *Phy. Rev. Lett.* **77**, 2981.

[156] Gonis, A., Schulthess, T. C., Turchi, P. E. A., and vanEk, J. (1997) *Phy. Rev. B* **56**, 9335.

[157] Ziesche, P. (1994) *Phys. Lett. A* **195**, 213.

[158] Ziesche, P. (1996) *Int. J. Quantum Chem.* **30**, 1361.

[159] Levy, M. and Ziesche, P. (2001) *J. Chem. Phys* **115**, 9110.

[160] Nagy, A. (2002) *Phy. Rev. A* **66**, 022505.

[161] Nagy, A. and Amovilli, C. (2004) *J. Chem. Phys* **121**, 6640.

[162] Ayers, P. W. and Levy, M. (2005) *Chem. Phys. Lett.* **415**, 211.

[163] Nagy, A. (2006) *J. Chem. Phys* **125**, 184104.

[164] Nagy, A. and Amovilli, C. (2008) *J. Chem. Phys* **128**, 114115.

[165] Nagy, A. and Amovilli, C. (2009) *Chem. Phys. Lett.* **469**, 353.

[166] Nagy, A. and Amovilli, C. (2010) *Phy. Rev. A* **82**, 042510.

[167] Li, S. and Percus, J. K. (1990) *Phys. Rev. A* **41**, 2344–2347.

[168] Li, S. and Percus, J. K. (1990) *J. Chem. Phys.* **93(6)**, 4266–4271.

[169] Bushong, N., Sai, N., and Venta, M. D. (2005) *Nano Latters* **5**, 2569–2572.

[170] Malik, R., Burch, D., Bazat, M., and Ceder, G. (2010) *Nano Latters* **10**, 4123–4127.

[171] Derrida, B., Evans, M., Hakim, V., and Pasquier, V. (1993) *J. Phys. A* **26**, 1493.

[172] Derrida, B. (1998) *Phys. Rep.* **301**, 65.

[173] Schütz, G. M. (2000) Phase Transitions and Critical Phenomena, volume **19**, Academic Press, London, .

[174] Stinchcombe, R. (2001) *Adv. Phys.* **50**, 431.

[175] de Gier, J. and Essler, F. H. (2005) *Phys. Rev. Lett* **95**, 240601.

[176] Alcaraz, F. C., Droz, M., Henkel, M., and Rittenberg, V. (1994) *Annals of Physics* **230**, 250.

[177] Alcaraz, F. C. and Bariev, R. Z. (1999) *Phys. Rev. E* **60**, 79.

[178] Alcaraz, F. C. and Bariev, R. Z. (2000) *J. Phys.* **30**, 13.

[179] Alcaraz, F. C. and Lazo, M. J. (2003) *J. Phys.* **33**, 533.

[180] Alcaraz, F. C. and Lazo, M. J. (2004) *J. Phys. A: Math. Gen.* **37**, L1.

[181] Lakatos, G. and Chou, T. (2003) *J. Phys. A. Math. Gen.* **36**, 2027.

[182] Shaw, L. B., Zia, R. K. P., and Lee, K. H. (2003) *Phys. Rev. E* **68**, 021910.

[183] Dong, J. J., Schmittmann, B., and Zia, R. K. P. (2007) *Phys. Rev. E* **76**, 051113.

[184] Dong, J. J., Schmittmann, B., and Zia, R. K. P. (2009) *J. Phys. A: Math. Theo* **42**, 015002.

[185] Hobbie, E. K. and Fry, D. J. (2006) *Phys. Rev. Lett.* **97**, 036101.

[186] Harvé, R. and Ibba, M. (2006) *Nature* **443**, 41.

[187] Derrida, B., Domany, E., and Mukamel, D. (1992) *J. Stat. Phys.* **69**, 667.

[188] Derrida, B., Evans, M. R., and Mukamel, D. (1993) *J. Phys. A* **26**, 4911.

[189] Derrida, B., Evans, M. R., Hakim, V., and Pasquier, V. (1993) *J. Stat. Phys.* **72**, 277.

[190] Blythe, R. A. and Evans, M. R. (2007) *J. Phys. A* **40**, R333.

[191] Krug, J. and Spohn, H. (1991) *Phys. Rev. Lett* **64**, 2332.

[192] de Gier, J. and Essler, F. H. (2006) *J. Stat. Mech. Theor. Exp* p. P12011.

[193] Evans, M. R., Foster, D. P., Godréche, C., and Mukamel, D. (1995) *Phys. Rev. Lett* **74**, 208.

[194] Evans, M. R., Foster, D. P., Godréche, C., and Mukamel, D. (1995) *J. Stat. Phys.* **80**, 69.

[195] Kolomeisky, A. B. (1997) *Physica A* **245**, 523.

[196] Karimipour, V. (1999) *Phys. Rev. E* **59**, 205.

[197] Karimipour, V. (2000) *J. Stat. Phys.* **100**, 999.

[198] Hager, J. S., Krug, L., Popkov, V., and Schütz, G. M. (2001) *Phys. Rev. E* **63**, 056110.